UNIVERSITÀ DEGLI STUDI DI PADOVA

DIPARTIMENTO DI INGEGNERIA DELL'INFORMAZIONE

DIPARTIMENTO DI INGEGNERIA DELL'INFORMAZIONE

CORSO DI LAUREA MAGISTRALE IN BIOINGEGNERIA INDUSTRIALE

"The use of "EMG driven" neuromusculoskeletal modeling in the Evaluation of the effects of rehabilitation in Parkinson's disease."

Relatore: Prof. Zimi Sawacha

Laureanda: Gloria Moro

Correlatore: Dott. Marco Romanato

ANNO ACCADEMICO 2022-2023

Data di laurea: 18 ottobre 2023

Abstract

The aim of this thesis is to perform a comparison between an innovative exoskeleton based robotic therapy (Eksobionics) and other conventional therapies on Parkisnon's disease subjects. To this end an innovative approach to assess the impact of the treatments is proposed which involves in terms of neuro-muscle-skeletal (NMS) models combined with surface electromyography (sEMG) (i.e. EMG-driven musculoskeletal models).

The advantage of this methodology is the possibility to estimate internal variables such as muscle forces in dynamic conditions (i.e. gait) and to base subjects assessment on these parameters. In the current work, these internal variables are used to compare the neuromuscular profile of people with Parkinson's disease before and after a rehabilitation intervention with a wearable robotic device (Ekso). In particular a sample of Parkinsonian subjects were acquired at Villa Margherita Fresco Parkinson Foundation (Vicenza) in collaboration with BiomovLab (University of Padova) within the research project "Quantitative assessment of training effects using a wearable exoskeleton in Parkinson's disease patients".

To realize this target, data from several gait cycles acquired simultaneously through a stereophotogrammetric system, force plates and surface electromyographic devices must be processed. The data pre-processing has a predefined pipeline that includes several steps: it is necessary to obtain data in compatible formats with OpenSim via a Matlab toolbox (MOtoNMS); then, through Opensim scaling, muscle analysis, inverse kinematics and inverse dynamics are carried on. Finally, in CEINMS the model associated with the subject must be calibrated, and then muscle forces and activations through Matlab are computed.

The final step will be to compare the pre-treatment and post-treatment data. In addition, data from people with Parkinson's will be compared with data from a population of normal subjects with the same age and body mass index to evaluate the overall effect of the therapy on restoring a more functional gait pattern.

Summary

Figure Index

Chapter 3

Chapter 4

Chapter 5

Chapter 8: Figure Appendix

x

Introduction:

Neuromusculoskeletal (NMS) modeling guided by electromyography (EMG) allows the mechanical function of multiple muscle-tendon units controlled by the nervous system to be simulated during the generation of complex movements. This can be helpful to identify the biomechanical aspects that lead to gait problems like those described in Parkinson's disease (PD) during a clinical evaluation.

The structures involved in the pathology are in the basal ganglia of the brain, which are responsible for the movement's execution. The disease manifests when degeneration of dopaminergic neurons occurs in the pars compacta of the substantia nigra of the midbrain.

The present thesis proposes the adoption of an EMG-based modeling pipeline to assess the effect of an exoskeleton-based therapy on the gait of a sample of Parkinson's disease subjects. The choice of a musculoskeletal modelling approach finds its bassis in the possibility to assess those muscle forces that would produce muscle activity and hence generate movements.

A sample of subjects were acquired at Villa Margherita Fresco Parkinson Foundation within the research project "Quantitative assessment of training effects using a wearable exoskeleton in Parkinson's disease patients".[1]

Subjects were included according to inclusion criteria such as absence of neurological pathology and of orthopedic pathologies. Each subject underwent a gait analysis including stereophotogrammetry assessment based on the IORGAIT protocol [2], force plate and surface electromyography. Raw EMG data were acquired considering these muscles bilaterally: biceps femoris, rectus femoris, gastrocnemius and tibialis anterior. This signal was recorded through a bilateral 8-channel EMG system called *Cometa Waveplus* that has a frequency of 1000 Hz. The s-EMG electrodes were placed following the guidelines of minimum crosstalk area to maximize the selective activity measured for the muscle.

For data processing, three trials of the right foot and three trials of the left foot were analyzed when the foot landed naturally on the force platforms. MOtoNMS was used to transform the motion data in a format compatible with Opensim software and to normalize the EMG. The following steps were performed in Opensim, including: linearly scale the geometry of each subject and applying an : optimization related to muscle analysis, inverse kinematics (IK) and inverse dynamics (ID), which were used to compute joint angles and moments and muscle-tendon moments and moment arms during the recorded trials, muscle forces estimation that better predict muscle activations, joint torques and muscle forces. All estimates were normalized with respect to the gait cycle and averaged over six walking trials.

CEINMS pipeline was used to compute muscle forces and activations for all the muscle groups involved in the movement of lower limb's joints.

For each subject, all dynamic tests were used for both calibration and execution. Calibration is required to identify subject-specific parameters that vary nonlinearly between anthropometric characteristics and force-generating capacity such as EMG-activation nonlinearity factor, optimal muscle fiber length, tendon slack length, and maximum isometric muscle force. CEINMS is used to predict knee and ankle moments, muscle forces, and activations from a hybrid EMG-based model capable of combining dynamics with static optimization procedure that adjusts experimental EMG excitations to minimize the instantaneous EMG predicted by joint moment estimates.

The thesis is organized in the following chapters:

1. Parkinson's Disease
2. Gait Analysis
3. Neuromusculoskeletal Model
4. Materials and Methods
5. Results
6. Discussion
7. Conclusions
8. Appendix

Chapter 1: Parkinson Disease

1.1   The Pathology:

Parkinson's disease is a progressively evolving neuro-degenerative pathological condition. More specifically, it is an extrapyramidal syndrome characterized by a dopamine deficiency that causes a range of motor and nonmotor symptoms including rigidity, bradykinesia, tremor, and as the disease progresses, postural problems such as instability and gait disturbances may also occur.

The structures involved in the disease are in the *basal ganglia* of the brain, which are responsible for the execution of movements. The disease occurs when degeneration of dopaminergic neurons occurs in the *pars compacta* of the *substantia nigra* of the midbrain.

This disease has multifactorial origins, and the possible etiological factors may be:

- *Genetic:* some genes such as alpha_synuclein, Parkin, DJ-1 and glucocerebrosidase GBA are some of the genetic mutations associated with the disease.
- *Brain Injuries.*
- *Infections.*
- *Neurotoxins*

From the motor point of view, gait disturbances are the most distinguishing features of this neurodegenerative disorder; in fact, all patients show abnormal increase in cadence, stance, and double support phases have been interpreted as a compensation in the reduction of stride length and range of motion of the lower joints [1]. The evaluation of PD-induced motor dysfunction is based on qualitative assessment. Since gait involves both the central nervous system (CNS) and the peripheral nervous system (PNS), rehabilitation must be able to restore both the mechanics but also the neurophysiological patterns of gait, which is why research has been implemented that aims at lower limb strengthening through an exoskeleton whose goal is to allow functional training in a realistic walking environment. Compared with grounding devices, in fact, the patient is more involved in therapy.

The main motor symptoms of Parkinson's disease are:

- <u>*Resting tremor*</u> which is perceived as oscillation with an average of five to six movements per second of the hands and feet.
- <u>*Internal tremor*</u>: is felt only by the patient but is not visible.

- *Rigidity:* muscle tone increases involuntarily. It may be the first symptom of the disease and often begins on one side of the body, manifesting in the limbs, neck or trunk.
- *Slowness of movement* is characterized by two different symptoms: *bradykinesia* i.e., a slowdown in the execution of movements and gestures, and *akinesia* which makes even the simplest movements very slow interfering with most daily activities. Symptoms related to bradykinesia are:
    - *Myographia*: change in handwriting, which becomes smaller.
    - *Sialorrhea*: increased amount of saliva, due to a slowing of the muscles involved in swallowing.
    - *Hypomimia*: reduced facial expression.
- *Balance disorder* appears later, and it involves the axis of the body; it is due to a reduction in righting reflexes, so the subject is unable to spontaneously correct any imbalances.
- *Freezing of gait (FOG):* represents one of the most common causes of falling in Parkinson's subjects; it interferes with activities of daily living and significantly impairs quality of life. It is defined as the unsuccessful attempt to initiate or continue movement without apparent cause. It is a condition in which the feet seem "glued" to the floor and can continue for several minutes and is often resistant to therapy.
- *Festination* is a phenomenon that generally occurs in the advanced stages of the disease, characterized by a tendency to chase one's center of gravity through an accelerated gait that appears in small steps. Together with the phenomenon of freezing, festination represents a little-known gait disorder that nevertheless causes frequent falls and disability in parkinsonian patients.

In addition to motor disturbances, Parkinson's also manifests with non-motor symptoms such as sensory disturbances (pain, olfactory and visual disturbances), autonomic (orthostatic hypotension, supine hypertension, urinary symptoms, sexual function disturbances), behavioral (impulse control disorders such as pathological gambling, compulsive shopping, hypersexuality and punding), cognitive, sleep, anxiety, and depression [2]. Other symptoms of this neuronal degeneration may also present with non-motor phenomena, which may begin many years before the onset of motor symptoms. They are most often evident in the early stages of the disease and most frequently in the more advanced stages. Non-motor symptoms may include sleep, cognitive, olfactory, and vegetative disorders.

1.2 Inclusion and exclusion criteria

Parkinson's disease patients present a hypokinetic gait with increased cadence, stance, and double stance phases that compensate for reduced stride length and speed. The combination of gait analysis and musculoskeletal modeling provides more accurate monitoring of disease progression. A neuromusculoskeletal model is created for each subject guided by signals from the individual's surface electromyography (s-EMG) and monitoring its biomechanics. In this manner, neuromuscular functions can be linked in vivo providing new markers to assess patients' motor deficits. Comprehensive gait and electromyographic analysis will be combined in NMSM to determine changes at both central and peripheral nervous system levels. To improve therapeutic outcomes, an exoskeleton is used.

This study is recruiting patients from January 2021, and an approval has been obtained from the Clinical Trials Ethics Committee (CESC) of the province of Vicenza [1]. Subjects recruited for this study must necessarily have certain inclusion requirements including:

- Age between 20 and 90 years.
- Patient with bilateral rigid-kinetic PD.
- Hoehn-Yahr between 3 and 4.
- At least 4-year history of the disease.
- Stable response to drug therapy with no changes performed in the 3 months prior to the study.
- Presence of postural instability and freezing of gait unresponsive to parkinsonian therapy.
- Mini mental status assessment greater than 24/30

All patients must have a clinically established diagnosis according to the Brain Bank diagnostic criteria of the Parkinson's Disease Society of the United Kingdom [1]. This diagnosis will be reviewed by a neurologist specializing in movement disorders. However, there are also exclusion criteria including [4]:

- Systemic diseases.
- Presence of cardiac pacemaker.
- Postural abnormalities or orthopedic comorbidities that do not correspond to active physiotherapy treatment and use of the proposed robotic device.
- Presence of deep brain stimulation.

- Obsessive compulsive disorder.

- Presence of severe dysautonomia with marked hypotension.

- Severe depression.

- Dementia and psychosis.

- History or active neoplasm.

- Pregnancy.

Figure 1.1 Subject wearing the wearable above-ground exoskeleton during training to robotic gait [1].

1.3 The Exoskeleton EKSO

The device used in this study is a battery-powered wearable exoskeleton that enables people with weakness or paralysis of the lower limbs to walk and participate in rehabilitation. This device has been calibrated for a height range between 158 and 188 cm and with a maximum authorized weight of 100 kg. This device is worn by the patient and is adapted to the patient's anatomy. In the first phase of therapy, the patient learns to manage both the static phase and the different walking modes [4].

This exoskeleton has four battery-powered motors placed on the two hips and two knees and has 15 position sensors. The device also includes two powered hip and knee joints and a semi-rigid ankle joint that is not powered, as well.

In general, Ekso is used with external aids such as crutches or walkers to support a greater balance by providing better interaction with the subject. The exoskeleton has several settings that adjust the level of assistance: unilateral, bilateral, fixed, adaptive, or no assistance.
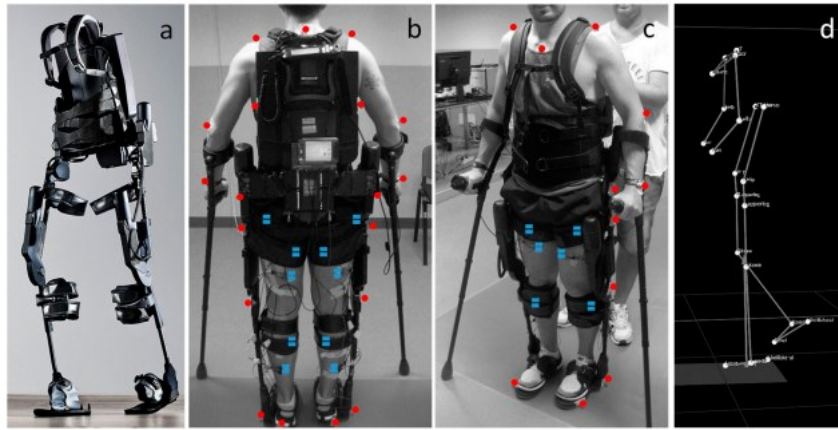
Figure 1.2: (A) Ekso exoskeleton; (B, C) Participants wearing the Ekso. The red dots indicate the positions of the
reflective markers for motion analysis and the blue rectangles indicate the locations of the electrodes,
surface electromyography (EMG). (D) Markers recorded by the motion analysis system (side view at the
center of the motion analysis laboratory pathway)[5]

Fixed assistance is used in Parkinson's rehabilitation to ensure constant motor power independent of the patient's ability. The Ekso also consists of three different control modes that vary according to the subject's abilities [5]:

1. *First step*: This modality is used during the first training session to formalize with the device. A physical therapist controls the beginning of each step by pushing a button.

2. *Active step*: the user controls the beginning of each step with an interface placed on the crutches or on the walker that communicates with the device.

3. *Pro step*: The user controls the beginning of the next step by moving his hips forward and laterally. When the device recognizes that the user is in the correct position allows the step of the contralateral leg.

With the exoskeleton, gait events and velocities can be detected, and based on foot position and velocity, gait cycle events including heel strike (HS), initial take-off (TO) can be detected. In addition, individual muscle activations can be detected, and muscle synergies can be analyzed.

Chapter 2. Gait Analysis

Human gait analysis is very important from both a sports and rehabilitation perspective. Thanks to science and medicine, one has the possibility of recreating neuro-muscular-skeletal (NMS) models guided by muscle activation signals, which allow one to obtain information about the execution of movements of each subject, but more importantly, one has the possibility of deriving information inherent to the onset and development of neurodegenerative diseases such as Parkinson's disease, Alzheimer's disease, and Multiple Sclerosis. Through the analysis of kinematics and dynamics, the construction of NMS models allows insight from a neurological perspective that can identify the control differences that are generated between healthy and pathological subjects. [6]

To best conduct these analyses, appropriate stereophotogrammetry systems and tools necessary for the acquisition of muscle activation signals such as s-EMGs, or sensors capable of detecting surface electromyography, are needed. Markers placed according to an established protocol, which are recorded through camera systems in the laboratory, will also be important.

The study of motion is based on the orientation of anatomical segments of the human body using several mathematical models of biological tissues. We can analyze different types of data:

- Kinematic data, which are used to measure position, velocity and acceleration in space through motion capture systems.
- Dynamic data, whose goal is to identify muscle forces and moments acting during human movement. These data are captured using sensors and force platforms.
- Electromyographic data, which allow the acquisition of electrical potentials of muscle contractions with electrodes.

Identification of the mentioned parameters is obtained in a motion analysis laboratory through appropriate instrumentation.

2.1 Instrumentation

The body kinematics is described using stereophotogrammetry, which allows a reconstruction of bone morphology and anatomical segments of interest. In this project we use a Vicon System with a sampling frequency between 100 Hz and 300 Hz. This technique is based on the use of external position markers, which are applied at anatomical landmarks points: points that allow intra- and inter-subject repeatability of the acquisition.
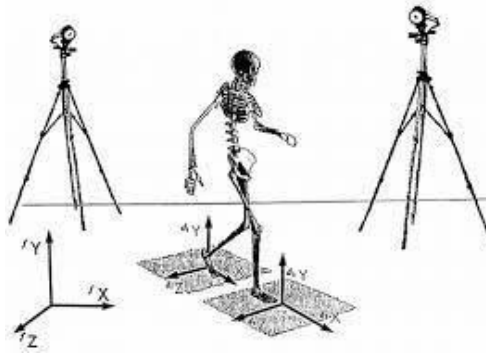
Figure 2.1 Stereophotogrammetry System

Kinematic analysis is based on the rigid body assumption where the soft tissue component is negligible. The points identifying the body segments move while keeping their mutual distances unchanged compared to a global reference system. The rigid body hypothesis allows approximations to be made along the bone segments sometimes leading to errors that are not always negligible. Therefore, a local reference system is introduced to refine the orientation and position of the bone segments in both time and space through an orientation matrix and a position vector [7].
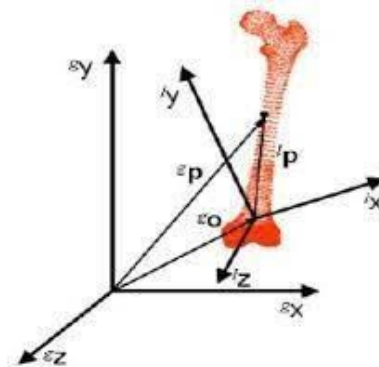
Figure 2.2 Local Reference System

The position of a portion of a bone segment with respect to the global reference system is defined by a position vector $^g_l P = ^g R_l \, ^l P + ^g O_l$ where:

- $^g P = [x_g, y_g, z_g]$ is the position vector of point P in relation with the global tern.
- $^l P = [x_l, y_l, z]$ is the position vector of point P to the local tern
- $^g O_l = [^g O_{lx}, ^g O_{ly}, ^g O_{lz}]$ is the origin of the position of the local tern in relation to the global one
- $^g R_l$ represents the matrix of direct cosines whose goal is to bring the local reference system into the global system and is represented as in the figure below. In analytic geometry, this matrix contains the cosines of the convex angles formed by the line along which the position vector lies and the Cartesian axes.

9

$$^gR_l = \begin{bmatrix} \cos\theta_{x_g x_l} & \cos\theta_{x_g y_l} & \cos\theta_{x_g z_l} \\ \cos\theta_{y_g x_l} & \cos\theta_{y_g y_l} & \cos\theta_{y_g z_l} \\ \cos\theta_{z_g x_l} & \cos\theta_{z_g y_l} & \cos\theta_{z_g z_l} \end{bmatrix}$$

In order to describe the trajectory of an anatomical reference point, we can consider a reference point of a global system, the [x,y,z] coordinates of the local system and the 9 components of transformation matrix and in this way we can obtain the possible combination of local system respect the global one. We can obtain 6 degrees of freedom of movement of the bone segment. The description of the movement of two adjacent bone segments is done as a relative motion of the proximal local system with respect to the distal local system. In order to describe the angular displacement unambiguously, we can use Euler Angles. These angles are characterized by a sequence of rotations about two axes of the selected reference system respecting the Grood & Suntay convention:

- Rotation about the Z axis of the distal reference system (γ) coincident with the proximal Z axis
- Rotation about the X axis of the distal reference system (α) after the first rotation.
- Rotation around the Y axis of the distal reference system (β) after the second rotation.
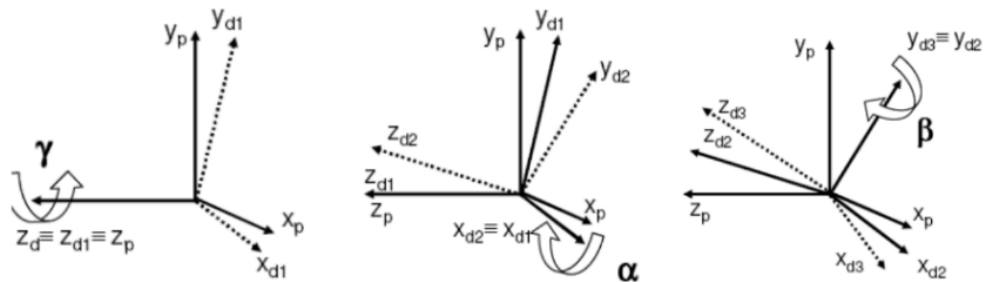
Figure 2.3 Eulerian Angles

Through stereoscopic viewing with two cameras, it is then possible to reconstruct the three-dimensional positions of the points of interest through the acquisition of two-dimensional images. Image processing begins with marker detection, where, with thresholding, the pixels identifying the markers can be distinguished and the center of gravity is calculated.

To calibrate the Stereophotogrammetry System, a geometrical parameter determination is necessary to reconstruct the markers three-dimensionally. Two types of parameters can be distinguished:

- *Internal*, which are characterized by a camera system that can identify the coordinates of the main points (N1 and N2), focal length and distortion coefficients.

10

- *External*, which differs as the position of the camera's changes. They can change coordinates between two different reference systems.

The data can be derived through a mathematical model called the Pin-Hole model, which is able to transform the 2D coordinates of the image recorded by the camera into 3D coordinates with respect to the global reference system.
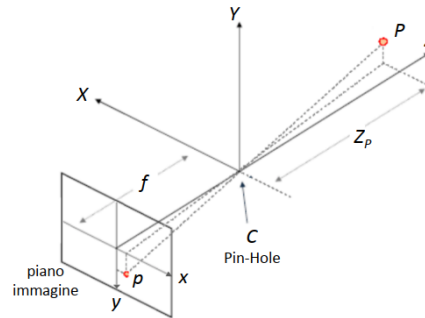
Figure 2.4 Pin Hole Model

From the image it can be noticed that

- (X,Y,Z) is the reference system with origin on the camera represented as infinitesimal point C defined as PinHole point;
- (x,y) is the image plane reference system originating along Z;
- P (X_p, Y_p, Z_p) is a point in the scene and p (x_p, y_p) represents its projection in the image plane;
- f is the focal distance between C and the image plane.

The calibration of the Stereophotogrammetric System is based on the perspective transformation of the 3D system of the laboratory to the 2D space of the camera located in the center of perspective and the perspective transformation of the 2D system of the camera to the 2D reference system of the image plane. There is also a transformation from the 2-dimensional coordinate system from the image plane of the camera to the 2-dimensional system of the sensor. However, corrections of distortions are required through static and dynamic calibration operations. In the former case the acquisition of a calibration object of known size and shape is saved in a calibration matrix, while in the latter case the acquisition is characterized by a pair of markers placed at a known distance within which the movements of a wand are reported.

2.2 Acquisition Errors

The stereophotogrammetric System is affected by instrumental errors and errors related to the presence of skin tissue since soft tissue causes several limitations in correct motion reconstruction. In the former case, one can identify:

- *Casual Errors* including flickering due to the digitization process, quantization errors related to the analog-to-digital conversion required to process the image, electronic noise.

- *Systematic Errors:* the measurement model assumed might cause poor estimation of model parameters, including inappropriate marker volume and calibration procedure.

For errors related to the presence of skin tissue, one can detect misapplication of the markers at anatomical landmarks such as incorrect definition of joint centers or failure to prepare the skin during marker placement.

Soft-tissue artifacts can also be detected, i.e., skin, muscle, and adipose tissue are all soft tissues, so involuntary movements may occur between these three tissues when markers are placed.

However, to compensate for the errors, there are various techniques for filtering and optimizing the calibration procedure or multiple calibration.

2.3 Acquisition Protocols

The protocols have precise characteristics concerning the placement of marker sets and the definition of reference systems. The choice of gait analysis protocol is based on the type of subject that requires monitoring and the type of instrumentation in the laboratory. The protocols ensure accuracy and repetition of human motion analysis through a standard acquisition scheme and appropriate processing of kinematic and dynamic data.

The motion of an anatomical segment of interest (TF) is described by the instantaneous positions of at least three unaligned technical markers associated with a technical cluster (CTF) relative to the laboratory reference system. In this way, the position and orientation of the technical markers relative to bone can be identified; a proper positioning of the markers ensures an accurate detection from the camera system and minimization of movement relative to bone. Technical reference systems and anatomical landmarks are both generated during the task on the anatomical segment of interest; in fact, a morphological technical reference system (MTF) can be defined based on bone morphology and the requirements of the motor task [7].
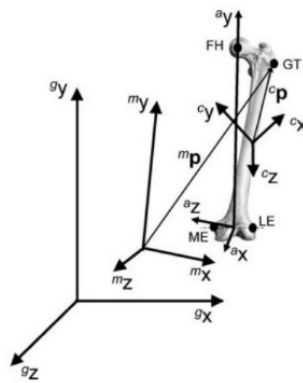
Figure 2.5 Morphological Reference system

To report all the instantaneous and morphological information of the technical structure (TF) of interest, transformations are required. For example, position vectors defined in the MTF system are converted to position vectors with respect to the coordinates of the technical cluster by a process of Anatomic Calibration. Anatomical landmarks must be easily identifiable to ensure intra- and inter-subject repeatability. Markers can be placed along major planes (forntal, transverse, sagittal) or at locations of morphological interest.

To reduce the number of markers needed to construct a technical reference system, virtual markers can be used that are defined by geometric relationships to technical markers. If the joints are spherically hinged, the virtual marker is the spherical center, which means that the virtual marker is shared by two adjacent segments and can be used in both segments for CTF construction [8]
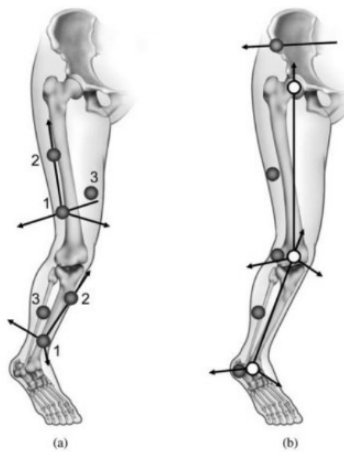
Figure 2.6 Markers Representation

The protocols related to gait analysis must meet some basic requirements:
- The experimental equipment must have a small footprint.
- The acquisitions must be very accurate.
- Markers must be easily applied including in the case of disabling conditions.

13

- Time dedicated to patient preparation including acquisition of motor tasks and data collection   must be reduced.
- Intra- and inter-subject and operator variability of results must be minimized.

There are three popular protocols in science that are mainly functional to describe the movement of the lower limbs:
- Davis Protocol
- CAST Protocol
- IOR-Gait Protocol

Davis's Protocol:

Davis's protocol had its first formulation in the 80's [8] as a standard procedure in cases of Cerebral Palsy of Childhood. Data can be acquired at different stages:

1. *Videotaping prior to examination*. Archiving a patient's gait analysis is recommended for several reasons, including the usage of support devices like walkers that may not be permitted during the test due to marker obstruction or the ability to closely examine anomalous foot dynamics with a camcorder record.
2. *Physical evaluation and measurement*. The subject's weight, height, and leg lengths are all anthropometric measurements. Additionally, measurements are made of the knee and ankle withs, the distance between the right and left anterior superior iliac spines (ASIS), and the vertical distance, measured in the sagittal plane of a subject lying on their back, between the ASIS and the greater trochanter.
3. *Marker placement*
4. *Statistic offset measurement*. The location of each lower extremity joint center in relation to the associated segmentally fixed coordinate system is determined using marker data while the subject is standing within the measuring volume of the motion camera system.
5. *Motion Test.* The motion test is applied to the subject for a minimum of three barefoot steps. The displacements of the segments, as well as their velocities, accelerations, and joint angles, are computed using the markers' 3D coordinates.
6. *Electromyographic (EMG) assessment*. Electromyographic signals from a group of muscles are recorded by electrodes during the step cycle and manually recognized by examining the videos.
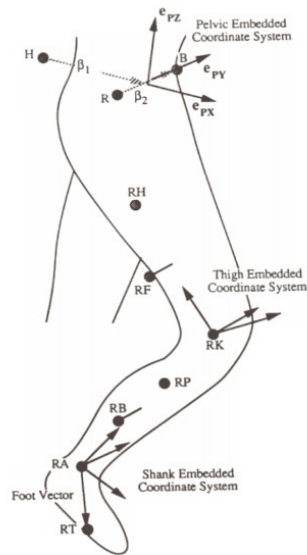
Figure 2.7 Davis Protocol

CAST Protocol

The CAST (Calibrated Anatomical System Technique) protocol ensures that the coordinates of the anatomical landmarks are obtained with respect to the technical reference system.

Combining the coordinates of a marker placed on the anatomical landmark and the markers forming the cluster of bone segments, anatomical calibration occurs [9].

Each bone section must undergo the same process, which must be visible to at least two cameras. Before the motor task starts, these markings are removed. Because of the usage of elastic clusters, there is a significant reduction in the markers' mobility, which minimizes soft tissue artifacts.

The CAST procedure tries to define the position and orientation of bone segments experimentally.
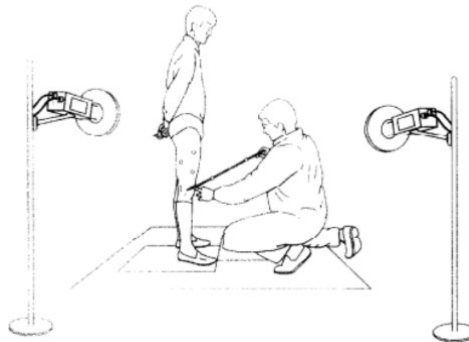
Figure 2.8 CAST protocol: Marker application

With the anatomical calibration, the anatomical reference systems for pelvis, thigh, leg, and foot can be identified.

Pelvi Reference System:

The midpoint between the Anterior Superior Iliac Spine (RASIS, LASIS) represents the origin of the reference system, O_p. The z_p axis is oriented along the axis through the anterior superior iliac spines in a positive direction, from left to right. The x_p axis is in the quasi-transverse plane defined by the anterior superior iliac spines and the midpoint between the Posterior Superior Iliac Spines (RPSIS, LPSIS) with positive anterior direction. Finally, the y_p axis is orthogonal to the plane generated by the xz axes and has a proximal positive direction.

Tight Reference System:

The origin O_t is in the middle between the epicondyles (LE, ME). The Femoral Head (FH) and the system's origin are connected by the y_t axis, which has a proximal positive direction. The z_t axis has a positive left-to-right direction and is situated on the quasi-frontal plane created by the epicondyles. The x_t axis has a positive anterior direction and is orthogonal to the plane created by the yz axes.

Shank Reference System:

At the intersection of the Malleoli (MM, LM), the system's O_s origin is situated. The malleoli and the Head of the Fibula (HF) form a quasi-frontal plane, while the malleoli's midpoint and the Tibial Tuberosity (TT) form a quasi-sagittal plane, which intersect to form the y-axis. On the other hand, the zs axis has a positive position from left to right and is located on the quasi-frontal plane. The x_s axis has a positive anterior direction and is orthogonal to the xy planes.

Foot Reference System:

The origin of the O_f system is located on the calcaneus (CA). The y_f axis with a positive proximal direction is defined by the intersection of the plane created by the First and Fifth Metatarsals (IMH, VMH) and the quasi-sagittal plane defined by the calcaneus and the Second Metatarsal Head (IIT). The z_f axis has a positive left-to-right orientation and is located on the quasi-transverse plane. Finally, the x_f axis has a positive dorsal direction and is orthogonal to the yz plane.

IOR-GAIT Protocol

The purpose of this protocol is to develop a new method for analyzing the kinematics of the pelvis and lower limbs that can describe 3D segment and joint motion on an anatomic basis and report these quantities according to current practices and guidelines. By the aid of a spherical marker with a 10-mm diameter, the anatomical landmarks are tracked in space and physiological reference points used in this technique are generally in accordance with the global standards. The virtual joint between the laboratory global frame as the "proximal" and the pelvis as the "distal" segments is used to determine the tilt, rotation, and obliquity of the pelvis using standard coordinate systems for each joint [2].

This approach satisfies the trade-off between minimizing the effects of experimental mistakes and identifying subject-specific anatomical references in the simplest and most reproducible approach possible. With a smaller marker set than the other protocols, applying markers and calibrating anatomical landmarks can be done so more quickly.

Marker trajectories and ground reaction force are collected with an eight-camera motion capture system and by two force plates.

Several participants were examined as part of our Parkinson's disease study using this modified protocol, which added the C7 marker and the L5 marker to assess the spinal cord length in addition to the markers that will be detailed.

The marker set used during this study is in line with that of the Rizzoli Orthopedic Institute in Bologna and includes the following marker arrangement:
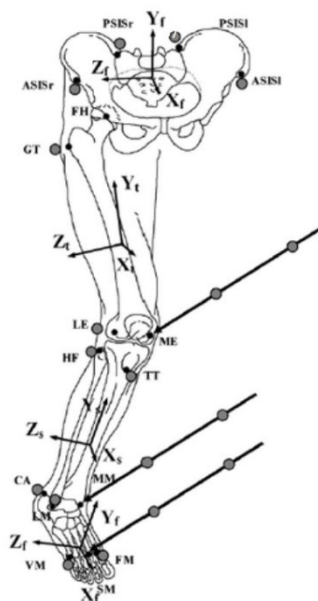
Figure 2.10 IOR-Gait Protocol

17

The anatomical landmarks are represented with small black circles and the reflective markers with gray circles, including a pointer for the three calibrations of each side and the orientation of pelvis (p), thigh (t), shank (s) and foot (f) segments.

2.4 Force Platform:

Force platforms consist of a rectangular base that can measure a ground reaction force at the instant that the foot touches the ground. In this thesis work we use an AMTI force platform with sampling frequency of 960 Hz. Through sensors, the force that the foot exchanges with the ground below is measured:

- *Strain Gauges:* the circuit consists of four strain gauges disposed in a Wheatstone bridge: two strain gauges are kept compressed and two are kept stretched, so the force can be measured in each direction. The elastic element inside each strain gauge, in case of deformation by a force, causes the electrical resistance to change, producing an output voltage. They maintain a good frequency response.
- *Piezoelectric sensor*: these crystals can produce an electrical charge when subjected to mechanical stress. The charge will be proportional to the strain, and due to amplifiers, it is possible to measure very small forces. Over time, the crystals tend to deteriorate by losing their correct orientation, and in a static case the centers of pressure are not calculated correctly.

From the force platforms, measurements can be obtained using a reference system defined on the platform that can measure the components along the axes (x, y, z) of the resultant forces, center of pressure (COP) and moments.

- COP: 6 Hz;
- Forces:13 Hz
- Moments 13 Hz
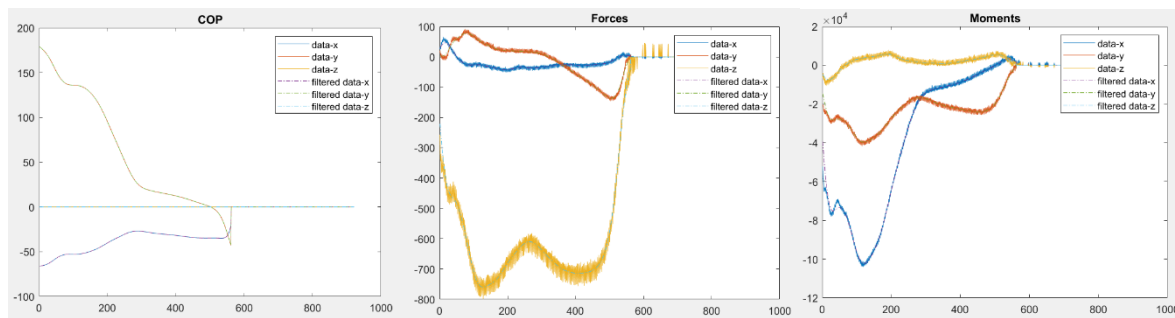
Figure 2.10 In these 3 figures there are represented COP, Forces and Moment respectively of an acquisition of a subject S3 in T0.

2.5 Electromyography

Electromyography is a diagnostic technique from the field of neurophysiology that allows analysis, using needles and electrodes, of muscle activity at rest and during voluntary activation. Its focus is to measure the electrical potential developed by muscle contraction generated during a motor task with electrodes. During a movement, nerve impulses are generated that generate an action potential. In surface electromyography, the signal can be:

- *Monopolar*: when the signal is detected between an electrode located above the muscle and one outside the electrically active (neutral) zone.
- *Bipolar*: when a differential amplifier is used to detect signals taken between two points on the same muscle, usually aligned in the direction of the fibers.

For the same motor task, the amplitude and frequency content of the measured signal change depending on the positioning of the electrode relative to the UM fibers.

The Motor Unit (UM) is the set of motor neurons and muscle fibers that it innervates. The motor neuron is a nerve cell on which all information from the nervous system converges and which sends the signal up to the muscle through its axon forming the peripheral motor nerve. The electrical impulse propagated by the alpha motor neuron, activated by the central nervous system or by a reflex, reaches the neuromuscular junction and causes the release of acetylcholine into the space between the nerve end zone and the muscle fiber membrane.

Acetylcholine excites the muscle fiber, which depolarizes from the junction and the depolarization propagates in the direction of the tendons. The alpha motor neuron simultaneously activates all the fibers of the motor unit to which it afferents. The depolarization impulse propagates in both directions toward the tendons.

19

Initially, one area of the axon generates the opening of sodium (Na+) channels, and the entry of these charged ions generates an action potential that depolarizes the region and the adjacent region. At this point the potential transfers to the new depolarized region ensuring the opening of potassium (K+) channels, thus K+ ions exit the axon and repolarize the membrane returning to an equilibrium state.

The motor unit action potential (MUAP) provides the representation of electrical activity over time. We can distinguish different electrodes that allow the variation of the electrical potential. We can have:

- *Insertion electrodes*: through needles it is possible to study the muscle activity of deeper muscles.
- *Surface electrodes*: mostly Ag/Ag-Cl electrodes are used because they are stable, inexpensive and low noise. Contractions of muscle activations are acquired noninvasively.

The electrodes are placed in a bipolar configuration where potential is measured between two electrodes placed on the same muscle at no more than a quarter of the muscle from a mass reference. the skin should be hairless and adequately clean and lightly abraded to ensure adhesion and reduce skin impedance.
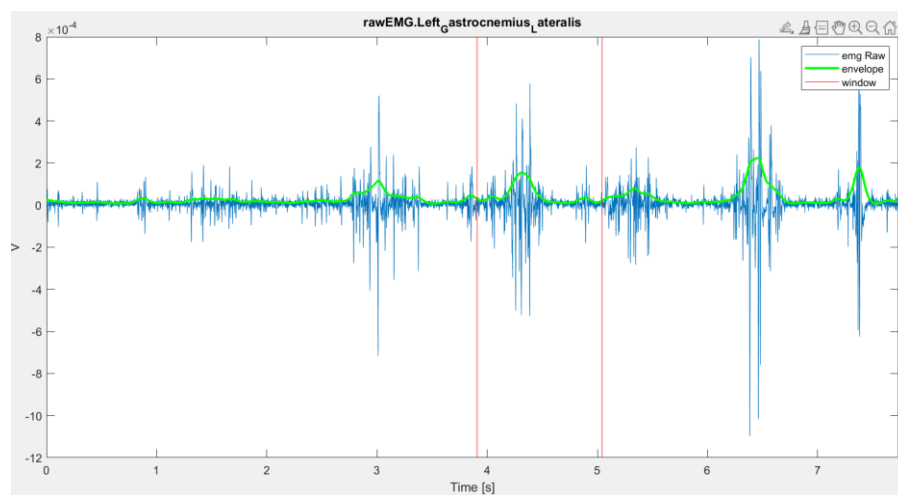
Figure 2.11 Raw EMG of a subject S3 at T0 time
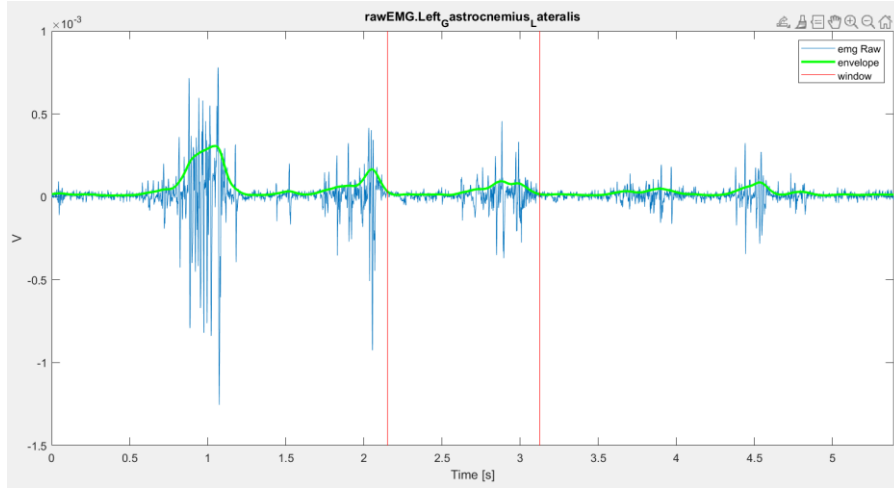
2.12 Raw EMGof a subject S3 at T1 time

However, the acquisition of surface electromyography (s-EMG) signals has some limitations including Cross-Talk that happens when some electrical signals not of interest are recorded [6]. In addition, muscle activation can cause electrode movement causing an overlap of the acquired signal.

The electromyographic signal is time-varying because it is a nonstationary signal. Processing of the raw EMG data yields crucial objective parameters.

Indices which are frequently employed in the clinic for the identification and monitoring of various disorders quantify and depict changes in the EMG signal. Important details about the signal's shape, amplitude (μV), temporal instants (seconds), and distinctive frequencies can be discovered by appropriate processing:

- *Envelope:* rectification of the signal is performed and then a Butterworth low-pass filter with a cutoff frequency of 5-9 Hz is applied.
- *Timing*: characteristic peaks are identified relative to a threshold value and muscle activation, duration of signal activation and deactivation (on-off) are defined.
- *Frequencies*: a relationship can be observed between the location of the muscle fibers and the amplitude of the frequencies, in fact, more fibers are closer to the electrode, more prevalent they are in the signal and compose the high frequencies.
- *Root Mean Square (RMS):* the following relationship applies, which is indicative of the strength of the acquired signal.

$$RMS(k) = \sqrt{\frac{1}{N}\sum_{i=0}^{i=N} X(k-i)^2}$$

(2.1)

21

The following parameters can be calculated:

- *Mean Frequency (MNF):* barycentric frequency of the power spectrum
- *Mean Frequency (MDF):* allows the signal to be divided into two equal parts
- *Power Spectrum*: physiological information of muscle contractions can be determined using the Fourier Transform
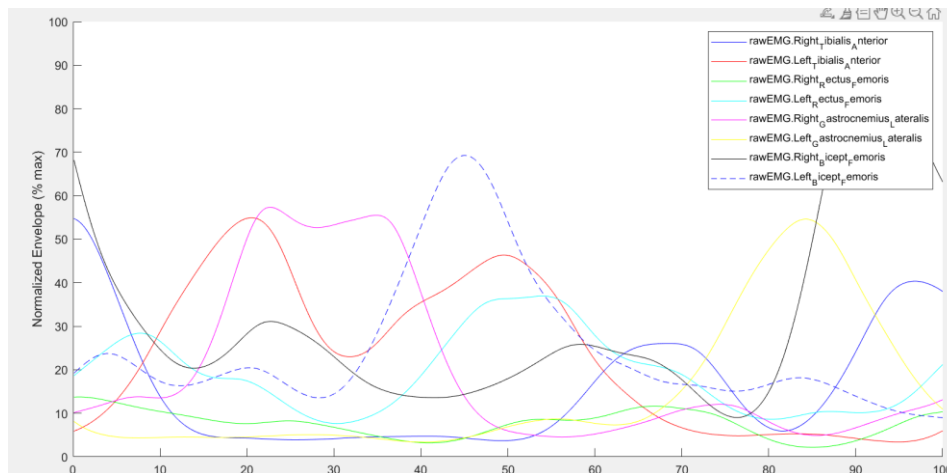
Figure 2.13 Raw EMG envelope

The acquisition of electromyographic signals represents a valuable tool in the study of many diseases that affect the motor abilities of those affected.

Neurodegenerative disorders like Parkinson's and Alzheimer's can be diagnosed by analyzing the muscle activity. Furthermore, the preservation of transient EMG signals enables follow-up in rehabilitation, for instance after a stroke or a sports injury. The assessment of muscle forces involved in the motions of healthy and diseased persons is made possible using electromyography in conjunction with suitable anatomical and muscular models.

The lower limb has been the area of focus for the investigation and modeling of muscle activation in this work. a summary of the main muscles that make up the lower limb and their purposes.

2.6 Biomechanics of the lower Limb

The muscle is essential for normal walking. In the case of its paralysis, patients tend to fall to the ground unless the knee is kept well extended. This is taken care of to some extent during flat walking by the force of gravity while all this is not possible in hill walking.

Neurodegenerative disorders like Parkinson's and Alzheimer's can be diagnosed by analyzing the muscle activity. Furthermore, the preservation of transient EMG signals enables follow-up in rehabilitation, for instance after a stroke or a sports injury. The assessment of muscle forces involved in the motions of healthy and diseased persons is made possible using electromyography in conjunction with suitable anatomical and muscular models.

It is fundamental to determine the proper anatomical reference to comprehend how muscles function and to analyze movement correctly. The human body is in an orthostatic where, the center of gravity is where the perpendicular anatomical reference planes meet each other around 3 millimeters in front of the sacral vertebra [10].

- *Sagittal plane:* a vertical plane that runs parallel to the acceleration of gravity and separates the body into two symmetrical, mirror-image halves on the left and right.
- *Trasversal Plane*: Is parallel to the ground.
- *Frontal (Coronal) plane*: This plane, which is perpendicular to both the sagittal plane and the transverse plane and rotates at a right angle to the sagittal plane, separates the body into the front and the back regions.

Hip Muscles
- *Anterior Muscles*: They are essential for thigh flexion. The muscles of the spine and iliac fossa insert on the small trochanter. Muscles are:
  - Iliopsoas: Is the most powerful hip flexor. It is a compound muscle, formed from the great psoas and iliacus muscles, which unite within the pelvic cavity and share the insertion tendon.
  - Great Psoas: Originates from the transverse processes of the last thoracic vertebrae and all lumbar vertebrae and inserts into the small trochanter of the femur and iliac fossa.
  - Iliac: originates from the anterior surface of the iliac fossa, the iliac spines and the lateral aspect of the sacrum.

- *Posterior Muscles*:These Muscles insert into the great trochanter. We find:
    o Great gluteus: It originates from the iliac crest and has insertion on the gluteal tuberosity of the femur.
    o Gluteus medius: originates in the iliac crest and has insertion on the great trochanter.
    o Tensor of fascia lata: originates in the anterior superior iliac spine and inserts into the iliotibial tract. It allows abduction and internal rotation of the thigh.
    o Gluteus minus: It originates from the gluteal aspect of the iliac wing and enters at the level of the great trochanter of the femur.

The great gluteus, with the gluteus medius and with the gluteus minus, allows the extension and rotation of the pelvis allowing a man to maintain an erect position [11].
- *Ventral Muscles*: they are used to maintain body balance with thigh adductors. The natural position of the foot is maintained outward to provide more support. The main muscles are:
    o Long Adductor/Great Adductor/Short Adductor: Originate from the pubis and insert into the rugged line of the femur.
    o Outer Obturated Muscle/Inner Obturator Muscle.
    o Pectineus Muscle: It originates from the pubic tubercle, the anterior aspect of the superior branch of the pubis, the pectine crest and the pubofemoral ligament. It inserts at the pectine line of the femur.
    o Gracilis Muscle: It originates near the pubic symphysis at the anterior aspect of the ischiopubic branch. It inserts on the medial aspect of the tibia

Thigh Muscles
- Anterior Thigh Muscles: They primarily act on the knee joint and except for the sartorius are all extensors. The main ones are:
    o Sartorius: It allows flexion and internal rotation of the knee and flexion and external rotation of the hip and external rotation of the thigh. Originates from the anterior iliac spine and inserts into the tibial tuberosity.
    o Quadriceps Femoris: consists of four muscle vents (Rectus Femoris, Vastus Medialis, Vastus Lateralis, Vastus Intermedius) that unite into a common tendon inserting into the tuberosity of the tibia.

- ▪ Rectus Femoris□ Originates in the anterior and inferior iliac spine and supra-acetabular groove and inserts into the proximal margin of the patella. It allows flexion of the hip.
  - ▪ Vastus Lateralis: Originates in the lateral section of the greater trochanter and inserts into the patella.
  - ▪ Vastus Medialis: The muscle originates from the medial labrum of the linea aspra and together with the other heads forming the Quadriceps Femoris join into a tendon that inserts into the patella and continues as a single ligament inserting into the tibial tuberosity.

- Posterior Thigh Muscles: They act as knee flexors.
  - o Biceps Femoris: the muscle is divided into two heads: the long head that originates from the ischial tuberosity of the thigh and the short head that originates instead from the lateral labrum of the linea aspra of the femur. These converge inferiorly in the terminal tendon that inserts on the head of the fibula. The Biceps allows flexion and outward rotation of the leg on the knee joint, particularly the long head acts as a retro-versus.
  - o Semitenineus: It originates from the ischial tuberosity and inserts into the medial tuberosity of the tibia along with the Sartorius and Gracilis tendon. Its activation allows extension of the thigh relative to the leg, flexion and internal rotation of the leg.
  - o Semimembranosus
  - o Popliteus
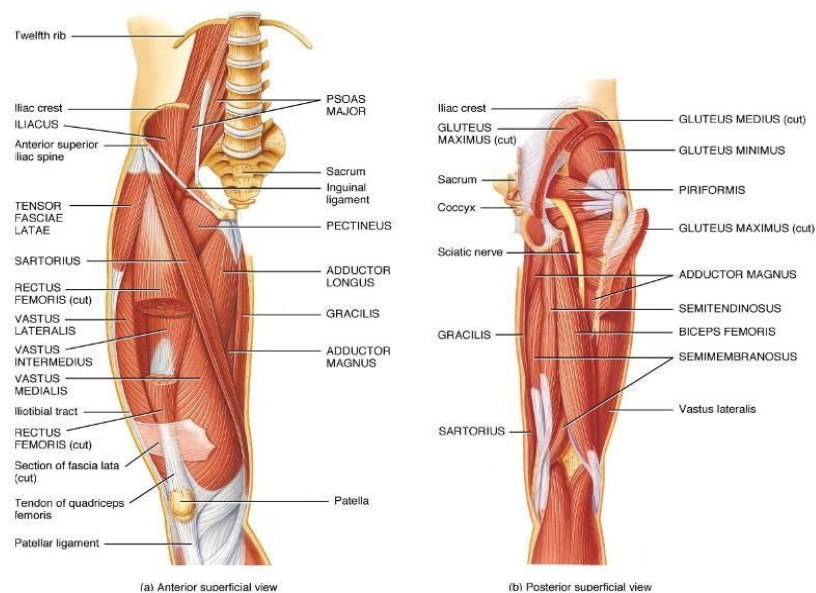
Figure 2.14 Thigh Muscles

Shank Muscles

All muscles originating in the shank have insertion on the foot.

- Anterior Muscles: here are collocated extensor and peroneal muscles. The extensor muscles are responsible for dorsiflexion of the foot; the main ones are:
    o Tibialis Anterior: It originates from the lateral aspect of the tibia, terminates in a tendon that is inserted on the first cuneiform bone and the base of the first metatarsal bone. Its activation allows dorsiflexion and medial rotation of the foot.
    o Long extensor of the fingers/long extensor of the big toe

Peritoneal Muscle: In the lateral region of the leg are the muscles that insert on the bone's metatarsals of the foot. Their main action is to operate plantar flexion of the foot.

    o Peroneal Long: It originates from the head and lateral region of the fibula and contains an oblique tendon that allows the muscle to insert into the tuberosity of the first metatarsal bone of the foot. It is essential for abduction, rotation, and plantar flexion.
    o Peroneal Short: it is essential for abduction, rotation, and plantar flexion with Peroneal Long

- Posterior Shank Muscles: Located in the posterior region of the leg are the flexor muscles responsible for plantar flexibility of the foot. The posterior muscles of the leg are divided into superficial and deep calf muscles.
    o Deep Calf Muscles:
        ▪ Tibialis Posterior
        ▪ The Long Flexor muscles of the big toe and the toes.
    o Superficial Muscles: the group of interest called the triceps sura is responsible for plantar flexion. In fact, it is composed of:
        ▪ Soleus: Originating from the head of the fibula and the popliteal line of the tibia, its tendon along with that of the Gastrocnemius inserts on the posterior tuberosity of the calcaneus as a Achilles tendon.
        ▪ Gastrocnemius: It originates in two regions of the knee joint capsule that identify the two heads: from the medial condyle of the femur originates the medial head while from the lateral condyle of the femur originates the lateral head. The two heads join in a tendon and with the

Soleus muscle tendon, together they insert onto the calcaneal tuberosity. The gastrocnemius muscle is critical during walking as it acts in the flexion.

▪ Plantar Muscle
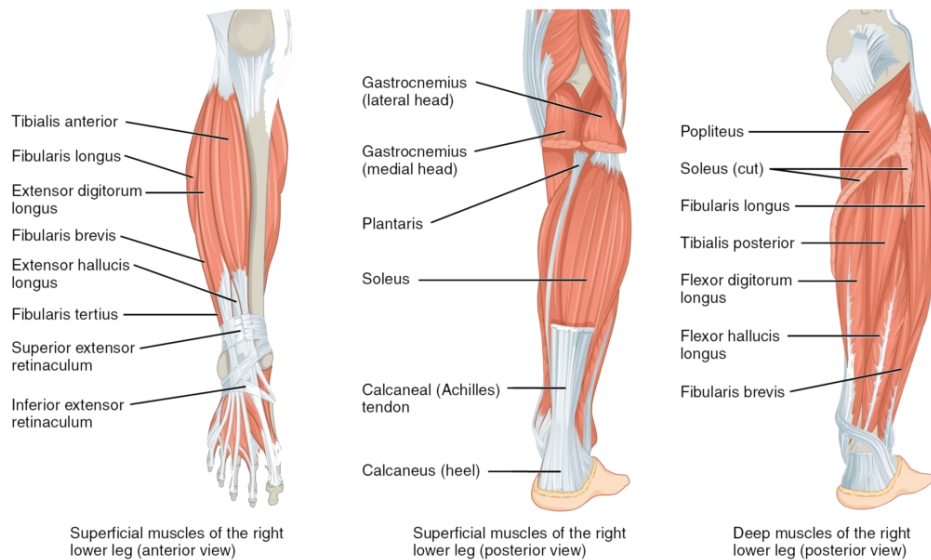
Figure 2.15 Shank and Plantar muscles

The muscles of the lower limb can also be described through body movements: external and internal rotations in the transverse plane, extensions, and flexions in the sagittal plane, and finally abductions and adductions in the frontal plane. A breakdown brief of the muscles by function now follows:

Hip and Thigh muscles:

- *External Rotation*: Great Gluteus (red), Gluteus Medium and Small (orange), Square of the Femur (blue), Internal obturator (yellow), Ileo-psoas (green), Adductors (purple), Piriformis (gray) and Sartorius.

- *Internal Rotation:* Gluteus Medium and Small (red), Great Adductor (yellow), Fascia Lata Tensor (blue)
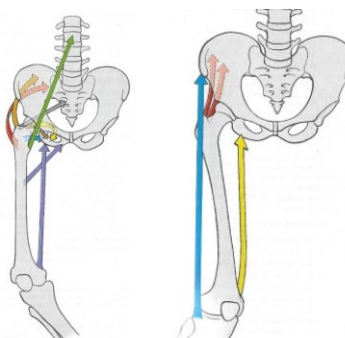
Figure 2.16 Thigh External and Internal Rotation

- *Extension*: Great Gluteus (red), Great Adductor (green), Medium and Small Gluteus (blue), Piriform (brown), Femoral Biceps (Violet), Semimembranosus (Yellow), Semitendinosus (orange)
- *Flexion*: Ileopsoas (red), Pettineus (green), Long and Short Adductor (brown), Fascia Lata Tensor (orange), Rectus Femoris (blue), Sartorius (yellow)
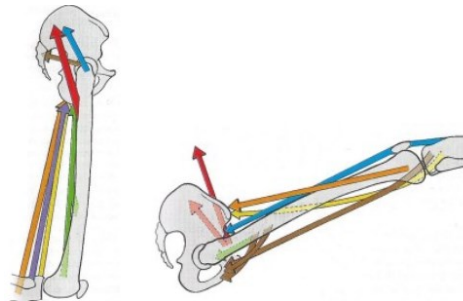
Figure 2.17 Thigh Flexion and Extension

- *Abduction*: Fascia Lata tensor (blue), Medium Gluteus (red), Great Gluteus (yellow), Small Gluteus (orange), Piriform (green), Inner Otturator (brown)
- *Adduction*: Great Adductor (red), Long and Short Adductor (blue), Great Gluteus (yellow), Gracil (orange), Semitendineus (Green)
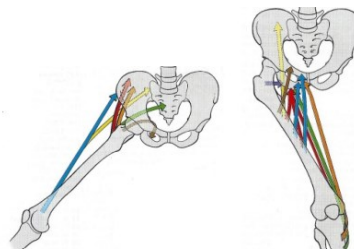
Figure 2.18 Thigh Adduction and Abduction

Shank Muscles:
- *Internal Rotation*: Semitendineus (blue), Gracil (yellow), Sartorius (Orange), Semimembranous (Red), Popliteus (green)
- *External Rotation*: Bicipt Femoralis (red)
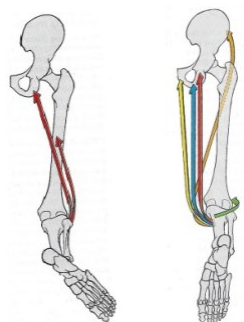
Figure 2.19 Shank External and Internal Rotation

- *Extention*: Rectus Femoralis (red), Vasto Lateralis (blue

28

-   *Flexion:* Semitendineus (blue), Bicipt Femoralis (yellow), Gracil (orange), Sartorius (green), Gastrocnemius (Purple), Semimembanous (red), Popliteo (Brown);
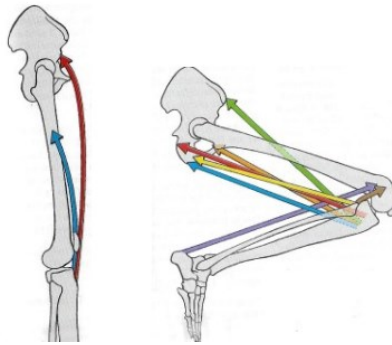
Figure 2.20 Shank Flexion and Extension

Foot Muscles:

-   *Dorsal Flexion*: Long extensor of the toes (blue) and Extensor long extensor of the big toe (yellow), Tibialis Anterior (red)
-   *Plantar Flexion*: Sura triceps (red), Long Peritoneus (blue), Short Peritoneus (yellow), Long Flexor of Hallux (orange), Long Flexor of Fingers (green) and Tibial posterior (brown).

Figure 2.21 Dorsal and Plantar Flexion

The range of muscle movements that become possible by these movements support a wide range of potential motor tasks. A stereophotogrammetry device is used to acquire kinematic data for gait analysis tasks, and surface electromyography can be used for helping the mechanics of movement. Test subjects must take part in a series of trials to examine the physical characteristics of lower limb muscles.

2.7 Gait Cycle

In the stride cycle, the legs repeat a sequence of movements that can move the body forward while maintaining a stable stance. Each sequence consists of a series of interactions between the various leg segments and the total body mass [12].

The two legs switch off during the walk; when one is employed as a stable support, the other one advances. A gait cycle is the name for each distinct sequence for a limb. Each gait cycle is divided into two periods: stance phase and swing phase and always begins and ends with both feet in contact with the ground, so the body weight is distributed equivalently on the two feet. During the second phase which starts when the opposite foot is raised, the weight is supported by one leg. The terminal phase of double stance, which starts with the contralateral leg touching the ground and lasts until the initial leg is raised to swing, is the last phase of the movement. Overall, the support phase occupies 60% of the gait cycle and 40% is the swing phase. The times for the loading phase, on the other hand, are divided as follows:

- 10% for double initial support

- 40% for single leg support

- 10% for the final double support.
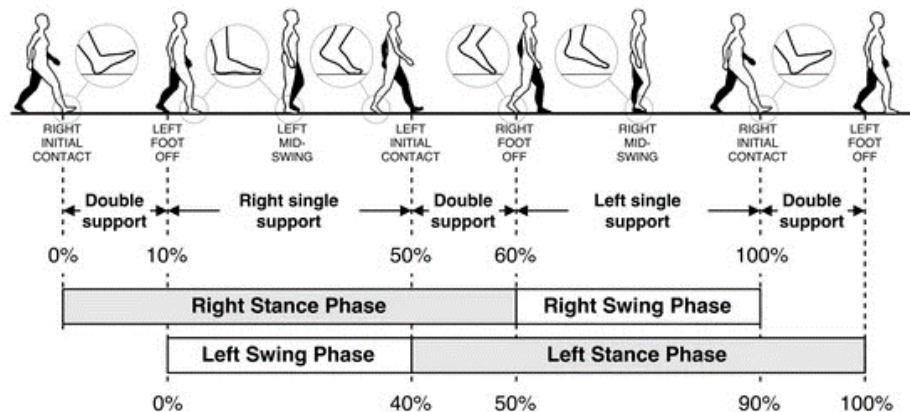
Figure 2.22 Gait Cycle

According to research in the literature, it is important to note that time frames are subject specific, so, the duration of these phases is inversely proportional to the speed at which one walks.

During walking, it is possible to consider the body functionally divided into two units: *passenger*, consisting of the Head, Arms and Trunk (HAT) that represent the 70 percent of body weight, and *locomotor*, consisting of the lower limbs.

To keep the vertebrae in neutral position during walking, muscular activity in the neck and trunk is required. The locomotor system is anatomically made up of the two legs and the pelvis. The eleven joints engaged in this system include the lumbosacral joint, the two hip joints, the ankles, the subtalar joint, and the metatarsophalangeal. The bone segments, thigh pelvis, leg, foot, and fingers serve as levers, and for each limb there are 57 muscles that control its movement [13].
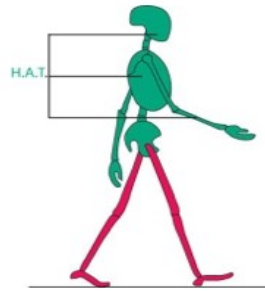
Figure 2.23 H.A.T. Model

The musculoskeletal system supports four main functions:

1.   Maintains stability despite changes in posture.

2.   Conserves energy by reducing the demand for muscle effort.

3.   It generates the propulsive force.

4.   Minimizes the shock of impact with the ground.

The Gait Cycle is divided into eight functional phases, which, combined, perform some basic functions, including limb progression, support on one leg, and limb stability.

First phase: Initial Contact

This phase begins when the foot touches the ground. The aim is to arrange the leg to start with the support phase so that the heel swings forward. The hip is flexed, the knee is extended, and contact with the ground is made with the heel. The other leg is at the end of the stance phase.
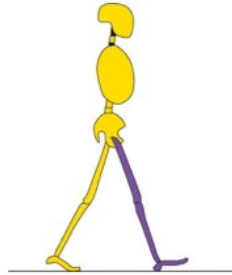
Figure 2.24 Initial Contact

Second phase: Load reaction

The phase begins with initial ground contact and continues until the other leg lifts for the swing. The body weight is shifted over the anterior leg. The heel is used as a fulcrum, while the knee is flexed to absorb the impact. Ankle plantar flexion limits the heel pivot for forefoot contact with the ground. The opposite leg is in its pre-oscillation phase. This period consists of two phases with two different mechanisms of progression: medial stance and terminal stance.
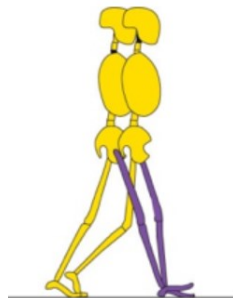
Figure 2.25 Load Reaction

Third Phase: Mid Load

In the first half of the single-leg stance phase, it supports the weight on the stable foot by dorsiflexion of the ankle, while the hip and knee are extended. At the same time, the opposite limb, moving forward, is in the middle of the swing phase.
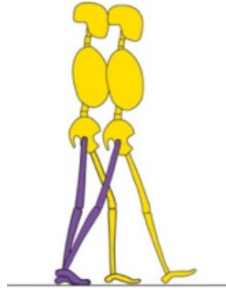
Figure 2.26 Mid Load

Fourth Phase: Terminal Load

In the second half of the loading period, the heel of the weight-bearing leg rises and the limb advances on the swinging forefoot. The knee increases its extension and begins to have flexion, the hip increases its extension while the other leg is in the terminal swing phase. The limb's forward performance and the support phase in which swinging occurs begins.
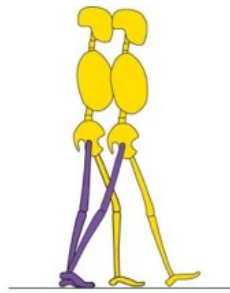
Figure 2.27 Terminal Load

Fifth phase: pre-swing

The weight is transferred and transferred to the other limb allowing the first limb to prepare for the swing. When the advancing leg contacts the ground, the terminal period of double stance begins. The reference leg responds with increased ankle plantar flexion, large knee flexion and small hip extension. The opposite leg is increasing its load.
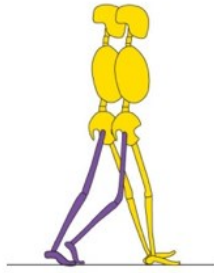
Figure 2.28 Pre-Swing

Sixth Phase: Start of the swing period

This phase represents 33 % of the swing period. It begins with lifting the foot off the ground by hip flexion and ends with swinging the foot on the other weight-bearing leg. The knee increased its flexion, and the ankle is partially in dorsi-flexion.
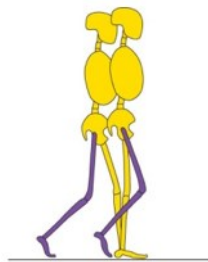
Figure 2.29 Start of swing Period

Seventh Phase: Mid Swing

This second phase of the swing period begins with the tibia vertical and leg swinging forward. The advancing forelimb brings the weight of the body forward for hip flexion. The knee can extend as a response to gravity while the ankle continues to go from dorsiflexion to neutral. The other leg is in the last part of mid-stance.
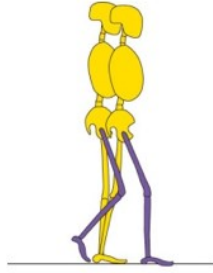
Figure 2.30 Mid Swing

Eighth Phase: end of the swing

This phase begins with the tibia vertical and ends when the foot hits the ground. The advancement of the limb is completed and the leg moves forward on the thigh. The knee is in extension, while the hip maintains flexion and the ankle continues to go from dorsiflexion to neutral. The other leg is at the end of the loading phase.
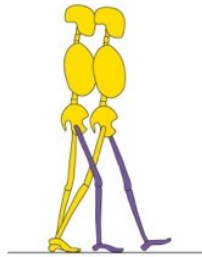
Figure 2.31 Terminal Swing

A passive balance between body vectors and the ligament tension can be achieved through hyperextension of the hips and knees, using the posterior knees oblique ligament and the ileo-femoral ligament of the hips. In this way the body weight passes anteriorly to the axis of the knees and posteriorly to the axis of the hips.
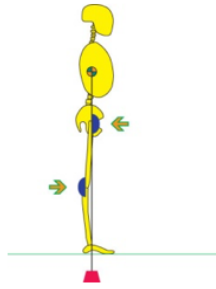
Figure 2.32 Balance

The joints are locked by two opposing forces: the weight of the body and the tension of the ligaments. A state of stillness is achieved if equilibrium is maintained by the body vectors that start from the center of the head and stop in the foot 1.5 cm in front of the ankle. It has been shown that an offset of 5 cm is indicative of mal alignment because there is a change in the location of the center of pressure. The distance from correct alignment is determined by the change in mobility of the joints of the ankles and knees and the relative lengthening of the soleus and gastrocnemius muscles. In a correct static posture, the projection of the body's center of gravity is placed 0.6 cm posterior to the hip axis and anterior to the ankles while the support area of the feet changes from heel to soleus to forefoot.

Chapter 3 Neuromusculoskeletal Modeling

The analysis of human motion is based on the study of quantities that characterize the orientation and position of body segments through stereophotogrammetry systems. Such information termed kinematic information, however, does not provide explanations related to the generation of motion. Therefore, it is necessary to make use of motion kinetics. We refer to direct dynamics if the model equations can predict features related to muscle activation through given forces over the entire duration of the task. In contrast, an inverse dynamic problem is defined when the forces that physiologically regulate muscle activation are unknown, the external forces applied to the system and the geometric, velocity and acceleration characteristics for certain frames are known.

The human musculoskeletal system can be represented as a rigid multi-body system, consisting of many muscles relative to the number of degrees of freedom (DOF) introduced by the skeleton.

The problem of estimating muscle activations forces management; it turns out to be indeterminate. In the inverse dynamics approach to reduce the number of unknown parameters in the problem, approximation techniques (e.g., optimization algorithms or use of sEMG signals) have been implemented. Both approaches use mathematical and computational models to quantify the forces generated within the muscle and the joint loads applied to it.

3.1 NMS Modelation

A model is composed of a series of mathematical equations describing the execution of specific tasks that allows its validation. The human body is considered as a multi-body articulated system with high degrees of freedom associated with joints, therefore, among muscle activation forces it is impossible to have an unambiguous determination [14]. Some preliminary assumptions must be satisfied including:

- The location of marker coordinates are known and depend on local density and segment size.
- Soft tissues are considered only in terms of inertial properties such as moment of inertia or mass distribution with respect to an axis of rotation.
- Bones and anatomical segments are assumed to be rigid bodies rotating about a joint axis;

- Anatomical segments are considered as homogeneous solids characterized by simple geometry whose moments of inertia can be calculated by known formulations. Their lengths are calculated as the distances between anatomical repere points, while masses are concentrated in the center of mass (COM).
- The joints are represented as ideal joints such as hinges or ball joints.

3.2 Muscle structure

Muscles are adhered to the musculoskeletal system through fibrous structures called tendons and can be subdivided into smooth muscles which are responsible for involuntary activations, control of the autonomic nervous system and are found in blood vessels, hollow organs, and airways. Striated muscles, instead, are characterized by a repetition of light and dark bands and are responsible for the musculoskeletal system. Based on the orientation of the fibers, muscles can be called pinnate if the fibers have oblique orientation with respect to the tendon axis; in this case their strength depends on the angle of pennation (α). If the fibers, in contrast, are arranged parallel to the length of the muscle, we will have fusiform muscles [15].

Skeletal muscles have the following functions:

- Maintaining balance and posture;
- Stabilization of joints;
- Execution of movement by contraction of motor units;
- Heat production to regularize body temperature.

The force that a muscle can generate is proportional to the number of functional units (sarcomeres) arranged parallel to each other and by the cross-sectional area of the muscle perpendicular to the fibers Physiological Cross-Sectional Area, PCSA.

$$F_o = k\,PCSA \quad (3.1)$$

F_o is the maximal force which can be generated when the muscle maintains its length unchanged during isometric contraction and PCSA is defined as:

$$PCSA = \frac{v}{l_0} = \frac{m}{l_0}\rho \quad (3.2)$$

l_0 is a resting length, v is the muscle volume, m is the mass e ρ is the density (1054 kg/m^3). In pinnate muscles, on the other hand, the useful force is given by the inclination of the fibers multiplied by the maximum force that can be generated:

$$F_u = F_o\,cos\alpha. \quad (3.3)$$

In the case of fusiform muscles, the value referred to PCSA will be lower than in the case of muscles pinnate, which therefore generate a greater force. However, the parallel arrangement of the fibers allows the achievement of maximum shortening and therefore maximum degree of movement.
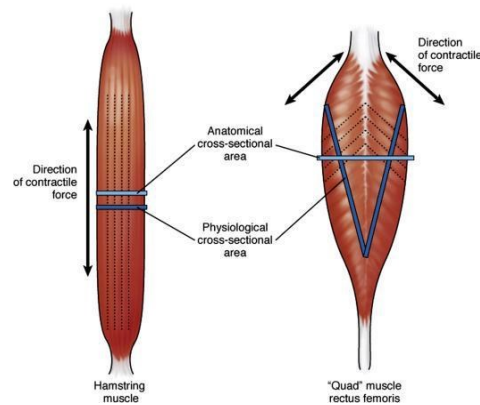
Figure 3.1 Shape of Muscles

The maximum force generated by muscle contraction is influenced by:

- Speed of shortening.
- Degree of excitation.
- Number type and size of motor units constituting the muscle.
- Angle of pennation.
- Fiber length.

The motor unit is the smallest functional unit of muscle and consists of a motor neuron, a synaptic junction, and a set of muscle fibers proportional to the precision of motor control required.

Muscles exhibit a hierarchical structure:

- *Muscle fiber:* collection of cylindrical polynucleated cells surrounded by a highly specialized membrane, the sarcolemma. Arranged longitudinally to the latter, within a fiber are contained myofibrils.
- *Myofibril:* is a 10 μm diameter filament that forms the contractile element of the muscle; it is responsible for muscle tension. From the present image, the structure of the myofibril can be observed where darker colored areas characterize myosin and are alternated with lighter bands of actin arranged neatly and transverse to the direction of the myofibril. The distance between two dark lines (Z lines) represent the length of the sarcomere.

- *Sarcomer:* Structural and functional unit of myofibril, consisting of thick threads (myosin) alternating with thin threads (actin).
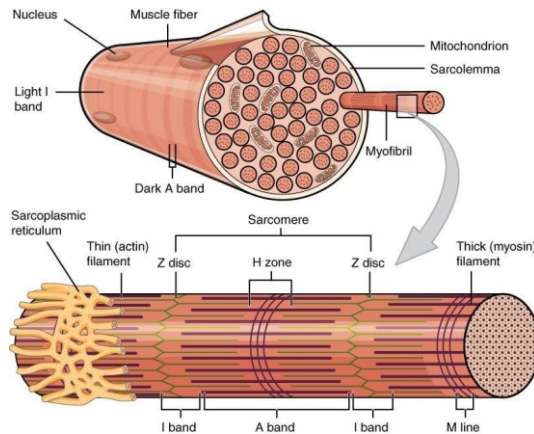
Figure 3.2 Sarcomere

The sarcomere, with its proteins, composes the mechanism of muscle contraction. The release of Ca2+ calcium ions into the sarcoplasmic reticulum is caused by the passage of the action potential down the axon. Actin filaments receive a conformational shift in response to the presence of these Ca2+ ions, revealing myosin binding sites. The weak link formed between myosin and actin facilitates movement of the thin filament, decreasing the distance. Myosin has an actin binding site and an ATPase site. The cross bridges are broken and the filaments return to their initial positions in the presence of a fresh ATP molecule. Sarcomere shortening is conceivable if calcium ions are found in the reticulum.

3.3 Muscular contraction

The muscle consists of a contractile element and passive connective tissue. The net force-length characteristics of a muscle are a combination of the force-length characteristics of both active and passive elements. At the resting length about 2.5µm there is a maximum tension possible related to the maximum number of cross-bridges of filaments [16].

The filaments are pulled apart, the number of cross-bridges decreases, and tension lowers as the muscle lengthens. There are no cross-bridges and there is no longer any tension when the length is full, which is around 4.0 µm. The cross-bridges meet as the muscle shortens to less than its resting length, causing interference. As a result, the tension is reduced, which lasts until the entire overlap, which happens at around 1.5 µm. These conflicting factors cause the tension to be significantly lowered rather than to zero.
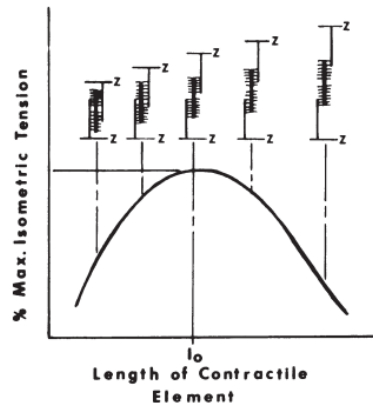
Figure 3.3 Elastic Element of Muscles

The connective tissue is called *parallel elastic component* and is like an elastic band. Its contraction influences the force-length curve. The parallel elastic component of the muscle is in a relaxed state with no tension when the muscle is at resting length or less. The parallel element becomes tighter as the muscle lengthens, causing tension to increase initially slowly and subsequently more quickly. The parallel element is extremely nonlinear, in contrast to typical springs, which have a linear force-length relationship.

The sum of the force generated by the elastic element F_p and the total force F_c generated by the contractile element represents the total force termed the tendon force F_t

$$F_t = F_p + F_c \quad (3.4)$$

The force of the parallel element represents the passive component F_p of muscle force and is always present during contraction, while the active component F_c is controlled by the fibers that constitute the elastic component. The total force F_t will therefore depend on the percentage of excitation of the muscle [16].
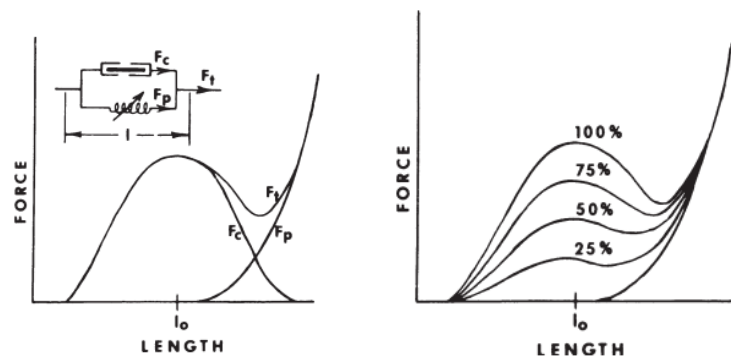
Figure 3.4 Relation between length and force

41

All connective tissues in series with the contractile component is called the *series elastic element.* During an isometric contraction, the length is changed within the limits, so there are no significant force-length relationships.

Since the overall length of the muscle is maintained constant, only a corresponding shortening of the contractile element itself can allow the series elastic element to stretch. The series elastic element lengthens by the same amount that the contractile element internally shortens, even though the exterior muscle length L remains unchanged due to the increased tension from the contractile element. In most muscles, the internal shortening from rest to maximum tension is only a small percentage (7%) of the resting length.

The tendon tension changes as the series element lengthens and the contractile element internally shortens during isometric contractions. The presence of the series elastic element is not very significant during normal human movement, but during high-performance movements, like jumping, it serves as in the position of saving energy as a muscle lengthens just before rapidly shortening [16].
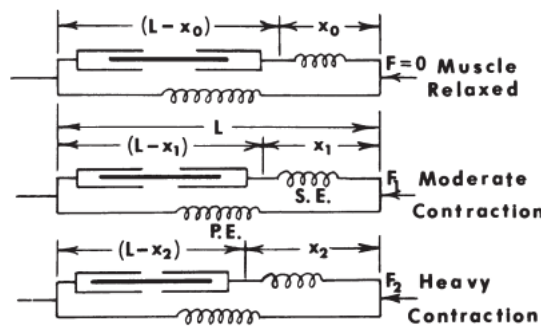
Figure 3.5 Muscle Contraction

We can also describe the force-velocity curve, where we can see concentric contractions. The usual curve is plotted for 100% which represents the maximum. Isometric contractions, which occur along the graph's zero-velocity axis, should be viewed as nothing more than a specific case among all conceivable velocities. It should be emphasized that this curve shows the features at a specific length of the muscle. Different levels of muscular activation are represented by the force-velocity properties of the skeletal muscle; these levels are 25%, 50%, 75%, and 100%. The length of the muscle must be recorded, and all such actions are required as the muscle shortens or lengthens at a specific length. The solid lines represent isotonic activity, while the dashed lines represent isovelocity activity; during shortening, the curves adhere to the hyperbolic Hill model, while during lengthening, the curves depend on the experimental technique [16]

42
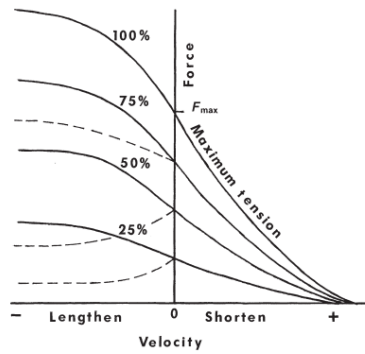
Figure 3.6 Muscular velocity representation

In our studies we have decided to apply Hill mathematical relationships that regard also the internal thermodynamics. Hill's curve has this form:

$$(P + a)(V + b) = (Po + a)b \qquad (3.5)$$

Where:

- Po is the maximum isometric tension.
- a is the coefficient of shortening heat.
- $b = a\,Vo/Po$
- Vo= is a maximum velocity when P=0

Eccentric contraction is the process through which the force placed on the muscle causes the fibers to extend as the tension created rises. The experimental information available for mathematical formulations regarding this case history is limited [16]. To conduct experiments on eccentric contractions it is necessary to perform external work greater than the human body can generate, 'in vivo' would mean using a motor that could cause muscle and joint breakdown. For the eccentric example, the relationships utilized for concentric contractions have been adjusted.
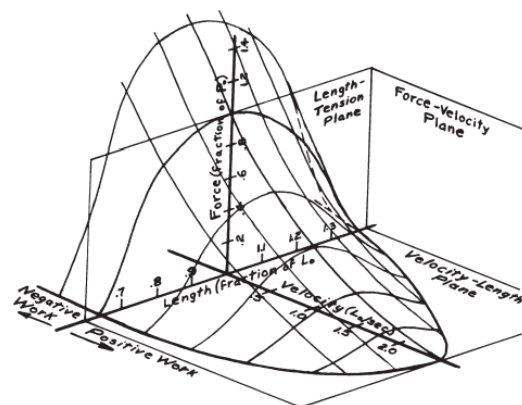
Figure 3.7 Relationship between length and force

43

Plot in three dimensions illustrating the relationship between length and velocity and the variation in contractile element tension. A new "surface" will be required to depict each level of muscle activation; the surface illustrated is for maximum muscular activation. The impact of the parallel elastic element is not demonstrated. The resulting curve, which here is only illustrated under the greatest contraction condition, is truly a surface. For each degree of muscular activation, let's say at 75%, 50%, and 25%, surface plots would be needed because the more typical contractions occur at a fraction of this maximum [16].

To enable muscle movement, muscles must maintain a state of equilibrium with the load to which they are subjected. If during muscle activation the load does not change either position or intensity it will be called a static load; if, on the other hand, the load changes its nature during muscle activation by invoking a muscle response it will be called a dynamic load. In the reality there are both types of load [16].
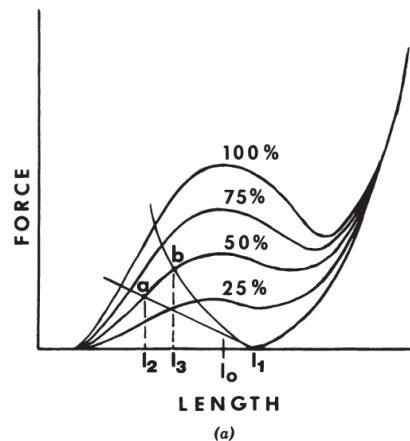
Figure 3.8 Relation between Length and Force in percentage

In the figure as we can observe the muscle force-length properties at four levels of activation, as well as the properties of a linear and nonlinear spring. The point of equilibrium is where spring (load) and muscle properties intersect. The point represents the muscular activation at 50%. Point b is the corresponding equilibrium point in response to a load assumed to be a spring with nonlinear characteristics.

We use the data from a typical walking stride to plot the time course of the contractions of the muscles about the ankle. We can assume that muscle lengths are proportional to ankle angle because the angular differences of the ankle are quite minor, and these length changes are also little. As a result, the event can be represented on a two-dimensional force-velocity curve [16]. It is possible to consider the lengthening or shortening velocity proportionate. The tendon forces are thought to be proportional to the angular velocity.

This image shows the time history of muscle moment-velocity during walking's stance phase. Plantarflexor moment is depicted as a solid line, while dorsiflexor moment is displayed as a dotted line. The stance starts off with negative work, then alternates positive and negative, and eventually, later in push-off, there is a significant burst of positive work that ends at toe-off.
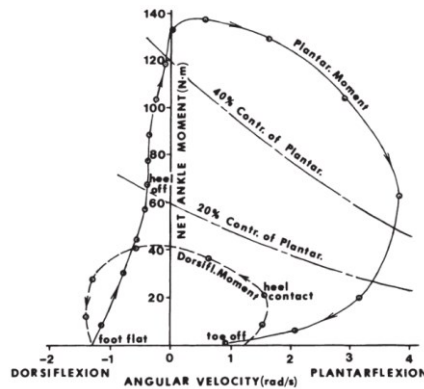
Figure 3.9 Representation of angular velocity of the foot

3.4 Hill's Model

Hill's model consists of three parts:

- A contractile component CC;
- Two elastic components SEC and PEC;

The contractile component CC is in series with the elastic component SEC and both are parallel to the elastic component PEC. The forces ft and fm represent muscle tendon force and muscle fiber force, respectively. The angle α, on the other hand, is the pennation angle defined as the angle between the direction of the muscle fibers and the line of action of the muscle force [17].
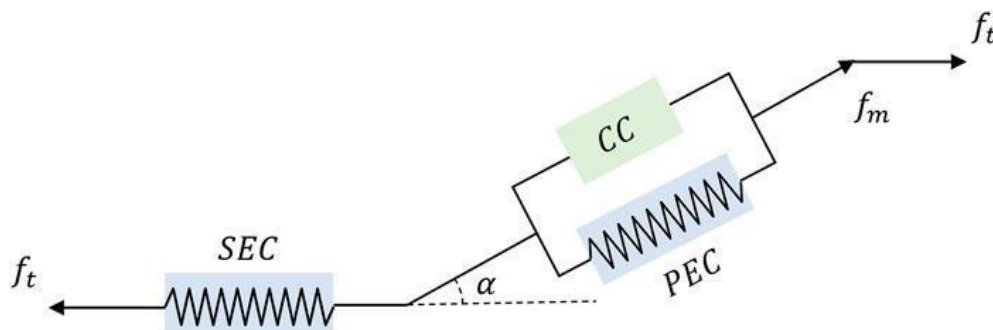
Figure 3.10: Graphic representation of Hill's model

3.5 *Muscle Activation Modeling*

The dynamics of muscle activation is one of the fundamental problems in musculoskeletal modeling. Approaches based on dynamics optimization and those exploiting the equation of state of variables involve onerous computational costs and complex implementations, respectively. In 2003, Thelen et al. proposed a new method based on a succession of ordinary differential equations called Computed Muscle Control (CMC). The purpose of the model is to reproduce the muscle activations involved in movement by feedforward and feedback control techniques.

Activation dynamics represents the pattern of muscle fibers with respect to activation time in response to calcium ions in the muscle structure.

The activation and deactivation states (α) of the fibers are contained in the continuous set of values between 0 and 1 where 0 identifies a state of no excitation and 1 a full excitation [18]. Activation dynamics were formulated as follows:

$$\dot{a} = \begin{cases} (u-a) \cdot \left[\frac{u}{\tau_{act}} + \frac{(1-u)}{\tau_{deact}} \right], & u \geq a \\ \frac{(u-a)}{\tau_{deact}}, & u < a \end{cases}$$

(3.6)

τ_{act} and τ_{deact} are the time constants responsible for fiber activation and deactivation, while u represents the excitation transmitted by the nervous system.

The dynamics of neuromusculotendinous concentration can be described by a concentrated parameter model that takes into account the properties of the tendon and the force, length and velocity properties of the muscle. Therefore, the following relationship holds:

$l_m = f_v^{-1}(l_m, l_{mt}, \alpha)$ where, l_m is the muscle length, l_{mt} is the tendon length and α is the muscular activation. The equations of motion, on the other hand, are used to calculate the model's generalized coordinate accelerations in response to applied forces as follows:

$$\ddot{\vec{q}} = \vec{A}^{-1}(\vec{q}) \cdot \{ \vec{G}(\vec{q}) + \vec{C}(\vec{q}, \dot{\vec{q}}) + \vec{R}(\vec{q}) \cdot \vec{f_m} + \vec{E}(\vec{q}, \dot{\vec{q}}) \}$$

(3.7)

Where $\vec{q}$ are the generic coordinates of the model, $\dot{\vec{q}}$ is the generic velocity of the model, $\vec{A}^{-1}$ is the inverse of mass matrix of the system, $\vec{G}$ is the gravity force vector, $\vec{R}$ is the muscular

moment matrix, $\overrightarrow{F_m}$ is the muscular force vector and $\vec{E}$ is the vector of generalized forces of interaction of the model with the extern.

During the muscle activation simulation, the desired accelerations $\overrightarrow{\ddot{q}_d}$ are calculated by exploiting the generic model accelerations $\vec{a}^*$, and then the optimization problem is solved for the calculation of forces generated under static conditions. Such obtained muscle activations satisfy the desired accelerations. The cost function (J) determined by the static optimization algorithm is given by:

$$J = \sum_{m=1}^{n} (a_m)^p$$
(3.8)

Where: n is the number of the muscles that are considered in the model, a_m is the instantaneous variation of the m-muscle activation and p is a constant defined by the operator. The neural activation u is calculated as the difference between the real muscular activation $\vec{a}$ and the optimization one.
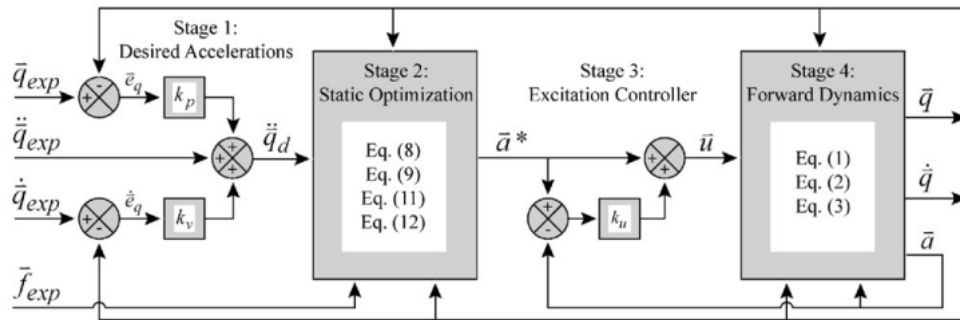
Figure 3.11: In this figure is represented a schematic computed muscle control algorithm (CMC) which is applied at each integration time step of a forward dynamic simulation [18] (D.G. Thelen 2003).

3.6 EMG driven Model

Any accurate representation of the motoneuron drive in a muscle must have a valid input. The output of the motoneuron pool to any specific muscle should be measured. Since there are not more motor units in the pick-up zone for surface electrodes than there are for persistent electrodes, surface EMG has been demonstrated to be more reliable than EMG recorded from indwelling electrodes. The surface EMG is a reliable signal to represent the average motor unit activity of most superficial muscles because of these benefits and simplicity of application. Each time a motor unit contracts, a distinctive action potential is produced, and the stimulated muscle fibers release a force impulse.

The study of the electromyographic signal is one of the most crucial methods for quantifying force and the activation of muscles during a movement during a Static Optimization (SO). The analysis of Inverse Dynamic of Human Movement, on which the static optimization is based, allows us to know the position, velocity, and acceleration of the system coordinates at any given instant. To create the force inside the system, external loads are applied. Surface electromyography (s-EMG) is a further method that can be used to approximate the impulsive signal of contraction of the musculotendinous units (MTUs) that are involved in muscle activation [19].

EMG-driven models were implemented because of their easy instrumental application and signal acquisition during a variety of motor tasks, with the goal of obtaining a simulation of subject-specific neuro-muscular control.

Isometric tasks showed quite different activation patterns between subjects to generate the same relative knee moments in flexion/extension and varus/ valgus directions, resulting in quite different amounts of support provided by the muscles and ligaments.

EMG-driven models have been developed to estimate muscle forces for the lower back, elbow, shoulder, knee, and ankle. These models are validated through the inverse dynamic approach to external joints moments because measures of muscle force in vivo are difficult.

The signals represent muscle activations implemented by the subject's characteristic CNS control of the people which could be distinct from that carried out by patients with neurological diseases. the muscular model is modified by calibration of the parameters for the muscle-tendon modeling.

The analysis of EMG signals can conduct in two different ways:

- With a forward approach that can predict EMG signal trends by knowing the properties of neuromuscular control (e.g., conduction velocity of the activation signal along muscle fibers, frequencies that characterize the spectrum of sEMG signals during isometric contractions).

- The inverse approach allows the identification of physiological processes underlying muscle activation by exploiting the processing of acquired EMG. This approach offers physiological solutions for a specific simulation with the help of proper models and applications for the neural control.

The EMG-driven modeling of the NMS system allows the prediction of joint's angular moments to a variety of movements. The model behavior is based on anatomical parameters of the lower limb. The muscular activation is obtained by a second order equation:

$$u_j(t) = \alpha\, e_j\,(t-d) - \beta_1\, u_j\,(t-1) - \beta_2\, u_j\,(t-2) \qquad (3.9)$$

where $e_j(t)$ is the j-th muscle excitation at time t, $u_j(t)$ is the neural activation, α is the muscle gain coefficient, $\beta 1$ and $\beta 2$ are the recursive coefficients and d is the electromechanical delay [20]. A stable solution must contain these constraints:

- $\beta_1 = C_1 + C_2$
- $\beta_2 = C_1\, C_2$
- $|C_1| < 1$
- $|C_2| < 1$
- $\alpha - \beta_1 - \beta_2 = 1$

Whenever compared to experimental parameters gathered from various motor activities, the calibration procedure makes sure that the model's and simulations' parameters are as accurate as possible [20]. When a model NMS's parameters are calibrated, a sizable number of even very dissimilar movements are performed. This enables for more physiologically accurate estimates of joint loads and muscle activation.
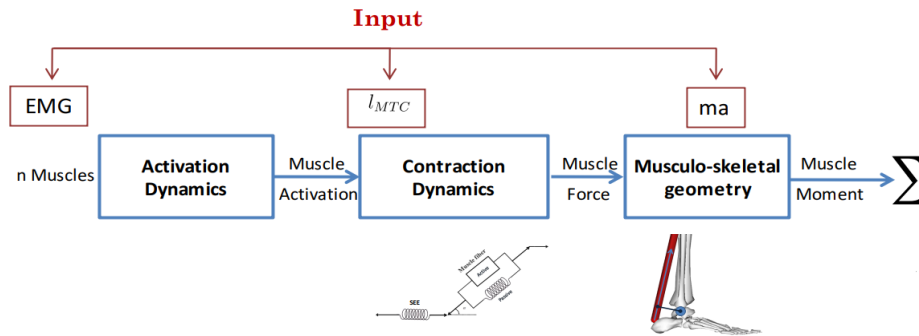
Figure 3.12 Schematic Input of NMS model

There are also NMS hybrid models, where, as the example proposed by Sartori et al. in 2014 [19], the model uses EMG-informed for the direct dynamic analysis of the lower limb calibrated with respect to the experimental excitations of a portion of the MTUs.

The hybrid model combines an EMG-driven dynamic model with a static optimization component. The parameters and coefficients were identified by calibrating the model parameters and tuning the static optimization coefficients.

EMG-driven model is based on a lower limb model with four body segments (pelvis, thigh, shank, foot), five degrees of freedom and 34 MTU of the specific OPENSIM model.
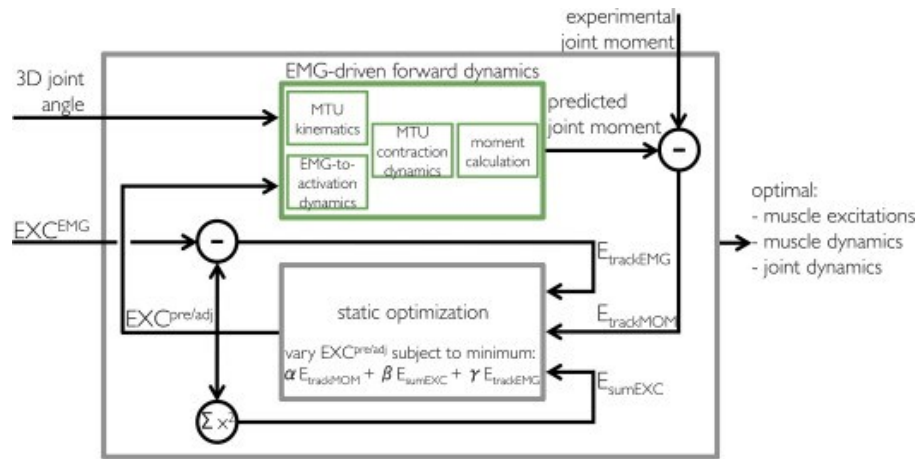
Figure 3.13 Scheme of s-EMG signal for NMS modeling

The use of s-EMG signals for musculoskeletal modeling has limitations including [19]:

- The signal acquisition instrumentation does not allow reaching deep muscles but is limited to ecording muscle activation at the skin level, thus detecting a limited number of muscles.
- The s-EMG signals approximate the activity of activated MTUs in the aggregate and not for individual units, and therefore the signal does not directly measure the action potentials generated.
- The signals are affected by errors:
    - Of motion artifact caused by the movement of the electrodes on the skin;
    - Significant if the electrodes are incorrectly positioned.
- The s-EMG signal is influenced by crosstalk i.e., the signal recorded at correspondence of a muscle of interest has a component related to the activation of surrounding muscles. There are numerous strategies that analyze this phenomenon to compensate for the errors it introduces into the parameters that characterize the neuromechanical mechanisms of muscle activation obtained from sEMG signal processing (e.g. Amplitude Analysis, Spectral Analysis and Cross-Correlation Analysis of the EMG signal surface)

3.7 Muscular Synergies

The Central Nervous System (CNS) acts on a large part of muscles but with an activation synchronized strategy of a limited muscle group in order to execute a movement. Muscle Synergy consists of the activation of a group of muscles in response to a neural command from the motor neurons located at the spinal and cortical level [21]. Instead of transmitting different neural signals

different for each muscle, the CNS uses the same set of signals for all the muscles required to perform the same movement. Muscle synergies are an important tool for understanding motor control mechanisms quantitatively and noninvasively in the pathological setting, especially for patients with neurodegenerative diseases or joint disorders.

The central nervous system, to generate movements, does not control muscles individually but through functional groups called muscle synergies. Muscles belonging to the same synergy exhibit similar EMG signals. The number and function of synergies depend on the number of EMG signal acquisition channels and the method of extraction [22].
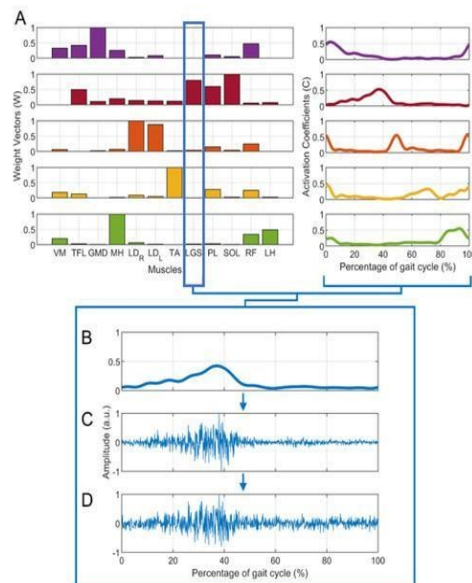
Figure 3.14 Muscular Synergies

Methods of factoring the acquired and processed EMG signal identify the activation signals (time-varying) and how these are distributed among the muscles (time-dependent weights) of each of the synergies. Among the most important methods are:

- Non-negative Matrix Factorization (NMF): ensures that the nonnegativity property of muscle activation signals is respected;

51

- Principal Component Analysis (PCA): using signals with Gaussian distribution, are extracts the synergies that best represent the variance of the data set and minimizes the covariance of the weights of the synergies.

3.8 Limitation of NMS modeling

Neuromusculoskeletal modeling is very useful for understanding many aspects related to human movement, including diagnoses, preparation for surgical operations and during rehabilitation courses, rather than athletic preparation of athletes. Despite all the advantages, modeling also has some limitations related to electromyography or stereophotogrammetry including:

- The amount of data required for modeling is significant in order to obtain realistic physiological parameters.
- Simplification of hard and soft tissues may adversely affect modeling.
- The presence of a soft artifact (ATM) can induce errors introduced by markers placed on subjects' skin.
- The acceleration of the markers is obtained by trajectory acquisition of inverse differential equations that sometimes do not coincide with the actual acceleration.
- The poor accuracy in parameter estimation regarding the size of the segments and the point of application of the estimated muscle forces, which cannot be validated during task execution but at later stages of movement analysis.
- The movement calibration and recording processes must be conducted through uncluttered equipment.
- Identification of joint rotation axis of joints is based on anthropometric methods using reference tables based on cadaver anthropometric measurements or obtained by measuring body segments from images.

3.9 Software for Neuromusculoskeletal Modeling:

Software for neuromusculoskeletal modeling were created to enable proper implementation of models. In fact, these programs were created so that users could freely enter and modify implementation algorithms. In the 1990s, Delp and Loan introduced a musculoskeletal modeling environment, called SIMM [23].

Using this software, researchers have been able to create musculoskeletal models for the dynamic modeling of numerous movements for various body parts. The software only offers a small selection of tools to allow for a thorough study of the muscle excitations, forces, and moments discovered at the conclusion of a dynamic simulation.

In addition, SIMM provides for the development, modification, and validation of numerous NMS models but does not provide unfettered access to source codes. For the biomechanics community, alternative software has been created, one of which is OpenSim.

OpenSim

The neuromusculoskeletal system can be modeled, simulated, and studied using the open-source platform OpenSim. It consists of low-level computing tools that an application invokes. Access to important functionality is provided by a graphical user interface. A rising number of contributors to Simtk.org are working to build and maintain OpenSim. Simtk.org acts as a public repository for information, models, and software for simulating biological structures using physics. The software is written in ANSI C++, and the graphical user interface is written in Java, allowing OpenSim to compile and run on common operating systems [23].

OpenSim's plug-in architecture invites users to create their own muscle models, contact models, controllers, and analytics to expand functionality. Several tools for validating musculoskeletal models, creating simulations, and visualizing findings are available via the OpenSim graphical user interface. Virtual markers are depicted as blue spheres, while muscles are represented by red lines. SimTrack is a tool that can quickly and precisely produce muscle-actuated simulations of subject-specific movements, as explained below.

OpenSim's structure is organized into computational and functional layers.

- Simbody is important to create and solve the multibody dynamics system. Is a computational layer and distinct state object which can contain several variables in the system equations like coordinates, speed, time, auxiliary states of force, user-defined

states for custom components, modeling options to enable/disable components like constraint and force elements, and model parameters such as masses and dimensions [24]. The base layer is the computational layer provided by Sinbody (in blue), where numerical methods and computational resources are available to all levels within the OpenSim API.

- Modeling Layer comprises two main classes Model Component and Model which are responsible for the physical part of the model and for assembling a coherent and consistent whole respectively (green). Model components include forces, constraints, controllers, and actuators with several subtypes, own dynamics, and state variables. When the system is constructed, it is time to analyze the layer.
- Analysis Layer comprises three categories of layers (orange):
    o Modeling
    o Solver
    o Reporter

There are some inclusion criteria of the model, then with the help of the solver equations it is possible to generate a trajectory of model kinematics or is possible to solve the inverse dynamics equations to determine joint moments.

- Application Layer contains a variety of applications. First, there is the OpenSim GUI, providing a visual interface to the Tools including plotting, animation and detailed models (red)
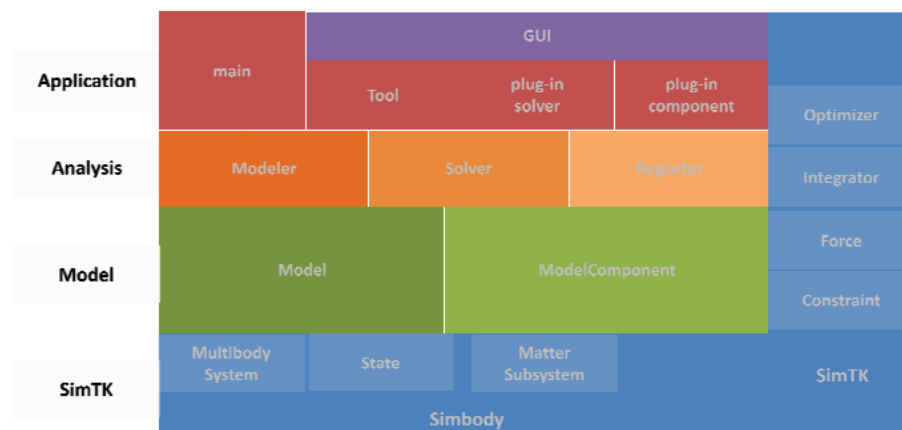
Figure 3.15 Opensim Layers [24]

The software offers a biomechanical simulation environment for the execution and evaluation of executable muscle movements. In addition, dynamic simulations can be performed for subjects with pathologies responsible for motor control. The ability to keep separate the

characteristic variables of the simulation under consideration and the set of information that constitutes a model ensures compliance with the principles governing the evolution of physiology and the dynamics of movement through Newton's Laws. Comparison of the results obtained from the simulation with experimental data allows for analysis and validation of the implemented model.

The structure of input files in Opensim is rigid:

- The models created are saved in the .osim format;
- Setup files used can be used to run different tools and are saved in .xml files to facilitate reading and deployment of a specific implementation.
- Marker files are obtained through stereophotogrammetry and are collected in .trc (track) format files. The first three lines constitute:
    - *Date Rate*: a header in which data on the frequency of data acquisition are also saved;
    - Camera Rate: the frequency of acquisition of the camera,
    - NumFrame: the number of instants of data acquired
    - Num Markers: the number of markers applied to the subject,
    - OrigDateRate: the unit of measurement of the position coordinates, the number of the first frame acquired
    - DataStartFrame: the corresponding initial instant of the first frame.

    This is followed by a line containing the names of the markers (*C7-RA-LA-L5-RPSIS-LPSIS-RASIS-LASIS-RGT-LGT-RLE-LLE-RME-LME-RHF-LHF-RTT-LTT-RLM-LLM-RMM-LMM-RCA-LCA-RVMH-LVMH-RIMH-LIMH-RIIT-LIIT*) and a line which contain the x-y-z coordinate of each point. Every row contains the number of frames, the temporal instant and every acquisition data.

Figure 3.16 Example of dataset of a .trc file of subject S5

- File Motion: here Ground Reaction Forces (GRF), center of pressure (COP) and free moments generated during task execution are saved in a motion file with *.mot* format. First lines consist in:
  - *Datacolumns and datarows;*
  - *Range;*
  - *Name labels* of GRFs (vx,vy,vz), their point of application (px,py,pz) and torques for each platform used
  - Each row contains the time reference and for each force of reaction are given the x-y-z components with respect to the model reference system.

```
datacolumns 19
datarows 1121
range 2.800000e+00 3.966667e+00
endheader

time        ground_force1_vx    ground_force1_vy    ground_force1_vz    ground_force1_px    ground_force1_py    ground_force1_pz
2.8          -7.65338169        248.05857885         35.85966148        -0.31919132          0.00000000        -0.17273373
2.80104      -8.22986325        260.92602636         37.40307066        -0.31869620          0.00000000        -0.17254625
2.80208      -8.90693343        273.61035028         38.84289643        -0.31819403          0.00000000        -0.17235637
2.80312      -9.69963197        286.08540828         40.16472449        -0.31768409          0.00000000        -0.17216213
2.80417     -10.62226977        298.33300963         41.35522566        -0.31716575          0.00000000        -0.17196104
2.80521     -11.68790775        310.34207478         42.40236125        -0.31663837          0.00000000        -0.17175044
2.80625     -12.90788102        322.10752049         43.29558367        -0.31610140          0.00000000        -0.17152783
2.80729     -14.29142652        333.62907511         44.02599287        -0.31555441          0.00000000        -0.17129139
2.80833     -15.84545335        344.91008553         44.58643842        -0.31499734          0.00000000        -0.17104021
2.80937     -17.57444472        355.95631919         44.97158793        -0.31443057          0.00000000        -0.17077430
2.81042     -19.48040759        366.77478965         45.17793959        -0.31385489          0.00000000        -0.17049443
2.81146     -21.56287063        377.37264953         45.20378038        -0.31327141          0.00000000        -0.17020205
2.8125      -23.81898650        387.75626884         45.04913275        -0.31268157          0.00000000        -0.16989911
2.81354     -26.24367507        397.93066866         44.71570579        -0.31208708          0.00000000        -0.16958768
2.81458     -28.82972567        407.89929217         44.20685669        -0.31148976          0.00000000        -0.16926976
2.81562     -31.56786498        417.66393686         43.52756208        -0.31089138          0.00000000        -0.16894710
```

Figure 3.17 Example of motion file .mot of subject S5

The Opensim Output files are in *.sto* storage format and have a similar structure to the motion input files, but they contain the results of the applications performed on the model. In fact, the muscle analysis allows the information inherent in the length, Force, FiberPassivePower, Moments-Ankle-Angle, Fiber Velocity, Moment-Hip, Moment-Knee (etc) of each muscle's tendon units to be saved in storage files.

```
FiberLength
version=1
nRows=141
nColumns=93
inDegrees=no

This analysis gathers basic information about muscles during a simulation (e.g., forces, tendon lenghts, moment arms, etc).
Units are S.I. units (second, meters, Newtons, ...)
Angles are in degrees.

endheader
time     glut_med1_r glut_med2_r glut_med3_r glut_min1_r glut_min2_r glut_min3_r semimem_r    semiten_r   bifemlh_r   bifemsh_r   sar_r   add_long_r
     2.79999977    0.10000000          0.10000000          0.10000000          0.10000000          0.10000000          0.10000000
     2.80833310    0.10000000          0.10000000          0.10000000          0.10000000          0.10000000          0.10000000
     2.81666643    0.10000000          0.10000000          0.10000000          0.10000000          0.10000000          0.10000000
     2.82499976    0.10000000          0.10000000          0.10000000          0.10000000          0.10000000          0.10000000
     2.83333309    0.10000000          0.10000000          0.10000000          0.10000000          0.10000000          0.10000000
     2.84166642    0.10000000          0.10000000          0.10000000          0.10000000          0.10000000          0.10000000
     2.84999975    0.10000000          0.10000000          0.10000000          0.10000000          0.10000000          0.10000000
     2.85833308    0.10000000          0.10000000          0.10000000          0.10000000          0.10000000          0.10000000
     2.86666641    0.10000000          0.10000000          0.10000000          0.10000000          0.10000000          0.10000000
```

Figure 3.18 This analysis gathers basic information about muscles during a simulation (e.g., forces, tendon lengths, moment arms, etc). Units are S.I. units (second, meters, Newtons, ...) Angles are in degrees.

Opensim makes it possible to determine the forces produced by the skeletal muscle system in response to electrical stimuli produced by the nervous system. In order to create personalized joints, it is also possible to use anthropometric information about a subject and the ratio of limitations to desired degrees of freedom. Even in the presence of some disorders, the dynamics of muscle stimulation can produce a variety of movements that allow for greater neurological and physiological control of the musculoskeletal system.

It is not always guaranteed to be possible to gather experimental data, such as measurements of the center of pressure or the locations where GRFs should be applied from force platforms. OpenSim utilizes Simbody for calculating the forces of interaction with the environment to model or predict motion. OpenSim uses the Hill's three-element model to represent the muscle-tendon system and the activation of muscle fibers while using equation (2.7) to model the dynamics of muscle activation. Additionally, OpenSim implements static optimization algorithms that address the indeterminacy issue underlying the neurological regulation of muscle excitation. The CMC method [18] is used to verify that the biomechanical simulations' kinematic outcomes are as compatible as possible with EMG data obtained using motion-capture equipment. The kinematics and dynamics of the model used to accomplish a movement can be examined using the tools provided by OpenSim. One of the features that has made the software popular among scientists is the capacity to compare, validate, and adjust a model using these tools:

- Scaling of a subject's parameters of a model;
- Inverse Kinematic (IK);
- Inverse Dynamic (ID);
- Static Optimization (SO);
- Direct Dynamic;
- Result's Plot obtained by Tools execution (IK, ID, SO).

In this work, OpenSim's Tools are used for trial analysis of each subject in this order: Scaling, Inverse Kinematics, Inverse Dynamics, and Analyze Tool.

OpenSim Tools:

Scaling:

To perform a motion simulation, a preliminary scaling analysis must be performed. The anthropometry of the musculoskeletal model must match that of the acquired subject; therefore,

the generic model of the system is modified to approximate the anthropometry of the test subject. Body segment sizes are scaled with respect to distances relative to marker coordinates acquired through a motion capture system with respect to virtual markers, muscle-tendon lengths are scaled with respect to the percentage of muscle-tendon units. Segment masses, on the other hand, are scaled with respect to total mass.

The masses and inertial properties of the subject are preserved. The use of scaling factors serves to keep the proportions of the model constant.

In OpenSim we have to apply a scaling step to adjust both the dimensions of the body segment and the mass properties. Scaling can be performed using a combination of two methods:

1. Manual scaling where each segment is scaled using some predetermined scale factor.
2. Measurement- based Scaling: Scaling that determines scale factors for a body segment by comparing distance measurements between specified landmarks on the model, known as *model markers*, and the corresponding *experimental marker* positions [25].
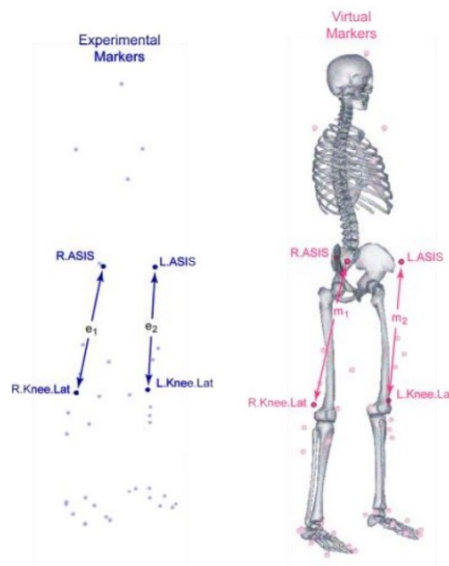
Figure 3.19 Experimental Markers (e_i) and virtual Markers (m_i)

The interface that opens when running the *Scale Model Tool* allows the user to have freedom in choosing the parameters to be used in scaling the subject. The Subject Data section allows the user to choose the name of the new scaled model, enter the mass and markerset. To ensure that the mass of the model equals that of the subject acquired you must select the option, also it is important to specify the file path of the marker set trajectories of the static acquisition and the frame interval of interest.

Similarly, to ensure that the model markers coincide with the experimental ones it needs to select the option.
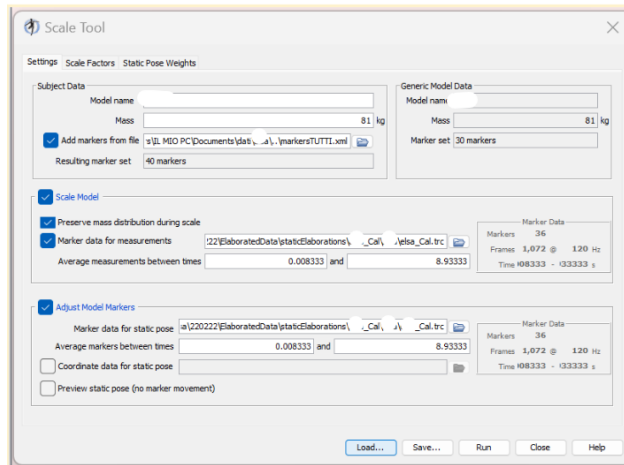
Figure 3.20   Scale Model Tool Interface

The Scale tool then needs a few files including Subject Setup Scale in .xml format containing all the information, data and choices made for scaling. In the Measurement Set are saved the names of the markers whose distance is used to calculate the scaling factor. In the IK TaskSet object are saved the weights for each marker needed to run an inverse kinematics problem.

Figure 3.21 : Input and Output of tool Scale. It is possible to observe that experimental data are in green, opensim's file are in red and setup file are in blue [25]

Body Name	Measurement(s) Used			Applied Scale Factor(s)		
pelvis	Pelvis_x	Unassigned	Pelvis_z	1.319503	1.0	0.879828
femur_r	thigh_r					0.841879
tibia_r	thigh_r					0.841879
talus_r	foot_r					0.937631
calcn_r	foot_r					0.937631
toes_r	foot_r					0.937631
femur_l	thigh_l					0.843855
tibia_l	shank_l					0.986698
talus_l	foot_l					0.902767
calcn_l	foot_l					0.902767
toes_l	foot_l					0.902767
torso	Unassigned	trunk_y	trunk_z	1.0	0.913181	1.283728

Figure 3.22 Editor to the creation of Measurement Set

Is important also observe that the Scale Marker set contains the .xml file with virtual marker coordinates that are on the model's segment. The Subject Static .trc file contains the trajectories markers acquired by a static trial: all the markers were positioned on the subject's skin during an erect position. The model NMS generated is a .osim file and contains the implementation of the neuro-muscle-skeletrical model during a motor task analysis. The measurement set is model-specific.

Model Gait2392

The model used in this work for gait analysis is gait2392 which represents the characteristics of an average subject of height 1.80 m and weight 75.19 kg, consisting of 76 muscles, 23 degrees of freedom, 92 muscle-tendon actuators. The upper limbs are not represented. The model considers 7 body segments: Pelvis, Femur, Fibula, Tibia, Patella, Astralagus, Calcaneus.
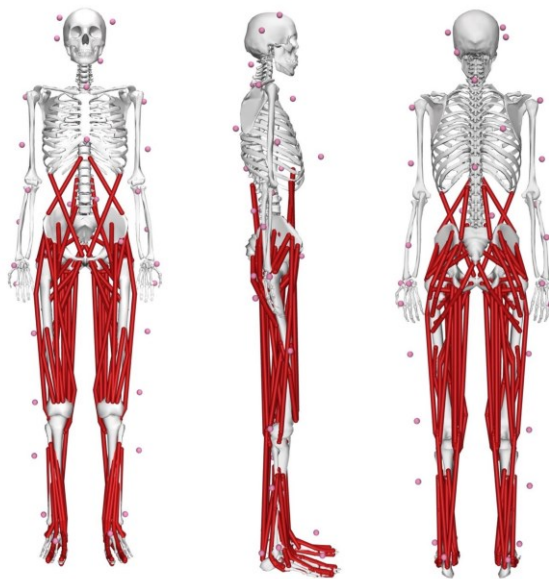
Figure 3.23 Model 2392 [26]

The muscles represented by the model are as follows: Great Gluteus , Gluteus Medio, Small Gluteus, Semimembranosus, Semitendinosus, Biceps femoris capitis Long, Biceps femoris capitis short, Sartorius, Tensor fascia lata, Pectineus, Gracilis, Iliacus, Psoas, Quadriceps femoris, Gemellus, Piriformis, Rectus femoris, Vasto medialis, Vasto internal, Vastus lateralis, Gastrocnemius medialis, Gastrocnemius lateralis, Soleus, Tibial Posterior, Tibialis anterior, Spinal rectus, Internal oblique, External oblique, Finger extensors, Hallux extensors, Peroneus longus, Peroneus shortus, Peroneus thirdus, Adductor longus, Adductor breve, Adductor grande (1,2 and 3), Finger flexors and Hallux flexors [27].

Muscle Optimizer:

The Muscle Optimizer Tool allows obtaining optimal estimates for fiber length and the resting length of tendons by exploiting data obtained from biomedical images [28]. This tool has been added as a plugin. A Reference Model is used to optimize the factors of scaling of the muscles you wish to select. The muscles selected in our case correspond to those acquired using the marker set
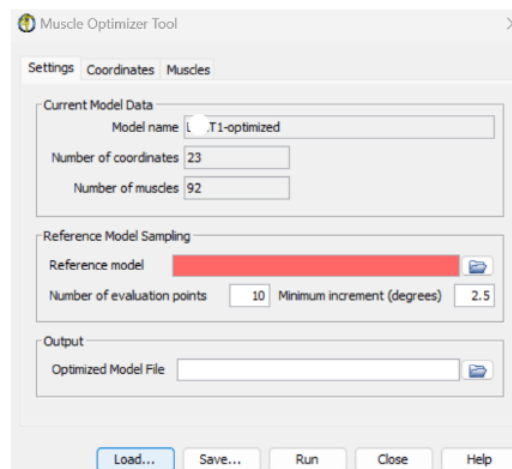
Figure 3.24: Muscle Optimizer tool

Inverse Kinematics (IK)

IK makes it possible to calculate the joint angles and body segment positions of the musculoskeletal model from data acquired during motor tasks. Its goal is to identify the coordinates that best reproduce the experimental data. The algorithm used by the tool can identify the reconstruction error that reproduces the inverse kinematics. This error is given by

the distance between an experimental marker and a virtual marker. Minimization of the error ensures a more accurate reconstruction of the motion of the coordinates of the markers recorded through a motion capture system.

$$Squared\ Error = \sum_{i=1}^{markers} \omega_i \left(\vec{x}_i^{subject} - \vec{x}_i^{model} \right)^2 + \sum_{j=1}^{joint\ angles} \omega_j \left(\theta_j^{subject} - \theta_j^{model} \right)^2$$

(3.10)

Where:

- $x_i^{\ subject}$ and $x_j^{\ model}$ represents the position of i-esim marker of the subject and of the model respectively
- $\theta_j^{subject}$ and θ_j^{model} represents the j-esim joint-angle
- ω_i and ω_j are markers weight and joint-angle weight.

Each marker is associated with a proportional weight and his aim is to reduce the error that is associated. The Inverse Kinematics tool can individuate the coordinates witch better represent the experimental data with the help of minim squared:

$$\min_{\theta} \left[\sum_{i=1}^{markers} \omega_i \left\| \vec{x}_i^{subject} - \vec{x}_i^{model}(\theta) \right\|^2 + \sum_{j=1}^{joint\ angles} \omega_j \left\| \theta_j^{subject} - \theta_j^{model} \right\|^2 \right]$$

(3.11)

In this way, for each temporal instant, the movement that make a subject is followed by coordinates of virtual markers and by joint-angle of the model.
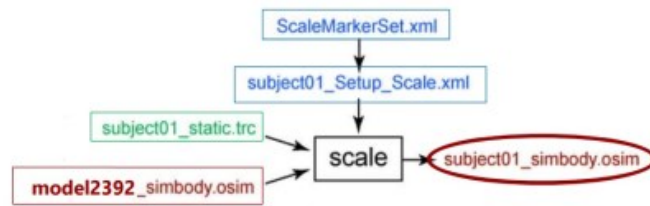

Figure 3.25: Input and Output of Inverse Kinematics. It is possible to observe that experimental data are in green, opensim's file are in red and setup file are in blue [25]

Input files of IK execution are:

- The previously scaled model (.osim) of the subject versus a generic model.
- Subject Walk: the trajectories of markers (.trc files) acquired during the execution of a motor task with a stereophotogrammetric system.
- Subject Setup IK: the .xml file contains all the information related to the execution of the IK, including the weights assigned to each marker.

62

Special feature of the IK is that the output (.mot) files must be generated before the execution of the Tool, otherwise this produces an error.
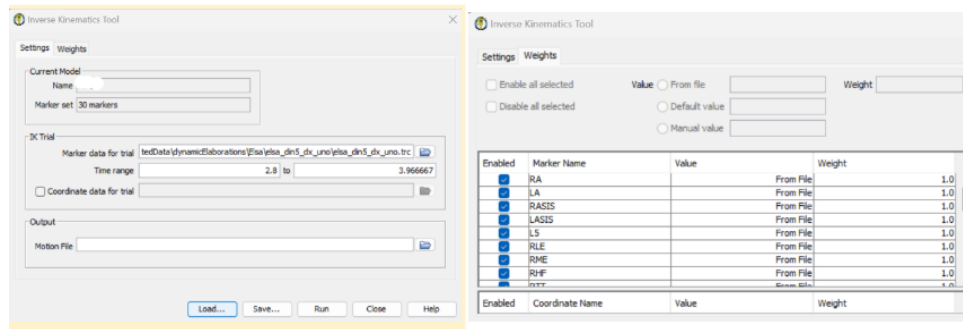
Figure 3.26: IK interface.

Inverse Dynamics (ID)

An inverse dynamics (ID) problem allows calculation of the internal forces of muscles and the moments generated by each joint during the execution of a movement. The tool uses the cardinal equations of dynamics, which are based on the following equations relating the forces (F) and angular moments (M):

$\Sigma F = ma$ (3.12)

$\Sigma M = I\alpha$ (3.13)

The first equation represents Newton's law, a and α are the acceleration obtained by the Inverse Kinematics, where a is applied at the body's center of mass (CM) and α represents the angular acceleration with respect to a rotation axis. I is the Inertial Moment and m is the rigid body mass.

The ID iteratively solves the equations of motion by exploiting data obtained from inverse kinematics and external forces applied to the model (e.g., ground reaction forces obtained from force platforms). The equation of motion can be generalized, for the N degrees of freedom of the model, as follows:

$$\tau = M(q) * \ddot{q} - C(q, \dot{q}) - G(q) - F \quad (3.14)$$

Where τ is the internal generalized force's vector, $(q, \dot{q}, \ddot{q})$ are vectors that contain coordinates, velocity and acceleration respectively, M is the mass matrix of the system, C is the vector of centrifugal and Coriolis forces, G is the vector of gravitational forces, and F is the vector of the forces applied to the model. Since all the parameters on the right side of the equation are known it is possible to calculate the unknown forces (τ).

63

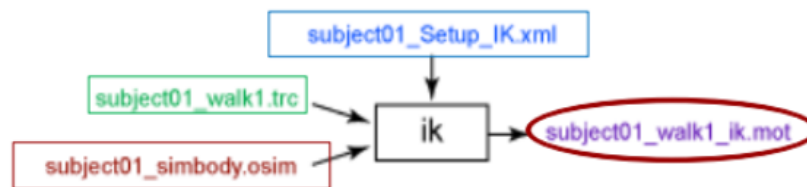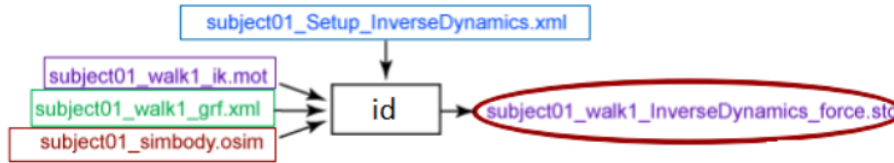*Figure 3.27 : Inverse Dynamics Input and Output. It is possible to observe that experimental data are in green, opensim's file are in red and setup file are in blue[25].*

During ID execution, we have several Input File:

- The previously scaled model (.osim) of the subject with respect to a generic model.
- Subject Walk IK: the motion (.mot) file containing the generalized coordinates of the model obtained from the execution of the IK.
- Subject GRF: the .xml file containing the external ground reaction forces, moments and the positions of the center of pressure. The creation of this file involves using not only the .mot file obtained from the IK but also of the motion file relating the forces acquired by the motion-capture system. The file also specifies the force application points and torques.
- Subject Setup ID: the .xml file contains all the information related to the execution of the ID.

Output file .sto, for each temporal instant, contains the application forces' value of joints and moments which are generated with respect to reference axis.
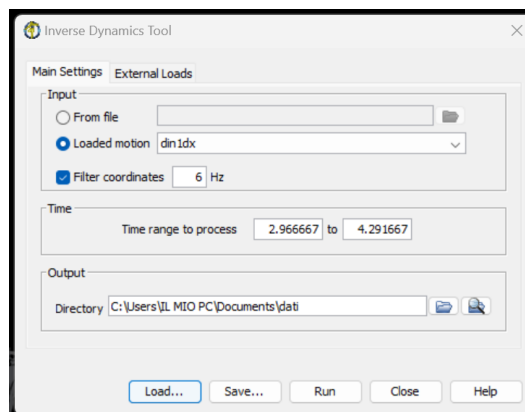
Figure 3.28 Inverse Dynamics Tool of the subject S8

In addition to the Inverse Dynamics Tool, there is also the ability to insert external loads as depicted in the following figure. In this study, however, the external loads were not used

because the subjects walk on the force platform, which is able to detect all the information of interest.
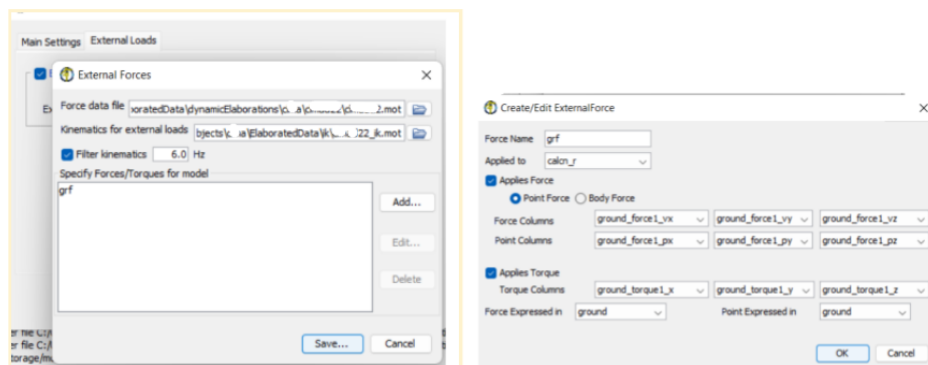
Figure 3.29 External Load tool

Analyze Tool

The Analyze tool based on the input files allows to obtain an analysis or simulation of the model. This tool offers the possibility to perform an analysis of kinematics, Actuation, JointReaction and many others.

Of interest to us is the possibility to perform MuscleAnalysis i.e., to obtain the parameters characteristic of muscles related to each instant regarding muscle fibers (e.g., length, velocity, activation power) and joint moments (e.g. arm of the angular momentum of the ankle joint) saved in .sto files . Only files (.mot) are needed as input. containing the temporal instants and motion coordinates saved in the output files of the IK.

Files obtained from running the various tools available in OpenSim are usable in other environments for human motion analysis such as Matlab, Excel, and CEINMS.

CEINMS

CEINMS (Calibrated EMG-Informed Neuromusculoskeltal modeling toolbox) inspired by electromyography-driven methods. Given the right anatomical and physiological information, CEINMS may work with any number of musculotendon units (MTU) and any number of degrees of freedom (DOF), as it was developed and written to be flexible and generic software. Additionally, the modular structure enables the independent choosing of various operation modes:

- *Full-predictive open-loop mode.* To directly drive the computations of the musculotendon forces, a neuromusculoskeletal model is provided with the experimentally recorded EMG signals and 3D joint angles as input.
- *Hybrid Mode.* The excitation patterns of muscles from which it is not practical to routinely collect EMG signals (e.g. deep muscles) are constructed using optimization algorithms.[29]
- *EMG-assisted mode.* Both the excitations derived from experimentally recorded EMG signals and the determination of the excitations of muscles without experimental EMG are adjusted using optimization techniques. The neuromusculoskeletal model is then fed information from the muscle excitations and 3D joint angles.
- *Static Optimization Mode.* An optimization algorithm is used to construct all the muscle excitation to drive the neuromusculoskeletal model.

CEINMS is divided into three application stages:

1. Calibration: uses an optimization loop of the initial parameters to adapt them to the muscle activations and experimental joint moments.

2. Execution: for those motor tasks whose data were not used in the previous calibration, the activation forces are calculated for each MTU and the joint moments.

3. Validation: the execution results are compared with the data acquired using the EMG signals [30].
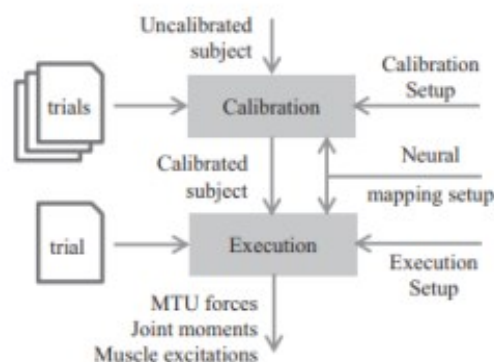
Figure 3.30 Schematic Representation of calibration setup and CEINMS execution

CEINMS Calibration

The aim of calibration is to determine the values for a set of parameters for each musculotendon unit. The first parameter set describes the kinetics of the musculotendon unit's activation, and the second parameter set describes the kinetics of the muscle-tendon contraction, which converts the kinematics and activation of the muscle into force. To enable close tracking of the experimental joint moments derived from EMG signals, which are acquired during the execution of various motor tasks, an optimization algorithm, such as simulated annealing, is employed to alter the values of the parameters.

The final set of model parameters can be guided by a variety of calibration control functions. To ensure that the muscles function within their physiological range, the parameters are also restricted to change within predetermined boundaries during calibration.

A subject-specific neuromusculoskeletal (NMS) model that represents the musculotendon physiology, activation, and contraction dynamics for an individual is the result of the calibration.

CEINMS can be validated with a novel set of input data, which has not been used for the calibration process, and run with any of the four execution modes.

Input files are needed to perform calibration and simulation using CEINMS, configuration files are needed:

- Calibration Setup: contains the parameters describing the characteristics of the MTUs.
- Neural Mapping Setup: each MTU is associated with a muscle excitation obtained from the recorded EMG signals.
- Execution Setup: contains specifications regarding the algorithm employed for the representation of the neural control of the model by exploiting the data not used for the calibration.

The sEMG signals are not usable without prior processing. The signals acquired by a motion-capture system are saved in a format (.tdf) that cannot be used in the major NMS modeling software such as OpenSim and CEINMS. The use of software data conversion (e.g., MOtoNMS) allows data to be extracted and converted into the formats appropriate for performing NMS modeling. MOtoNMS is a public toolbox of Matlab, which can be configured via XML files.

With the algorithm execution of MOtoNMS some data to the OpenSim and CEINMS execution can be obtained:

- *Static Elaboration:* .trc files save the coordinates related to the markers applied to the subject necessary for the execution of the Scale tool in OpenSim.
- *Data Processing:* data related to the dynamics of the motion i.e., .trc files are computed marker trajectories are saved for the IK execution and the values related to the external forces applied to the model to be used in the ID in OpenSim. Envelopes of the EMG signals to be used as experimental muscle activations are normalized.

From the data acquired during a subject's movements, it is possible to calculate using OpenSim the joint kinematics and the data needed as input to use CEINMS:

- Length of muscle-tendon units obtained from OpenSim's Analyze Tool.
- Arm joint moments obtained from the Analyze Tool of OpenSim.
- Muscle activations obtained from sEMG signals (after processing with MOtoNMS).
- Joint moments obtained by an ID problem in OpenSim to perform the calibration.

Neural Control

The problem related to the lack of EMG signals for some muscles that electromyography of the surface presents in CEINMS is overcome. The software thanks to the possibility of combining linearly any time-varying signal obtains new muscle excitations from signals of recorded muscle activation. These new signals, related to the excitation of those MTUs belonging to undetectable or inaccessible muscles, are used together with the other excitations as inputs to the Neural Control Solution Algorithm. This algorithm by means of a simulated annealing technique minimizes a function to guarantee the solution of an optimization problem The operation modes require solution of an optimization problem. Except for full-predictive model, the objective function is defined as:

$$F_{obj} = \alpha * \Sigma_{k \epsilon DOFs} \ (\tau_k - \widetilde{\tau_k} \ )^2 + \beta * \Sigma_{j \epsilon MTUs} \ (e_j - \widetilde{e_j})^2 + \gamma * \Sigma_{j \epsilon MTUs} \ (e_j)^2 \quad 3.15)$$

Where τ_k is the moment at joint k as estimate by CEINMS, $\widetilde{\tau_k}$ is the experimental moment at joint k, e_j is the estimated excitation for MTU j and $\widetilde{e_j}$ is the experimental excitation for MTU j; α, β, γ are the positive weight factors which characterized different behaviors that the function can assume. With this algorithm there are different neural controls:

- *EMG-driven mode*: this algorithm is characterized from EMG signals registered for each MTU, so there isn't any results' optimization;
- *EMG-assisted mode*: an optimization problem for the excitation obtained by EMG experimental data is executed. For muscles without EMG signals, the excitations are calculated by a linear combination of available signals.
- *Static Optimization*: with the experimental EMG signals, every muscular excitation is synthetized by an optimization algorithm.
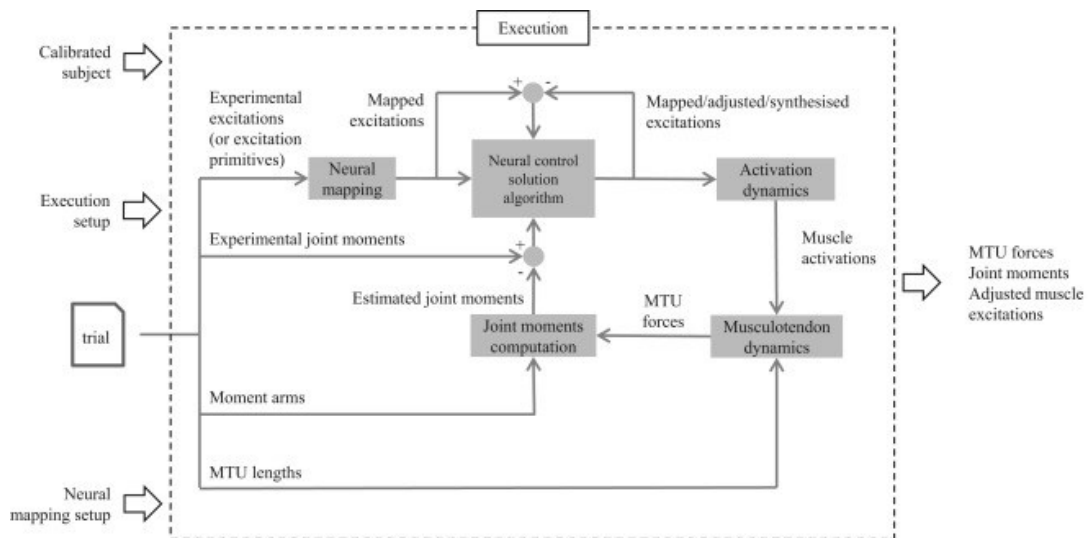
Figure 3.31 Schematic representation of CEINMS execution. It is shown the use of the Neural Mapping and the Neural Control Solution Algorithm [30]

Neuromusculoskeletal models used in CEINMS.

Two separate models of muscle activation dynamics are implemented by CEINMS, and three different models of muscular contraction dynamics are used to reflect the conversion of muscle activation and muscle kinematics into force. Extracted from experimental EMG readings are signals that represent muscle excitation (e(t)), which represents the neural drive muscles. Raw EMG signals are often first rectified fully, then high-pass filtered using a zero-lag fourth-order recursive Butterworth filter (30 Hz), and then low-pass filtered using a Butterworth with a 6 Hz cutoff frequency. Muscle excitation is used as an input signal for CEINMS software.
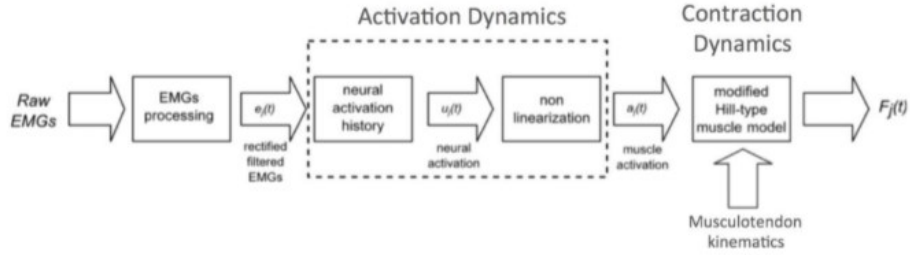
Figure General 3.32 Data processing flow showing activation dynamic and contraction dynamic.[29]

The activation dynamic model, which has been demonstrated to improve muscle force predictions, is used to simulate the muscle's twitch response to infer neural activation from muscular excitement. A critically damped linear second-order differential system described in a discrete form using backward differences serves as a representation for this:

$$u_j(t) = \alpha \, e_j \, (t-d) - \beta_1 \, u_j \, (t-1) - \beta_2 \, u_j \, (t-2) \quad (3.16)$$

The relation between neural activations and muscle activations is non-linear and CEINMS has two solutions. The first was introduced by:

$$a_j(t) = \frac{e_j^{Ajuj} - 1}{e^{Aj} - 1} \quad (3.17)$$

Where a_j (t) is the activation of the j-th muscle, and Aj is the non-linear shape factor.

With the second model, the uj☐ aj transformation is defined as a piecewise parametric function:

$$\alpha_j \, (t) = \alpha_j^{act} \, ln \, (\beta_j^{act} \, u_j(t) \, +1), \; with \; \; 0 \leq u_j \, (t) \leq u_0 \quad (3.18)$$

$$\alpha_j \, (t) = m_j \, u_j \, (t) \, +c_j, \; with \; \; u_0 \leq u_j \, (t) \leq 1 \quad (3.19)$$

For each muscle, j, α_j^{act}, β_j^{act} , m_j , c_j, depend only on the shape Aj constraint in the interval (0, 0.12].

Contraction dynamics Modeling

Muscle-tendon kinematics and muscle activation are used as input for a modified Hill-type muscle model, which comprises an active force-generating component, the muscle fibers, in series with a passive one, the tendon.

The muscle fiber force depends on three factors:

- The active force-length that express the ability of muscle fibers to produce force at different lengths: $f_\alpha\ (\widehat{l}_m)$

- The passive force-length that represents the force response of the fibers to strain: $f_p(\widehat{l}_m)$

- The force contribution of the velocity of the fiber contractions: $f_v\ (\widehat{l}_m)$

These curves represented are normalized to maximum isometric muscle force F^{max} to optimal fiber length $L^0{}_m$ (figure a) and the maximum muscle contraction velocity v^{max} (figure b). The figure c represents the exponential tendon force-strain relationship.
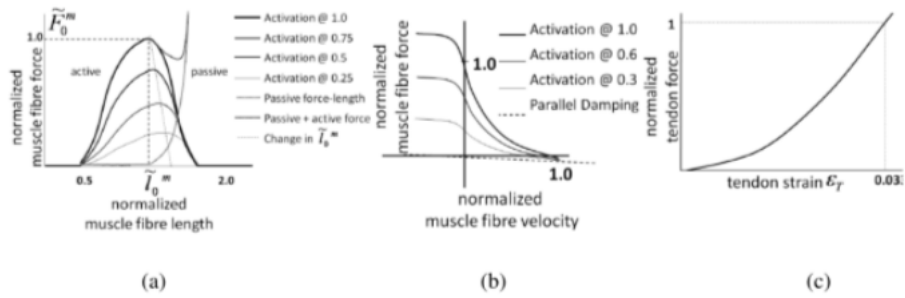
Figure 3.33: Representation of active and passive force-length curves.

The optimal fibre length decreases as the activation increases with this relationship:

$$F^{mt}=F^t=F^{max}[\ f_\alpha(\widehat{l}_m)\ f_v(\widehat{l}_m)\ a\ +f_p\ (\widehat{l}_m)\ +\ d_m\ \widehat{v_m}]\ cos\varphi \quad (3.20)$$

Where F^{mt} is a function of muscle activation and muscle kinematics produced by musculotendon unit (MTU), F^t is the tendon force, a is the muscle activation, d_m is the muscle damping element and φ is the pennation angle of the fibers witch is function of the instantaneous fiber length l_m.

The angle φ is given by this equation:

$$\varphi = sin^\wedge - 1\frac{L^0_m\ sin\ \varphi_0}{L_m} \quad (3.21)$$

Where l_m is the instantaneous length of the fibers and φ_0 represents the pennation angle when the fibers are at their optimal length $L^0{}_m$:

$$l_m = \frac{l_{mt} - l_t}{coscos\ \varphi} \quad (3.22)$$

The estimation of fibers' length depends on the passive element's length: the tendon. CEINMS implements three model to the estimation of the forces produced by MTU of each muscle:

1. *Integration Elastic Tendon (IET).*

   This method does not produce robust results because it is based on integrations of tendon stiffness relationships. The rate of contraction of the fibers v_m is calculated by optimization to then be integrated through the algorithm of Runge-Kutta-Fehlberg to obtain the relative lengths of the muscle fibers l_m and tendon l_t. Next, the strain of the tendon is calculated:

$$\epsilon = \frac{l_t - l_{ts}}{l_t} \quad (3.23)$$

   Where l_{ts} is the reposed length of the tendon. The force produced by the tendon F^t is calculated by exploiting its force-strain relationship, and to divide its active and passive, the muscle activation signal (α) was used. Finally, v_m is obtained from the inversion of the force-velocity relationship of contraction and is used for the subsequent iteration as the initial parameter.

2. *Equilibrium Elastic Tendon Model (EET)*

   The model uses a Van Wijngaarden-Dekker-Brent optimization routine to find the root of the equation:

$$F^{mt}(\widehat{l_m}) = F^t(\widehat{l_m}) \quad (3.24)$$

   Where $F^{mt}(\widehat{l_m})$ is the solution of the previous equation (3.20) with the derived calculation of v_m. $F^t(\widehat{l_m})$ is obtained as a combination of three different equations (3.21) and (3.22) and (3.23) and from the relationship force-deformation where the tendon deformation ϵ is expressed in function of the MTU $\widehat{l_m}$ length.

3. *Stiff Tendon (ST)*

   The tendon is an element of infinite stiffness whose length is equal to that at rest so as to reduce the time required to perform calculations.

   The use of models based on ordinary differential equations (ODEs) produce results that are not always correct in the case of high levels of stiffness or excessively small length of the tendon. The EET and ST models have similar behaviors. In particular, the EET

model produces reliable solutions with respect to changes in the lengths l_{ts} , l_{mt} and their ratio especially during calibration where these parameters are optimized.

CEINMS implements algorithms to calibrate the model to the parameters of the individual who performed the motor activities during the EMG signal acquisition phase. Identifying the parameters that most accurately depict the activations of each acquired MTU is the calibration's goal. Typically, a small number of dynamic or static collected trials are utilized against all the tasks that a subject completes. The initial calibration parameters are taken from the literature and kept as uncalibrated. They are then compared to the relevant experimental data, and the error between them is iteratively decreased.

A CEINMScalibrate setup file consists of element named *ceinmsCalibration* that contain these elements:

- *subjectFile* the location of the subject description file
- *exctitationGeneratorFile* the location of the Excitation mappings description file
- *calibrationFile* the location of the calibration parameters file including trials to calibrate on
- *outputSubjectFile* the name of the output calibrated subject file

The following equation defines the function that must be minimized as:

$$f_{cal} = \sum_t^{Ntrials} \sum_d^{NDOFs} E_{t,d} \quad (3.25)$$

where:

$$E_{t,d} = \frac{1}{N_r} \sum_r^{N_{rows}} \left(\frac{\left(\overline{M_{t,d,r}} - M_{t,d,r} \right)^2}{var\left(\overline{M_{t,d}} \right)} + p_r \right)$$

$$(3.26)$$

p_r is obtained by:

$$p_r = \sum_j^{NMTUs} P\,(r,j) \qquad (3.27)$$

and P(r,j) is obtained by:

$$P\,(r,j) = \begin{cases} 100\left(\tilde{l}_{mr,j} - 1 \right)^2, & if \; \left| \tilde{l}_{mr,j} - 1 \right| > 0.5 \\ 0 & , \; otherwise \end{cases} \qquad (3.28)$$

In order to reduce the length differences between the proofs, is possible to normalized the sum of the square difference between the predict particular moment $\underline{M_{t,d,r}}$ and the experimental one ($M_{t,d,r}$) to the variance of test and number of row for each t-esim trials.

The penal solution P (r,j), discourages the adoption of non-physiological solutions which correspond to values outside its operational range (0.5-1.5).

After calibration, the optimized parameters are used to run CEINMS using a new test set as input and any neural control solution algorithm [30].
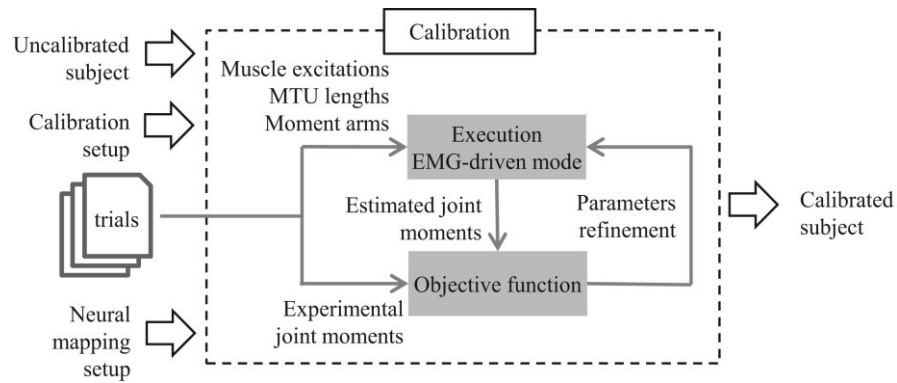
Figure 3.34 Calibration of CEINMS

Chapter 4: Materials and Methods

In this thesis work, a dataset including kinematic, dynamic and electromyographic data of subjects with Parkinson's disease was analyzed. Two types of different treatments were considered: in the first case subjects were treated with classical strategies, meanwhile on the other hand, EKSO robotic therapy was considered. Gait analysis took place at the motion analysis laboratory of Villa Margherita, Arcugnano, Vicenza. Right and left dynamics were analyzed.

Through MOtoNMS software the movement data were converted in order to be applied into OpenSim and then, CEINMS musculoskeletal modeling software. Muscle activation data were simultaneously processed in Matlab in order to validate the results of the therapy.

On the subject's lower limb, at the skin level, markers were placed at the anatomical landmarks points according to the IOR-GAIT protocol to acquire trajectories. Each subject then walked at a self-chosen pace. Several trials were performed, but only trials in which adequate support was visible within the two force platforms were chosen for subsequent processing.

Below the specifications regarding the data set, information about the acquisitions and the methods used to process the kinematics and dynamics data are reported.

Finally, the methods implemented for the calibration and extraction of muscle forces, muscle activations and torque are presented, which, through the averages and standard deviations of the individual subjects, will be fed back into Matlab to visualize and compare the forces and muscle activations of the groups of subjects combined.

4.1 Data Set

In this project, several trials of different patients were analyzed, some of them treated with an EKSO therapy and others treated with classical therapies that will be named with the acronym FKT who will be used as control subjects. The mean and standard deviation value was calculated based on the body mass expressed in kilograms of the patient at the time they were recruited. The mass, in all patients, was considered unchanged from time T0 to time T1 More specifically, the dataset will consist of:

- EKSO's subject

Subject	Weight (Kg)
S1	74
S2	90
S3	76
S4	70
S5	81
S6	96
S7	85
Mean	*81,71*
STD	*8,56*

Specifically, of these subjects, S1, S2, S3, S5 were processed from MOtoNMS, while S4, S6, S7 were previously processed. However, all subjects have three right and three left bearings recorded correctly on the footplate in both the early phase at time T0 and the late phase at time T1.

- FKT's subject:

Subject	Weight (Kg)
S8	55
S9	68
S10	80
S11	70
Mean	*68,25*
STD	*8,90*

For FKT patients, we do not have all the trials as in the previous case, but we are in possession of only a limited portion of corrected footplate bearings.

Therefore, we have the following data available:

Subject	T0 trials	T1 trials
S8	four right and two left steps on the footplate;	three right steps and three left steps on the platform;
S9	one left dynamic was recorded correctly on the number one force platform on the platform.	two left dynamics were recorded correctly on platform two and one right dynamic was recorded on platform 1.
S10	one left dynamic was recorded correctly on the number one force platform on the platform.	three right dynamics were recorded correctly on the force plate one and three left dynamics were recorded correctly on the force plate two.
S11	one left dynamic was recorded correctly on the number one force platform on the platform.	Three left and one right dynamics were correctly recorded on the platform.

- Complete Dataset:

Subject	Weight (Kg)
S1	74
S2	90
S3	76
S4	70
S5	81
S6	96
S7	85
S8	55
S9	68
S10	80
S11	70
Mean	*76,82*
STD	*10,84*

4.2 Data Acquisition

Gait and posture have been measured at the Motion Analysis Laboratory of the Fresco Parkinson Center of Villa Margherita in Arcugnano (VI) with a 10m walkway. [3]. Gait Cycles are collected with an 8-cameras optoelectronic system (Vicon) with a frequency of 120Hz which are synchronized with two force plate with 1000 Hz of frequency and 8-channel electromyographic system named Cometa Waveplus with a frequency of 1000 Hz. The 8 channels analyzed are: Left Biceps Femoris, Left Gastrocnemius Lateralis, Left Rectus Femoris, Left Tibialis Anterior, Right Biceps Femoris, Right Gastrocnemius Lateralis, Right Rectus Femoris, Right Tibialis Anterior.

A modified version of IOR GAIT protocol is used for both anatomical landmarks identification and joint angles calculations. In our study we associate 28 of the 40 markers present in this figure, and, in addition to this we have C7 and L5 markers too. Here there is a description of our markerset:

- C7☐ seventh cervical vertebra
- L5☐ fifth lumbar vertebra

Pelvis:

- RASIS/LASIS☐ Superior Anterior Iliac Spine
- RPSIS/LPSIS ☐ Superior Posterior Iliac Spine

Thigh:

- RGT/LGT ☐More lateral prominence of the outer surface of the greater trochanter
- RTH/LTH ☐ They should be placed near the midline of the thigh. They are used only to distinguish the right side from the left side.
- RLE/LLE ☐ More lateral prominence of the lateral femoral epicondyle. Together with LM markers, it determines the position of the knee joint axis.

Shank:

- RTT/LTT ☐ Most anterior border of the tibial tuberosity.
- RLM/LLM ☐ Distal apex of the lateral malleolus.
- RMM/LMM ☐ Distal apex of the medial malleolus.
- RTT/LTT ☐Most anterior prominence of the tibial tuberosity

Foot:

- RCA/LCA Upper ridge of the posterior surface of the calcaneus.
- RVM/LVM Dorsal aspect of fifth metatarsal head.
- RFM/LFM Dorsal aspect of first metatarsal head.
- RVMH/LVMH Head of the fifth metatarsal, dorso-lateral aspect of the fifth metatarso-phalangeal joint
- RIMH/LIMH Head of the first metatarsal
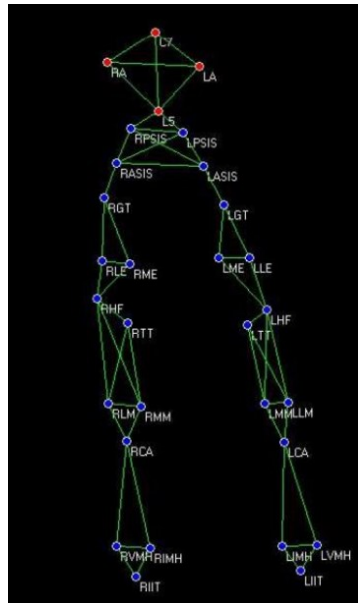
Figure 4.1 IOR gait Model

4.3 Data Processing

Nexus is a part of a Vicon System and is important for the capture application. This system is made up of several elements: MX Cameras, MX Connectivity Units, MX Host PC, MX Cables, Vicon Calibration Devices and accessories, Cameras [31].

First, there are data files that are generated by Nexus during motion capture and analysis. For our study we need .c3d files. Then it is possible to create and edit these Vicon configuration file types during Nexus motion capture and analysis.

From the Nexus screen, you can retrieve the trajectories that will go into determining the track files in .c3d format. However, it is necessary to perform a calibration of the system each time you need to record the walks of a subject to verify that all the cameras are filming the subject correctly. Next, we need to recognize the markers acquired by the Vicon system and assign labels to each marker according to the IOR-GAIT protocol, in addition, we need to identify the

force platforms, and select only valid trials, that is, when the whole foot rests completely on the platform for an entire step cycle. At this point, in our specific case, only three right and three left trials were selected for EKSO subjects. Once the trials under consideration have been selected, it is necessary to specifically derive the frames to identify a complete stride. Two different ways can be used to obtain the specific frames:

1. by observing the markers of the calcaneus (CA) and first metatarsal head (RIMH/LIMH) and recording their footing on the footplate.

2. by observing the vector of GRFs indicating exactly the instants with its minimum values.

MOtoNMS

The software MOtoNMS (*Matlab Motion data elaboration Toolbox for Neuromusculoskeletal application)* is a tool that permits to obtain movement elaboration data that are necessary for modellation software [32]. The most important steps are:

1. *C3DMAT:* kinematics data are converted from C3D format in structure compatible with Matlab (.mat)

2. *Data Processing*: processing of the trajectories of the markers, ground reaction forces, and the electromyographic signals contained in the dynamic tests produces the trace(.trc) and animation(.mot) needed by OpenSim.

3. *Static Elaboration*: processing dynamic evidence by calculating joint centers and saving them in the corresponding trace files.
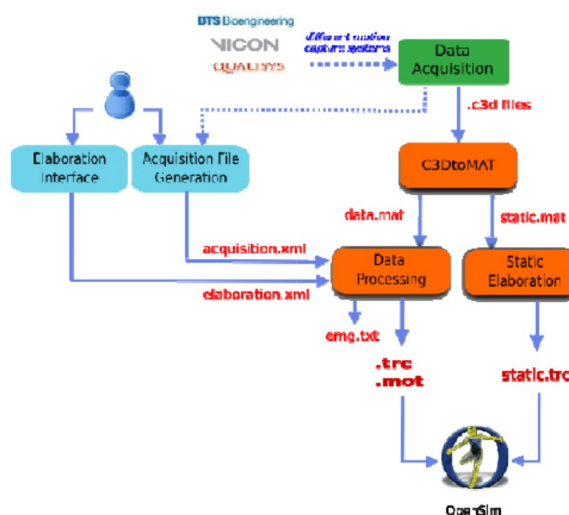

Figure 4.2 General Scheme proposed Matlab Tool [32]

After data loading from .mat files, marker trajectories are interpolated and then are filtered with a Butterworth filter at 6Hz. EMG signals are processed in the same way.

The configuration of each step is done through graphic user interfaces in Matlab, which create the following three XML configuration files:

- *Acquisition.xml* is created from Acquisition Interface and contains all the information about the movement acquisition like EMG protocols, marker set, the coordinate orientation system…
- *Elaboration.xml* is created from Elaboration Interface and contains all the parameters of data elaboration as dynamic trials or input data filters.
- *Static.xml* is created by Static Interface and contains all the parameters for the static elaboration.
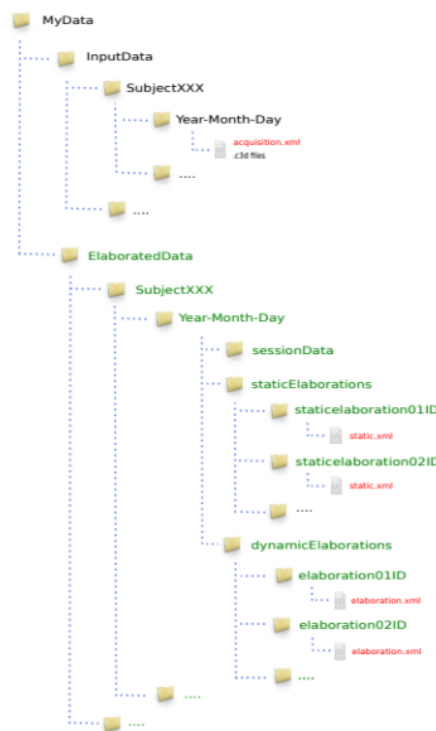
Figure 4.3 Data Organization

From this figure it is important to observe that input data are in black, the configuration's file created by MOtoNMS are in red and the folder created by toolboxes are in green.

In black, it is possible to notice that the data from the individual acquisition, in each collection along with the C3D files, is the 'acquisition.xml' file that describes the data collected [33].

The execution of MOtoNMS automatically creates new data collections by replacing the name of the InputData collection with ElaboratedData. Running different tools creates:

1. C3DMAT

Data collected with a motion capture and force plate system are labeled and then exported as a .c3d file, and they are converted in Matlab's structure with .mat format. To perform this operation, however, it is necessary to specify the path to the input file. This path can generate the corresponding collections containing the data in the .mat format by saving them in the sessionData folders.

The developed tool is divided in three main parts: (1) C3DtoMAT, (2) Data Processing, and Elaboration for scaling OpenSim models. This avoids having continuous accesses to .c3d files, which are computationally expensive and redundant. Starting from these structures, the second part produces .trc and .mot files for OpenSim, storing markers and ground reaction forces (GRF) information respectively.
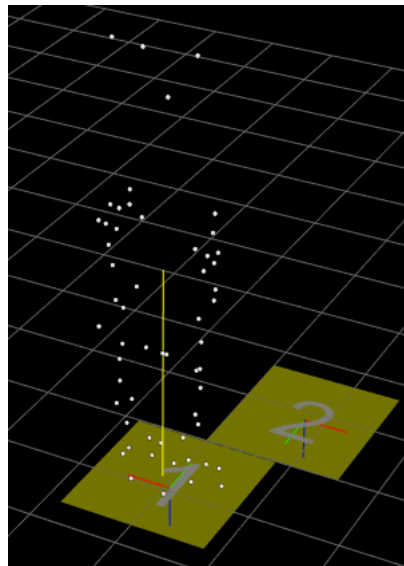
Figure 4.4 Force Platform and Marker position of a subject.

2. Acquisition Interface:

A graphic interface (GUI) needs to create an acquisition file (acquisition.xml) which must be created and inserted in the *InputData* folder with C3D data before the execution of other instructions. It is important to follow this procedure:

1. Select the file *mainAcquisitionInterface.m* and then select the input folder of a subject at T0 or T1 instant.
2. Select the correct acquisition laboratory that in this case is Villa Margherita;
3. Select the staff: is required the voice "person in charge" where we have to put 'zs'
4. Insert the Patient's characteristics like Name or Acronymous, code, birth date, age, weight, height, foot size and pathology.

5. Insert the Acquisition Date (yyyy-mm-dd).

6. Insert the Frame Rate: 120Hz in Villa Margherita Laboratories.

7. Select the Marker's protocols: UNIPD_IORgait_forOpenSim

8. Insert the number of EMGs System Used: 1;

9. Insert the EMGs System:

    a. Name: Cometa waveplus;

    b. Frame: 1000Hz

    c. Number of used channels: 8

10. Select the EMG's protocol: VM-8 muscles and then we must select all the 8 channels ID as follows.

```
<EMGsProtocol xmlns:xsi="http://www.w3.org/2001/XMLSchema-instance">
    <Name>trial-</Name>
    <MuscleList>
        <Muscle>rawEMG.Right_Tibialis_Anterior</Muscle>
        <Muscle>rawEMG.Left_Tibialis_Anterior</Muscle>
        <Muscle>rawEMG.Right_Rectus_Femoris</Muscle>
        <Muscle>rawEMG.Left_Rectus_Femoris</Muscle>
        <Muscle>rawEMG.Right_Gastrocnemius_Lateralis</Muscle>
        <Muscle>rawEMG.Left_Gastrocnemius_Lateralis</Muscle>
        <Muscle>rawEMG.Right_Bicept_Femoris</Muscle>
        <Muscle>rawEMG.Left_Bicept_Femoris</Muscle>
    </MuscleList>
    <InstrumentedLeg>Right</InstrumentedLeg>
</EMGsProtocol>
```

Figure 4.5: 8 channels of muscles

11. Associate each trial with the force platform on which it rested its foot.

In this way the procedure can be completed, and this data can be saved in a xml setup file named *Acquisition.xml*.

3. Data Processing

This tool can create the dynamicElaboration folder. Data Processing uses motion data saved as matlab structures by C3DMAT and produces trace files (.trc) containing marker information and motion files (.mot) containing force information for OpenSim. It is possible to perform this step thanks to the GUI that allows a choice of parameters saved in the elaboration.xml file.

The fundamental data processing's steps are:

1. Run the file ElaborationInterface.m and select the correct Input data folder.

2. Insert the identification filter (the acronym of the subject).

3. Select the dynamic trials to elaborate: (all files without the static one).

4. Filter the cut-off frequencies for filtering:

- o the trajectories of the Markers: 6Hz.
- o the forces: 13Hz.
- o the center of pressure (COP): 13Hz.
5. Select method for the analysis of window computation: Manual.
6. Insert the initial and final frame for each trial.
7. Select markers to insert in the .trc file: select all the 40 markers.
8. Select the EMG labels: *VillaMargherita-CEINMS*
9. Select EMG: all
10. Select EMG to max: all files without the static one.
11. The elaboration.xml file has been created, now it is possible to run data and see some graphic images.

Normalization of EMG signals is performed on trials that are selected by the user, which may involve the performance of maximal voluntary contraction (MVC) trials. In this work, EMG signals were normalized against all trials acquired for one same subject.

The Data Processing tool allows processing the acquired positions of the markers and Ground Reaction Forces to be used as input files in Opensim, i.e., in the NeuroMuscleSkeletal (NMS) modeling environment. The analysis window in MOtoNMS is used to select the part of the data to be processed. Figures are then created for visual analysis of:

- raw EMG;
- Envelopes;
- CoP

The processed GRFs, on the other hand, are used to calculate free angles based on the filtered forces, moments, and centers of pressure for selected instants. The markers and GRFs are saved for use in Opensim.

DataProcessing also performs the processing of EMG signals which represent the muscle activations. A subset of all acquired muscles can be selected. The maximum value for each EMG signal is estimated by one or more trials and saved in a text file (maxemg.txt). The envelopes for the EMG signals are calculated and normalized with their maximum value, they are saved in a motion file (emg.mot), the name can be chosen by the user. Storage text formats are also available for the recording of EMG processing.

MOtoNMS execution was done for each subject's data. The processing dynamics of the EMG signals from each trial were used in the analysis, conducted in MATLAB, to identify the

muscles that best represented muscle synergies. This small number of muscles provide the muscle activations for the NMS modeling relative to each subject in CEINMS.
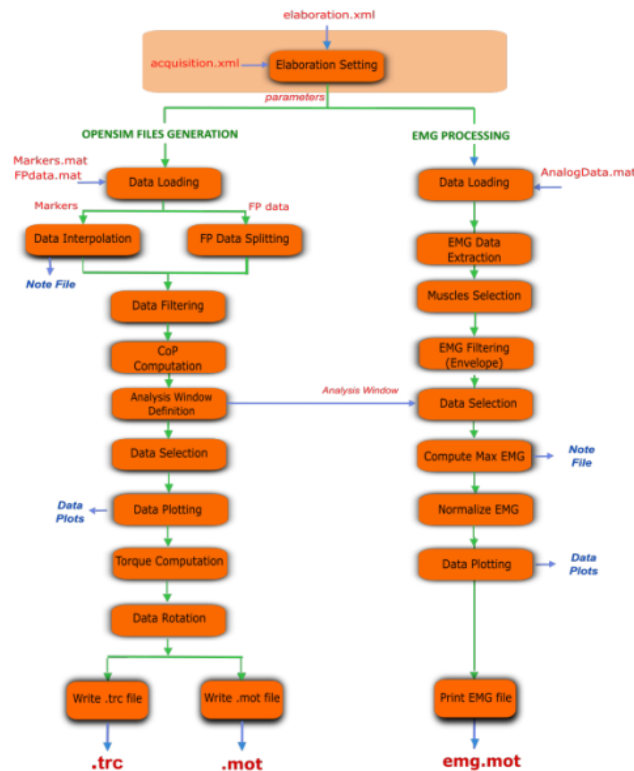

Figure 4.6 Data Processing general scheme [32].

4. Static Elaboration

This procedure is useful to create a StaticElaboration folder. Using as input the .mat files created by C3DMAT, Static Elaboration applies the same filtering procedure used in Data Processing. The main step is the estimation of the center of articulation (JC), being the points that allow to improve the accuracy of scaling in OpenSim. The method for calculating the center of joint of the pelvis (HJC) exploits the equations defined by Harrington while the calculation of the knee joint centers (KJC) and ankle joint centers (AJC) uses the midpoint between the specific anatomical landmarks in the corresponding setup files. The trajectories obtained are added to the list of user-defined markers, and then the list complete is converted to the OpenSim reference system and saved in the trace file (.trc). It is important to check the setup files for the names of the individual protocols of markers, as they use different labels. The execution of this step is completely defined by a set of user-selected parameters that are saved in the static.xml configuration that is obtained through a graphical user interface (GUI).

The main steps are:

1. Run the file StaticInterface.m and select the correct Input data folder.
2. Select the static file from the folder.
3. Insert the acronym of the subject.
4. Filter the markers trajectories with a cut off frequency of 6Hz.
5. Compute the joint centers and select joints (Ankle, Knee, Hip).
6. Select all the 40 markers.
7. The static.xml file has been saved.
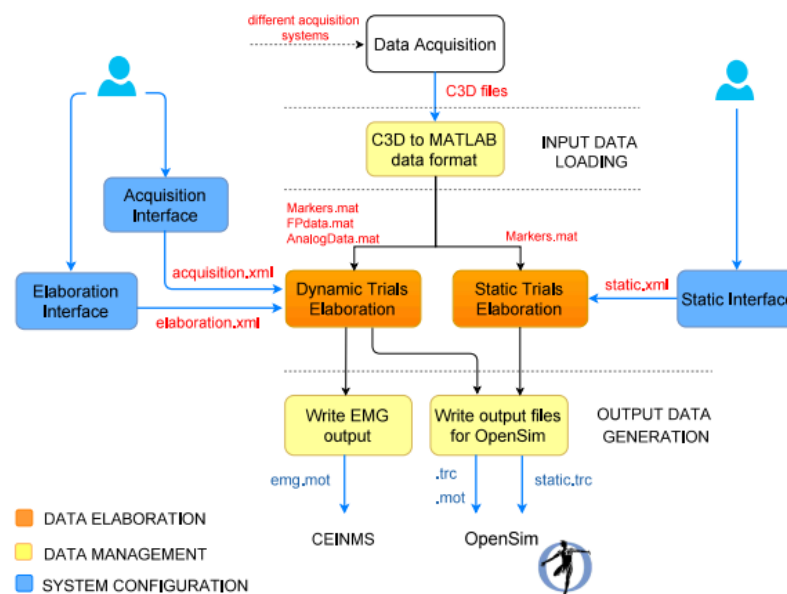
Figure 4.7 MOtoNMS scheme

OpenSim

a. Scaling Tool

The following input data were used for the Scaling process:

- The subject's mass in kg.
- An .xml file containing marker-set specifications consisting of 40 markers set according to the IOR-Gait acquisition protocol.
- The starting model for each subject is the gait2392 described in the previous chapter.
- The .trc files obtained from the static processing of each subject are then entered.
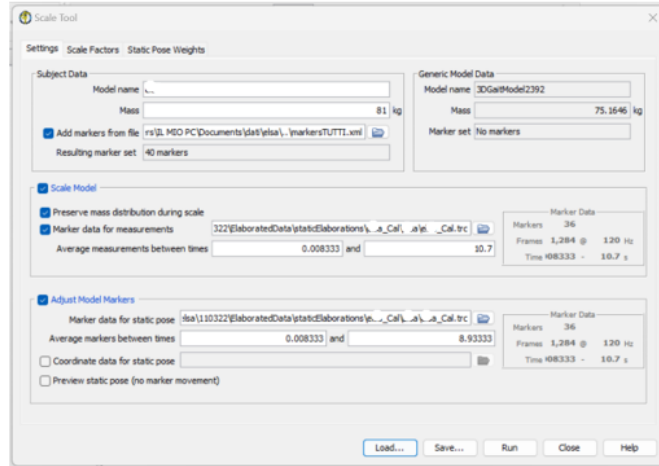
Figure 4.8 Scaled Tool of S5 Subject

b. Muscle Optimizer Tool

The Inverse Kinematics' parameters obtained by the scaling tool are optimized respect on gait2392 model for these muscles of lower limbs: Semimembranosus, Semitendinosus, Biceps femoris capitis longus, Biceps femoris, Sartorius, Adductor Longus, Tensor Fascia Lata, Rectus Femoris, Vastus Medialis, Vastus Internal, Lateral Vasto, Medial Gastrocnemius, Lateral Gastrocnemius, Soleus, Tibialis Anterior, Short Peroneus, Long Peroneus, and Third Peroneus. The model related to the optimized scaling of each subject was saved in the same folder of the previous tool.
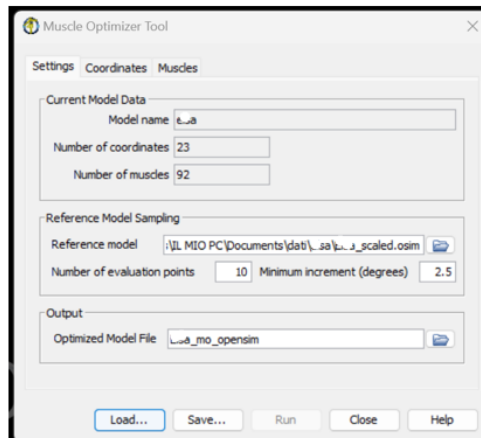

Figure 4.9 Muscle Optimizer Tool of S5 Subject

Batch Processing

Before using CEINMS, through a pipeline, it is necessary to create the MuscleAnalysis, InverseKinematics and InverseDynamics folders through batch processing. The main steps are:

1. From the BOPS-v9 folder run the file main.m
2. Select the subject folder in ElaboratedData\DynamicElaboration\subject_name\
3. Select the subject model .osim that was previously created and optimized.
4. Insert the subject acronymous for the IK setup.
5. Select the templates for the IK processing: IKsetup_VMdynamicTasks.
6. Select the trials to elaborate.
7. Select the templates for ID processing:
   a. ExternalForce_L1_6: a trial in left platform
   b. ExternalForce_L1R2_6: all trials left are in the force platform one and all the right trials are in the force platform two.
   c. ExternalForce_R1_6: a trial is in the right force platform.
   d. ExternalForce_L2R1_6: all right trials are in the force platform one and all the left trials are in platform two.
8. Choose the low pass cut off frequency for coordinate: 6Hz.
9. Insert the subject acronym for the Muscle Analysis.
10. Select the templates for Muscle Analysis processing: MA_setup.
11. Choose the low pass cut off frequency for coordinate: 6Hz.

In this step it is possible to have a different combination of trials, so this procedure can be made more than one time for each subject.

With batch processing, data can be processed without using the OpenSim GUI, running numerous complete analyses in shorter periods of time.
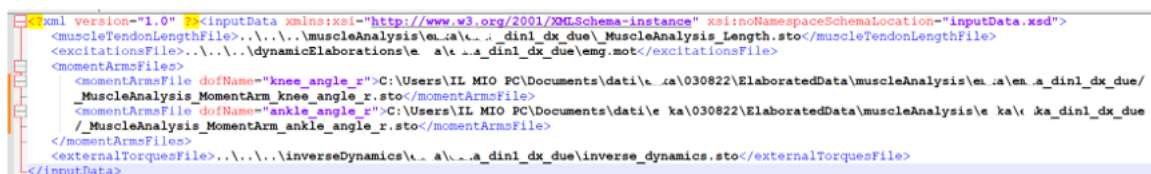
CEINMS

The execution of CEINMS involves a data calibration phase and subsequent data visualization.

Calibration:

Once the scaling and the Muscle Optimizer Tool were run, file paths leading to some specific data were copied and pasted for each patient trial including [29]:

An input data description file consists of a root element named inputData that contains the following elements:

- *muscleTendonLengthFile*: the location (absolute or relative) of the file containing the length of the muscle-tendon units during the trial. We can find this information in the Muscle Analysis folder of each trial of each subject.

- *momentArmsFiles:* a list of momentArmsFile elements, each being the location (absolute or relative) of the file containing the moment arms of the muscle-tendon units, relative to the degree of freedom given as dofName attribute, during the trial. Those can be found in the Muscle Analysis folder of each trial.

- *excitationsFile*: the location of the file containing the excitations (EMG signal envelopes) recorded for the trial. It can find this in the Dynamic elaboration folder of each trial.

- *externalTorquesFile:* the location of the file containing the torque that the subject exerts at each joint. It can be found in the Inverse Dynamic folder of each trial

Figure 4.10 Script of setup muscle file of a trial

For this work, we have used 8 channels of s-EMG system and they are mapped to 19 MTU and we have considered all the DOF of the lower limbs. Before using the CEINMSCalibrate executable from the command prompt, it is necessary to create an additional Setup XML file. In this file all data related to the execution of a simulation in CEINMS:

- The position of non-calibrated parameters of each subject obtained by the literature.

- The position of the muscular activation obtained by the input signals and how it is possible to mapping each MTU. In this work we have considered these muscles: Biceps femoris long head, Biceps, Short head femoris, Lateral gastrocnemius, Medial gastrocnemius, short peroneus, Peroneus long, Rectus femoris, Semimembranosus, Semitendinosus, Soleus, Tibialis anterior, Vast Internal, Lateral Vast, Medial Vast, Gluteus Major, Gluteus Medius, Tensor fascia lata, Sartorius and Adductor Longus.
- The position of the configuration file.
- The position of the output file where we can save the calibrated parameters.

Figure 4.11 Output of 15 muscles

This file describes the control of the muscular excitation. The *inputSignal* element contains the identification of the s-EMG signals contained in the emg.mot files obtained by MOtoNMS.

Next, it is necessary to implement configuration files for each trial used. From the CEINMS calibration folder, there are files renamed Cfg (configuration files) in which the file path must be changed to insert the file paths of the trials divided into right and left trials.

A calibration configuration file consists of a root element named calibration that contains the following elements [29]:

- algorithm: a description of the optimization algorithm to use.
- NMSmodel: a collection of options for the simulation of the model.
- calibrationSteps: a list of step elements (at least one) that describe an optimization procedure.
- trialSet: a list of XML files, each describing a trial to be used for calibration (Trial input data).

Now, it is possible to open the command prompt and perform the actual calibration. It is then necessary to type CEINMScalibrate -S " " where the file path of the right and left trials of the setup file will be entered in the superscripts.

It uses an optimization approach that minimizes a cost function to refine the muscle parameters that control how these tissues produce force. Since the implemented cost function is obtained as the discrepancy between the estimated and measured joint moments during a series of tasks, changing this file could have very different results in terms of the subject's calibrated parameters.

There are several methods by which all the muscle parameters describing the subject can be calibrated, but the technique used in this project turns out to be the most accurate.

If setup and data files can be correctly found, calibration will start after the number of total parameters is printed to screen. Calibration time may be variable and depends on the number of calibration's parameters.

When software execution finishes, an XML description of the calibrated subject will be written to the file that was specified as *outputSubjectFile* in the main setup XML file. [29]

These files are helpful for gaining a better understanding of how each muscle behaves and for ensuring that there are no errors or artifacts in the input data or in the model parameter.

Output File:

A subject description file (output file) consists of a root element named subject that contains the following elements:

- *mtuDefault* that contains the parameters that describe muscle-tendon unit and parameters common to all muscles as:
  - electromechanical delay (d in activation dynamics)
  - percentage Change in optimal fiber length depending on activation in γ Contraction dynamic.
  - damping the muscle damping coefficient (dm in Contraction dynamics);
  - maxContractionVelocity the normalized maximum contraction velocity of the fiber.
  - four curve elements, describing the normalized force/length (active and passive), normalized force/velocity, normalized tendon force/strain curves shown in the active and passive force curves) figure in section Contraction dynamics. Each curve has a name, a list of y-coordinates, and the corresponding x-coordinates that can be interpolated to provide the complete curves.

```
  <name>activeForceLength</name>
  <xPoints>-5 0 0.401 0.402 0.4035 0.52725 0.62875 0.71875 0.86125 1.045 1.2175 1.43875 1.61875 1.62 1.621 2.2 5</xPoints>
  <yPoints>0 0 0 0 0.226667 0.636667 0.856667 0.95 0.993333 0.77 0.246667 0 0 0 0 0</yPoints>
</curve>
<curve>
  <name>passiveForceLength</name>
  <xPoints>-5 0.998 0.999 1 1.1 1.2 1.3 1.4 1.5 1.6 1.601 1.602 5</xPoints>
  <yPoints>0 0 0 0 0.035 0.12 0.26 0.55 1.17 2 2 2 2</yPoints>
</curve>
<curve>
  <name>forceVelocity</name>
  <xPoints>-10 -1 -0.6 -0.3 -0.1 0 0.1 0.3 0.6 0.8 10</xPoints>
  <yPoints>0 0 0.08 0.2 0.55 1 1.4 1.6 1.7 1.75 1.75</yPoints>
</curve>
<curve>
  <name>tendonForceStrain</name>
  <xPoints>-10 -0.002 -0.001 0 0.00131 0.00281 0.00431 0.00581 0.00731 0.00881 0.0103 0.0118 0.0123 9.2 9.201 9.202 20</xPoints>
  <yPoints>0 0 0 0 0.0108 0.0257 0.0435 0.0652 0.0915 0.123 0.161 0.208 0.227 345 345 345 345</yPoints>
```

Figure 4.12 Output file: Parameters

- *mtuSet* a list of MTU elements, each describing a muscle-tendon unit that actuates the model. Each muscle-tendon unit is described by:
    - the identification name of each MTU.
    - c1 and c2 are the constants C1 and C2 that describe the recursive coefficients in Activation dynamics.
    - shape Factor that describes the relation. between neural excitation and the muscle activation. It is nonlinear.
    - Optimal Fibre Length is the optimal fiber length at maximum activation.
    - Pennation length.
    - Tendon Slack Length.
    - Max Contraction Velocity that normalizes the maximum contraction velocity of the fiber.
    - Max isometric force
    - strength Coefficient is a multiplicative factor for maxIsometricForce; the rationale for its inclusion is that, instead of calibrating the maxIsometricForce parameter for each muscle.

```
<mtu>
  <name>rect_fem_l</name>
  <c1>-0.49290694455431</c1>
  <c2>-0.94628663260088</c2>
  <shapeFactor>-0.00100000002355613</shapeFactor>
  <activationScale>1</activationScale>
  <optimalFibreLength>0.110609847428617</optimalFibreLength>
  <pennationAngle unit="rad">0.08726646</pennationAngle>
  <tendonSlackLength>0.300781164054358</tendonSlackLength>
  <maxContractionVelocity>10</maxContractionVelocity>
  <maxIsometricForce>1169</maxIsometricForce>
  <strengthCoefficient>0.500000000004114</strengthCoefficient>
</mtu>
```

Figure 4.13 Output file: MTUs

- dofSet a list of dof elements, each describing a degree of freedom of the model. Each degree of freedom is defined by the name of the identifier and by the mtuNameSet (a list of the muscle that act on it)
- calibrationInfo that reports whether the subject has been calibrated.

```xml
<dofSet>
  <dof>
    <name>knee_angle_l</name>
    <mtuNameSet>bifemlh_l bifemsh_l lat_gas_l med_gas_l semimem_l semiten_l rect_fem_l vas_int_l vas_lat_l vas_med_l</mtuNameSet>
  </dof>
  <dof>
    <name>ankle_angle_l</name>
    <mtuNameSet>lat_gas_l med_gas_l per_long_l soleus_l tib_ant_l</mtuNameSet>
  </dof>
</dofSet>
<calibrationInfo>
  <calibrated>
    <startSubjectFile>C:\Users\BioMovMarco\Documents\DatiTesiGloria\dati\elsa\110322\ElaboratedData\ceinms\
    calibration\calibrationSetup\standardCalibrtion\../../uncalibrated/UniPD_uncalibrated_Delp_L.xml</startSubjectFile>
    <calibrationSequence>C:\Users\BioMovMarco\Documents\DatiTesiGloria\dati\elsa\110322\ElaboratedData\ceinms\
    calibration\calibrationSetup\standardCalibrtion\../../Cfg/standardCalibration/calibrationCfg_L.xml</calibrationSequence>
  </calibrated>
</calibrationInfo>
</subject>
```

Figure 4.14 Output file: DoF

Data Extraction:

Once the final output from the calibration has been obtained, the next goal is to visualize the results obtained through graphs. Through Matlab codes (exe_HybridParaOptimizer.m and exe_nmsDataExtration_visualization.m), a data structure can be visualized, which represent muscle activations, muscle forces, and moments.

exe_HybridParaOptimizer.m

This code allows us to estimate the best coefficients to run the hybrid model in CEINMS after the calibration of the model. There is a pathStart where is insert the file location that we need and we have to define the range of coefficients (α,β,γ). Then we have to extract the trials name by the execution from the trials simulation and from the 'execution\Setup\standardCalibration' path.

Next, a for loop is implemented with the goal of calculating the α,β,γ coefficients for all trials under consideration. A new Cfg file that contains the updated version of the coefficients will be saved. Next there will be the extraction of the variables involved in the cost function defined as:

$F_j = \alpha * E_{mom} + \beta * E_{act} + \gamma * E_{emg}$ where:

- *E_{mom}* represents the sum of squared differences between predicted and experimental joint moments.
- *E_{act}* represents the sum of squared excitations.

- *Eemg* represents the sum of the absolute difference between adjust and experimental EMG excitations for the MTUs with EMG data available.

As a final step there will be the extraction of files from the inverseDynamics and DynamicElaboration folders in order to create an output directory.

exe_nmsDataExtration_visualization.m

Input is assigned a data path corresponding to the file path leading to the ElaboratedData folder of the test subject. To display the images, the loaded data are those of activation calibration, muscle force and torques. As output, we will have the following images:
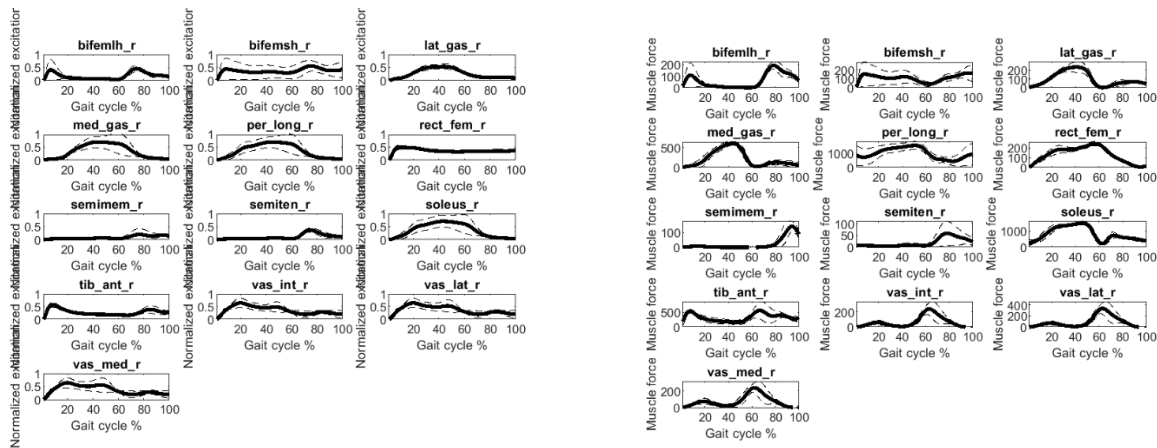
Figure 4.15 Normalized Activation and Muscle Force respectively

These data were obtained for each subject at both time T0 and time T1 regardless of the total number of trials we had available. Through the muscle activations, it is possible to visualize the normalized Gait Cycle trends of the 13 muscles under study, where, on the x-axis is represented the percentage of the gait cycle, where at 100% a full stance is identified, while on the y-axis the values of the muscle activations are normalized all between 0 and 1. Similarly, the muscle forces produce graphs with the same parameters.
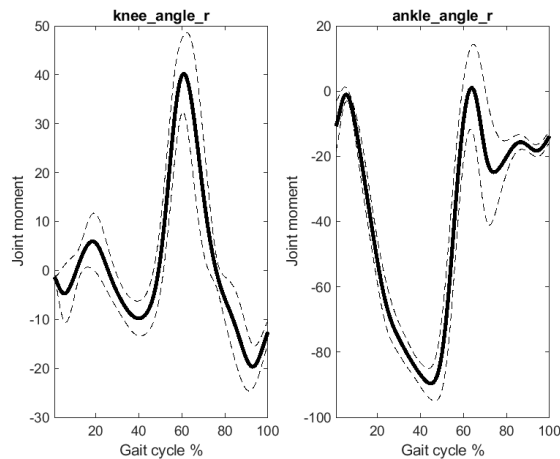
Figure 4.16 Torques

For torques, only knee and ankle moments are expressed. In this case on the x-axis is still represented the step cycle in percent, while on the y-axis are expressed the joint moments, which this time are not normalized between 0 and 1 but present a specific value.

Comparison between subjects:

The subjects are compared with each other according to the following matlab code: *matrixGroup_muscleFunctionalGroup.mat* by which different combinations were analyzed:

- All subjects at time T0 vs all subjects at time T1;
- EKSO subjects at time T0 vs all EKSO subjects at time T1;
- FKT controls at time T0 vs all FKT controls at time T1
- EKSO subjects at time T0 vs all FKT subjects at time T0
- EKSO subjects at time T1 vs all FKT subjects at time T1

The dataset consists of three different groups of subjects:

1. pathStoredT0, in which are placed all file paths up to the nmsData.mat folder that was obtained from the previous step of all subjects belonging to the T0 category. Associated with this pathStored is a *weightPd* matrix in which the masses of the subjects are entered.

2. pathStoredT1, in which are entered all file paths up to the nmsData.mat folder of the T1 population. Again, a matrix of masses is associated with this, which can be the same or different from the weightPd matrix depending on the data analyzed.

3.PathStoredCs in which healthy controls are present. During all comparisons, the same 13 subjects were always considered with the following mass matrix:

95

Then, it is important to load muscle force from each simulation of each participant. We also have to normalize in percentage of the body weight.

When we extract activation and muscle force, we have to identify each muscle group as follow:

- Posterior kinetics chain: lateral gastrocnemius, medial gastrocnemius, tibialis anterior, biceps femoris lh, biceps femoris sh, semimembranous , semitendineus
- Knee flexors group: biceps femoris lh, biceps femoris sh, semimembranous, semitendineus.
- Knee extensor group: rectus femoralis, vast internal, vast lateral e vast medial.
- Anterior Kinetics chain: biceps femoris lh, biceps femoris sh, semimembranous, semitendineus, tibialis anterior
- Ankle plantar Flexor Group: Lateral Gastrocnemius, Medial gastrocnemius, soleus
- Ankle Dorsal Flexor group: Internal Vast.

For the torquestwo groups have been considered:

- Knee Angle
- Ankle Angle

For this reason, we don't have to sum columns to identify different groups.

In addition to this code, however, a function defined as *statisticsSPM_1independent2paired. m* [34] whose purpose is to perform a t-test between the three groups, where the group of healthy subjects is identified as the independent group, while the two groups pathStoredT0 and pathStoredT1 are identified as paired Group in case a comparison between the same subjects is performed (Ekso T0 vs Ekso T1), while if the subjects are different (Ekso T1 vs FKT T1) a line of code is changed and the t-test is performed in the conventional way.

```matlab
% Non parametric paired test to compare the same sample in two different
% time frames, yA and yB
snpm1       = spm1d.stats.nonparam.ttest_paired(yA, yB);
snpmi1      = snpm1.inference(alpha, 'two_tailed', two_tailed, 'iterations', iterations);


% Non parametric paired test to compare the same sample in two different
% time frames, yA and yB
snpm1       = spm1d.stats.nonparam.ttest(yA, yB);
snpmi1      = snpm1.inference(alpha, 'two_tailed', two_tailed, 'iterations', iterations);
```

Figure 4.17 Matlab Code script

It is also important to note that a two-tailed t-test with a significance level value of 0.05 (alpha) was used for all statistical tests, i.e., we accept the risk of rejecting the true hypothesis 5 out of 100 wants. In this case, considering:

- yA as paired group 1;
- yB as paired group 2;
- yC ad indipendent group

it is possible to assume that the H0 hypothesis is that the mean of the group is the same.

Nonparametric t-tests, which are based on the comparison of the sums of the ranks, will be performed.

In our work, t-tests will be performed on the following combinations:

- Non-parametric paired test to compare the same sample in two different time frames, yA and yB.
- Non-parametric test to compare two different time frames, yA and yB (in the case where we have EKSO vs FKT)
- Non-parametric test to compare two different samples, yA and yC.
- Non-parametric test to compare two different samples, yB and yC.

The following chapters will specifically describe the outputs of these trials.

Chapter 5: Results

In the following chapter results of the processed data are reported.

The subjects were compared as follows:

1. EKSO subjects at time T0 vs all EKSO subjects at time T1
2. FKT controls at time T0 vs all FKT controls at time T1
3. EKSO subjects at time T0 vs all FKT subjects at time T0
4. EKSO subjects at time T1 vs all FKT subjects at time T1

For each of the four combinations of subject groups, the results from the graphical and statistical point of view of the six muscle groups described in prediction will be shown:

- Ankle plantar flexor group
- Ankle dorsal flexor group
- Anterior kinetic chain
- Posterior kinetic chain
- Knee flexor group
- Knee extensor group

In each graph, there are also bands and three dotted lines of three different colors that identify the three standard deviations and the averages between the three subject paths. From a literary point of view, if we are analyzing EKSO subjects, we will have the following colors:

- CS is black (k)
- T0 is blue (b)
- T1 is red (r)

In the case of the FKT control subjects, they will have the following colors:

- CS is black (k)
- T0 is yellow (y)
- T1 is green, where the mean is identified by 'g' and the standard deviation is identified by an interval [0-0.5-0] that represents a type of green color.

It is possible to analyze the graphs from the time point of view. In these cases, if we want to have T0 confronts, they will have the following colors:

- CS is black (k)
- EKSO T0 is blue (b)
- FKT T0 is yellow (y)

98

For the T1 time they have:

- CS is black (k)
- EKSO T1 is red (r)
- FKT T1 is green, where the mean is identified by 'g' and the standard deviation is identified by an interval [0-0.5-0] that represents a type of green color.

5.1 Muscle Force

EKSO subjects
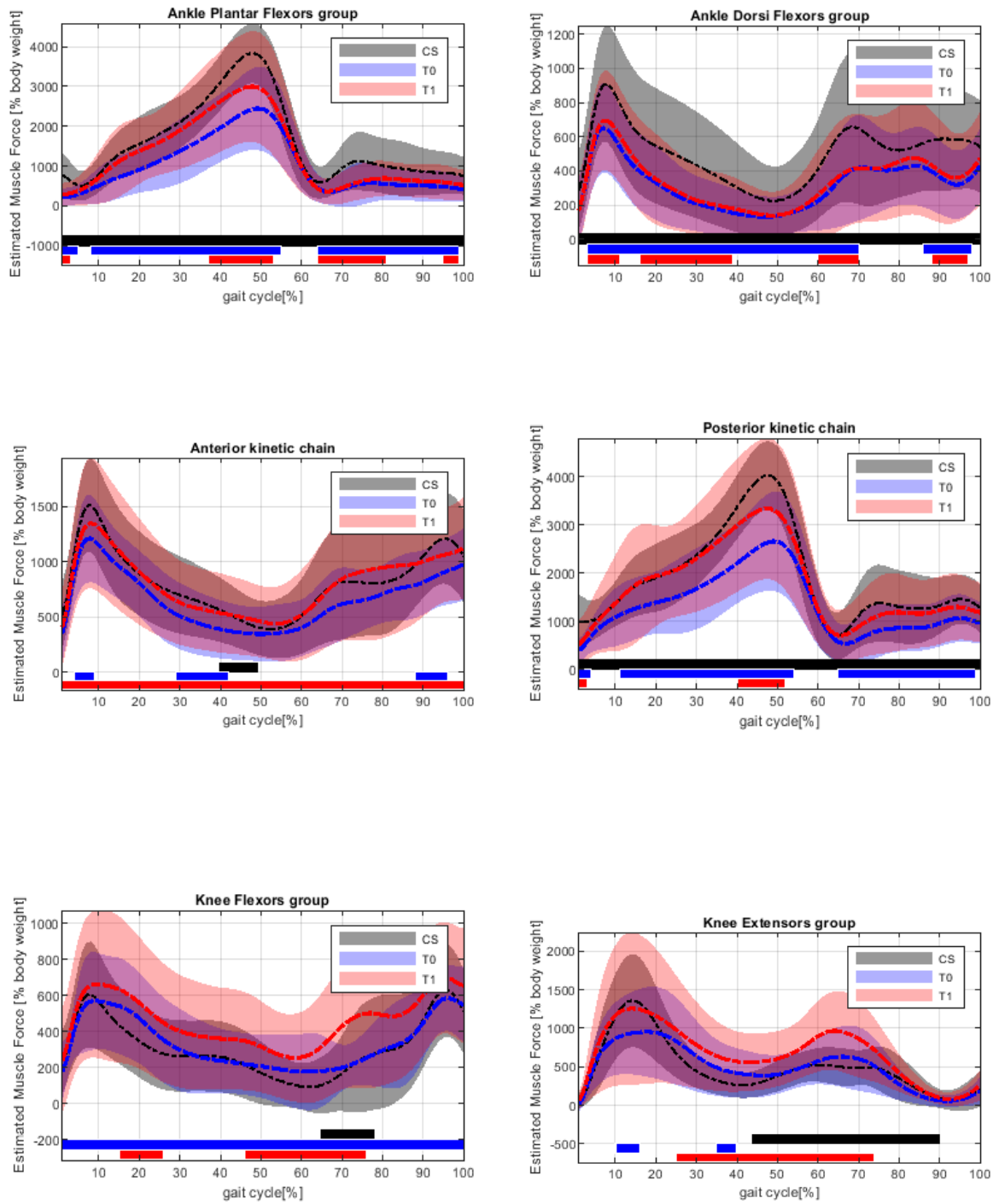
Figure 5.1: Muscle force of all EKSO subjects at time T0 and time T1 are represented.

FKT subjects
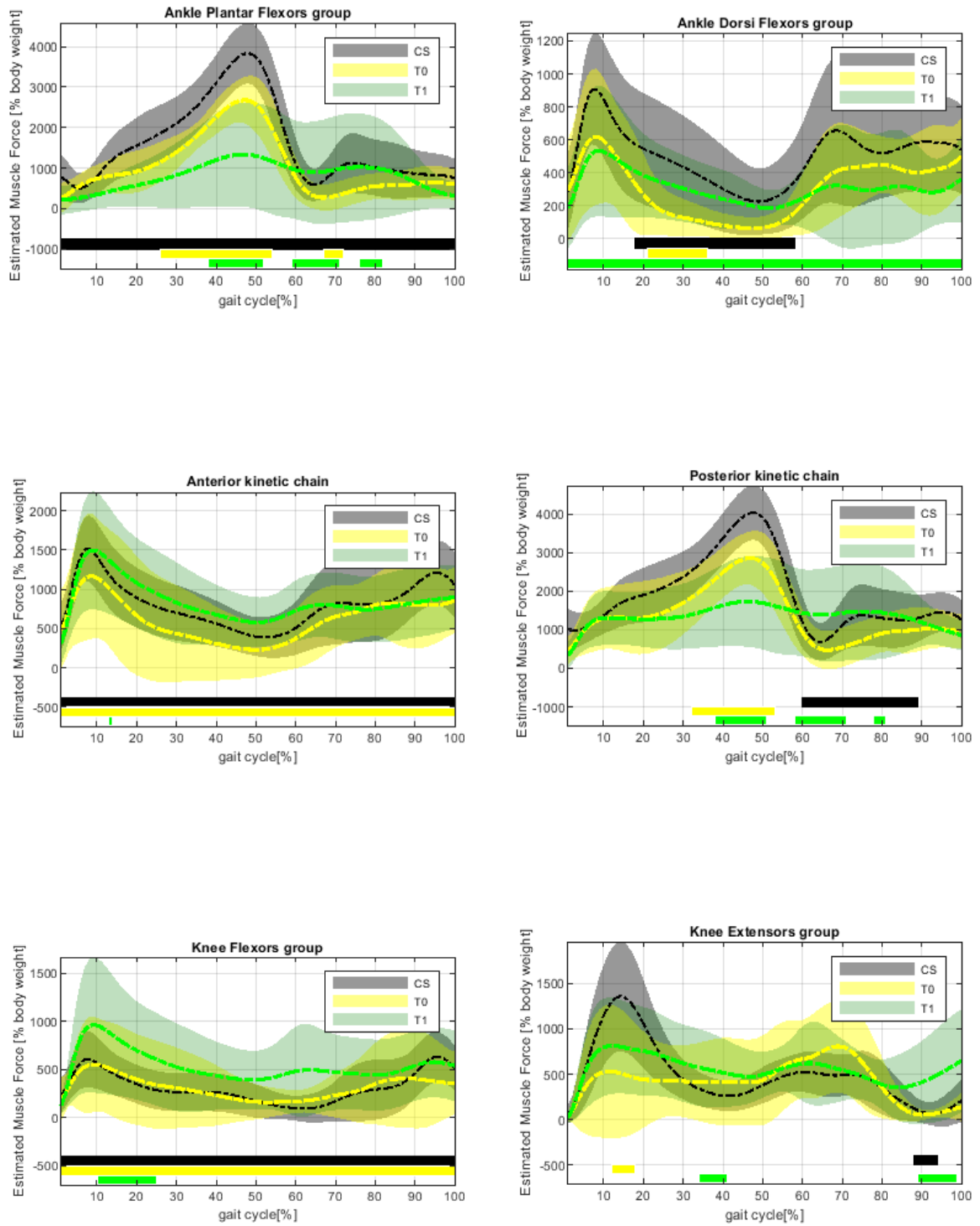
Figure 5.2 : Muscle force of all FKT subjects at time T0 and time T1 are represented

EKSO vs FKT T0 subjects
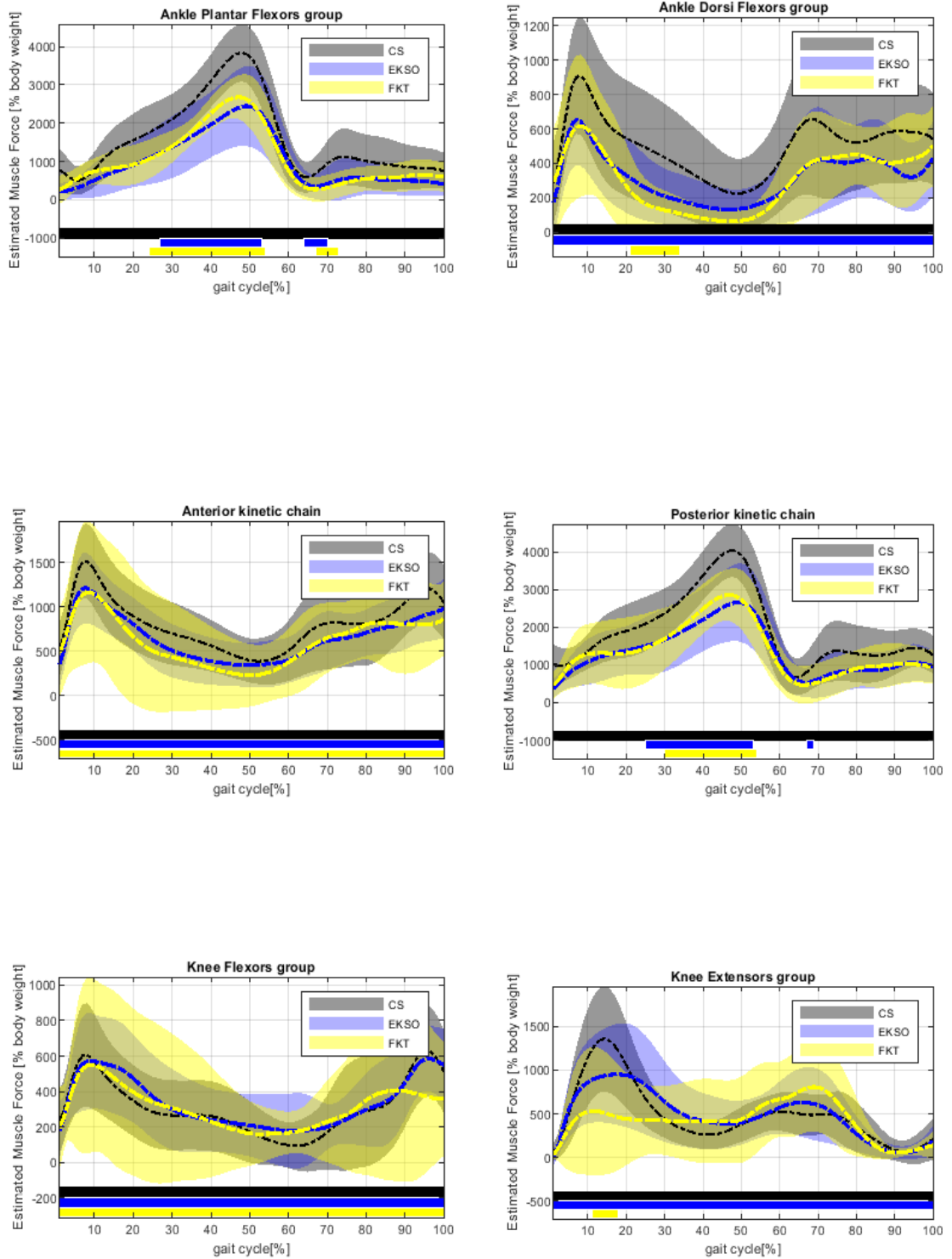
Figura 5.3: Muscle Force of All T0 subjects

EKSO vs FKT T1 subjects
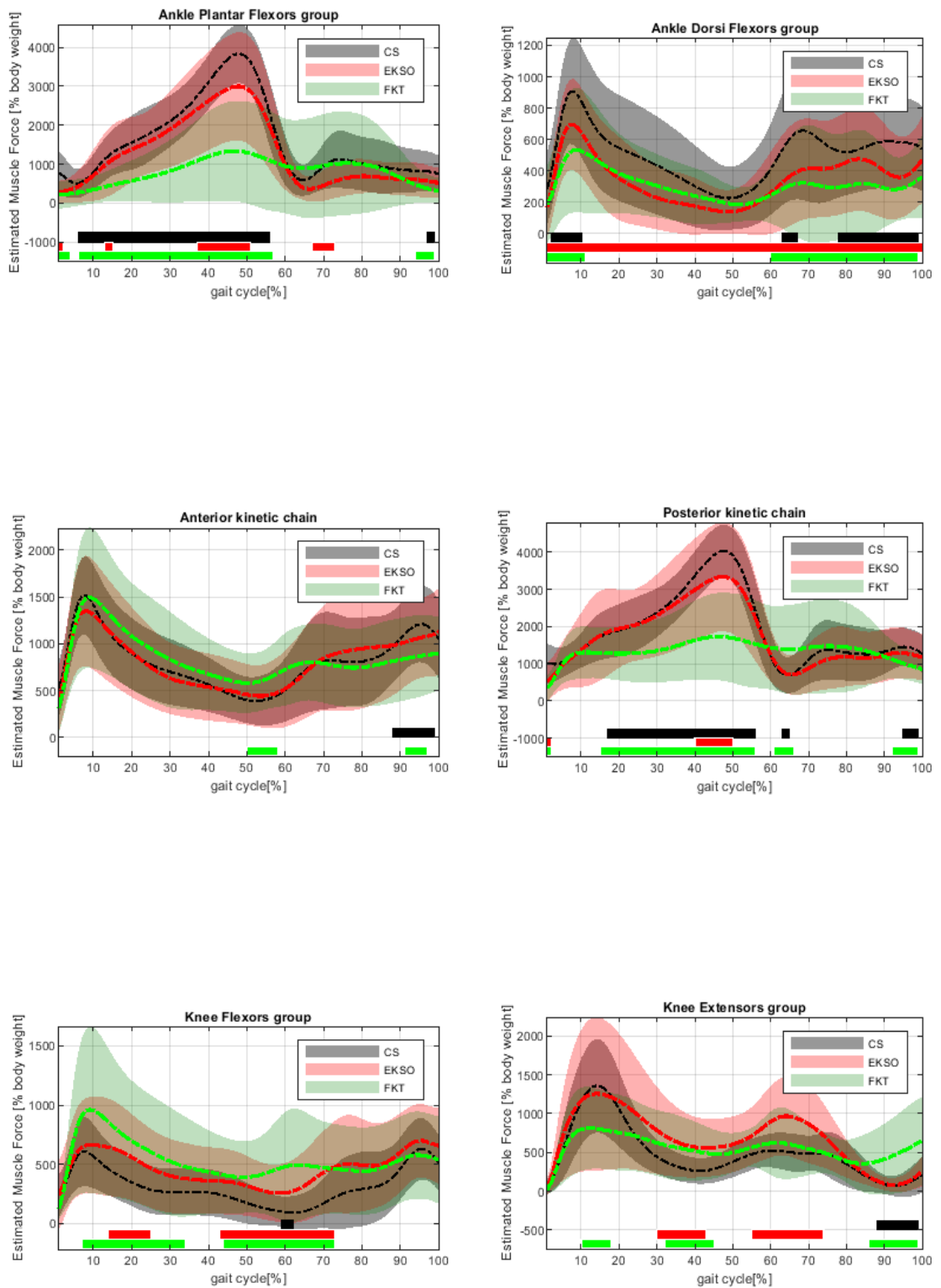
Figure 5.4: Muscle Force of all subjects at T1 time

5.2 Activations

EKSO subjects
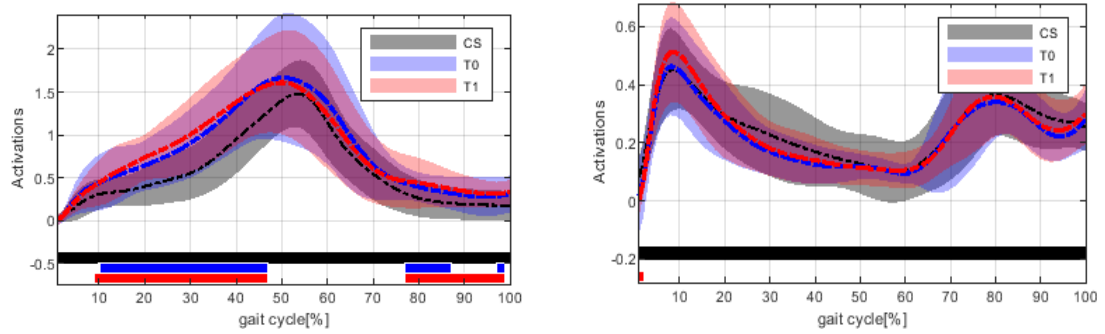
Figure 5.5 Activation of Ankle Plantar flexors group and Ankle Dorsi Flexors group respectively.
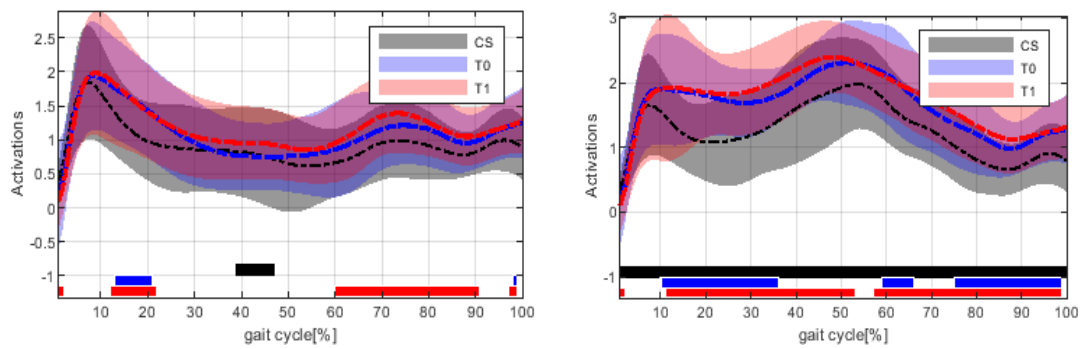
Figure 5.6: Activation of Anterior Kinetic chain and posterior kinetic chain respectively.
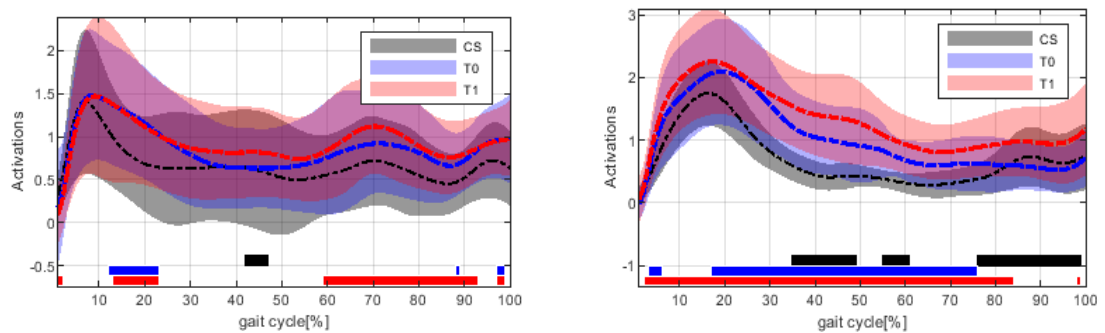
Figure 5.7: Activation of Knee Flexor group and Knee Extensor Group respectively.

FKT subjects
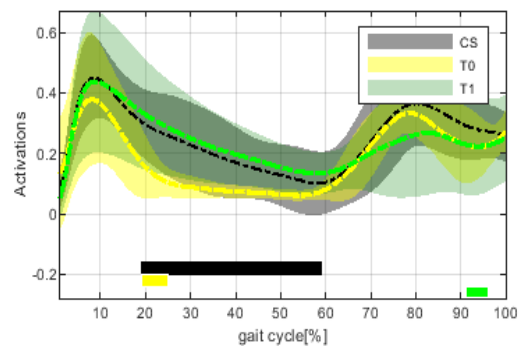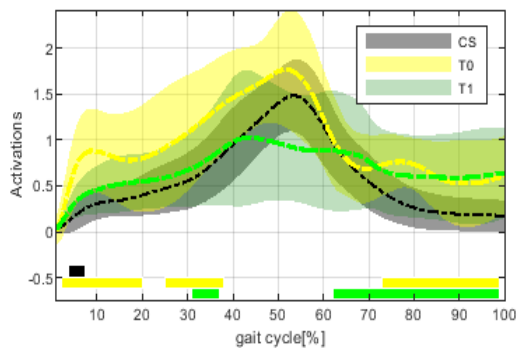
Figure 5.8 Activation of Ankle Plantar flexors group and Ankle Dorsi Flexors group respectively.
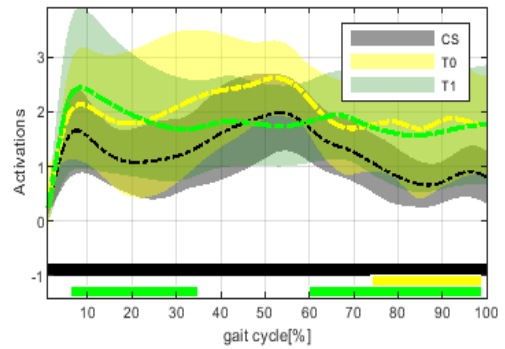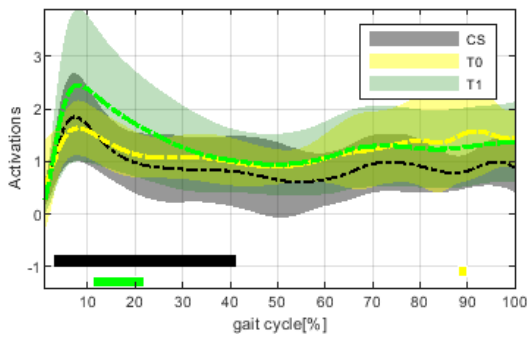
Figure 5.9: Activation of Anterior Kinetic chain and posterior kinetic chain respectively
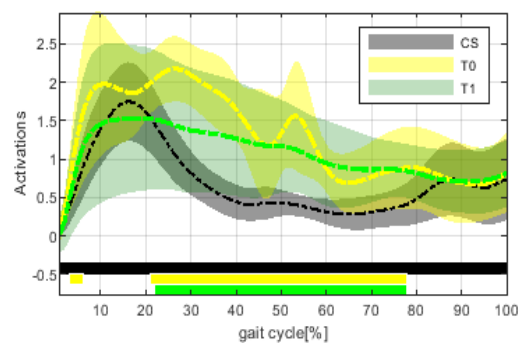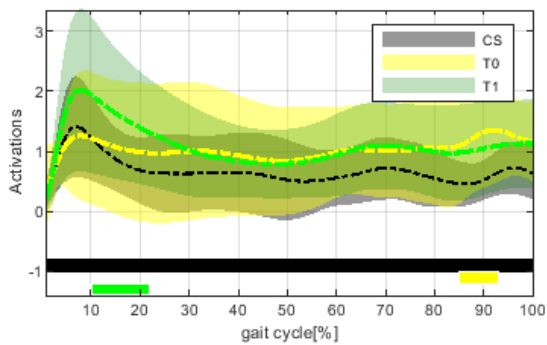
Figure 5.10: Activation of Knee Flexor group and Knee Extensor Group respectively.

EKSO vs FKT T0 subjects
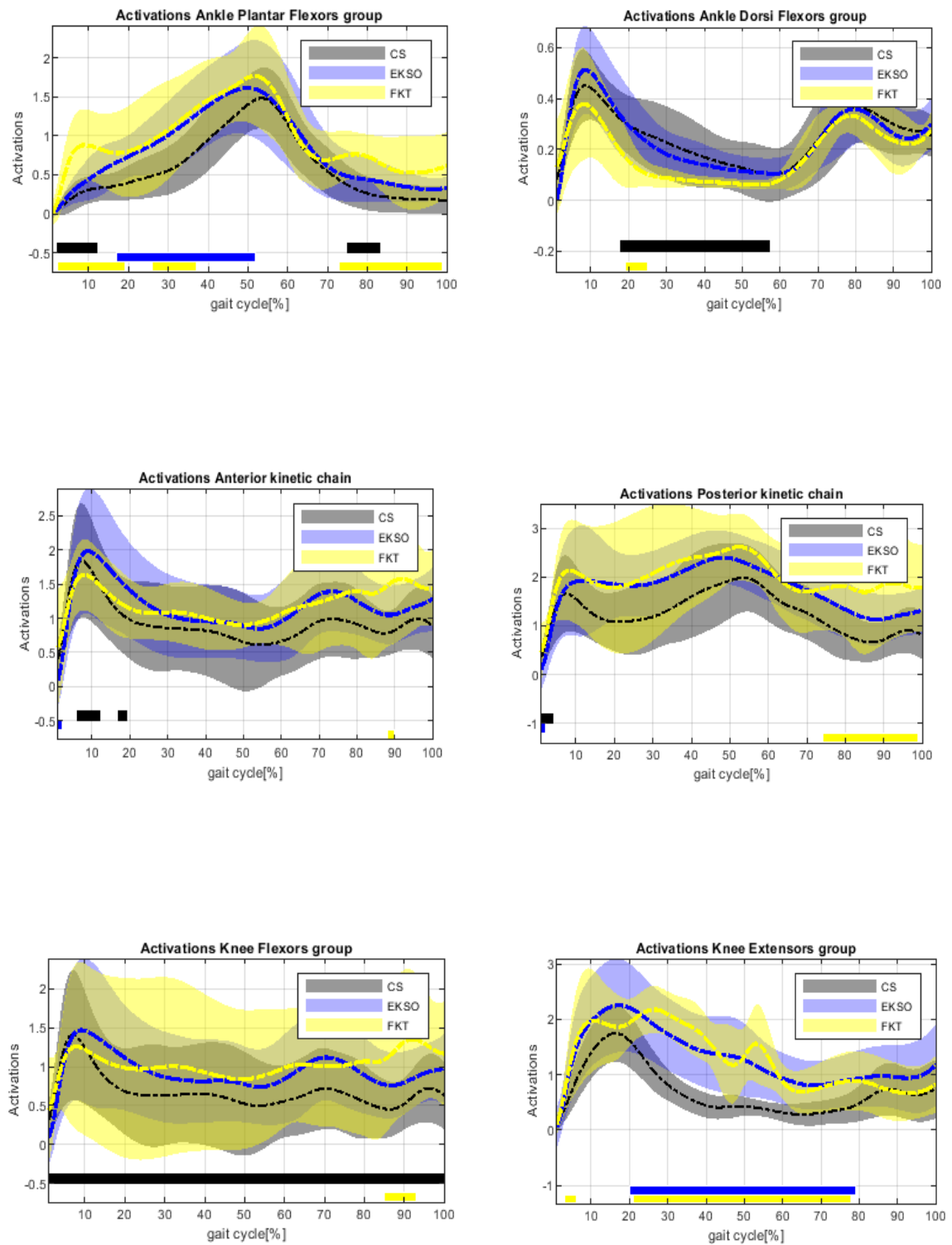
Figure 5.11 Activations of all subjects at T0 time

EKSO vs FKT T1 subjects
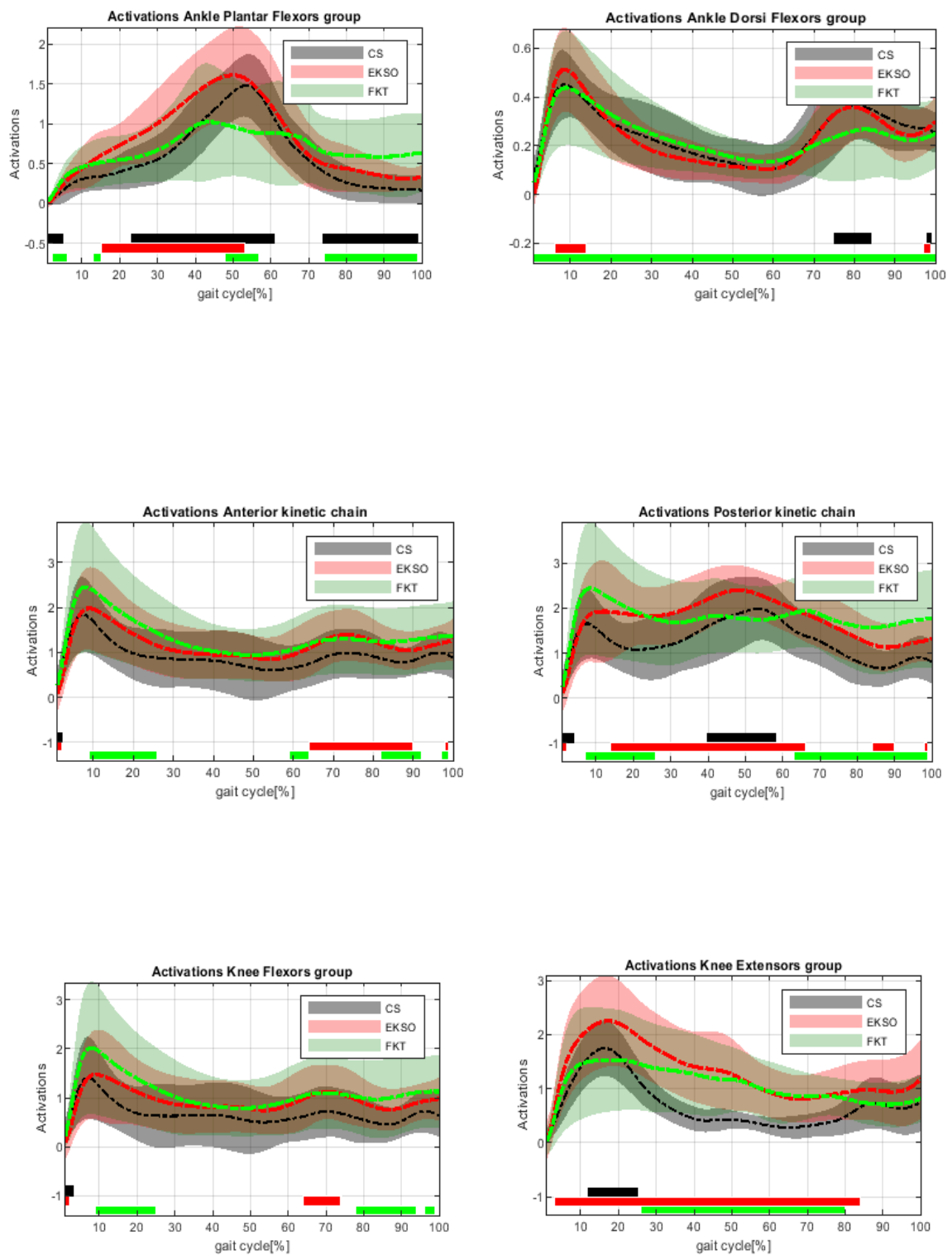
Figure 5.12: Activations of subjects at T1 time.

Chapter Six: Discussion

In this chapter I discuss the results of this thesis project. In all graphs (see Chapter 5), along the x-axis the various phases of the step cycle are represented in percentages ranging from 0% to 100%, where more precisely we can recall that:

- 0%-60% we have stance phase.
- 60%-100% we have swing phase.

On the y-axis, on the other hand, the magnitude corresponding to Muscle Force or Activations is reported.

Furthermore, it is important to observe the width of the bands identifying the standard deviations. The narrower the bands, the more promising the results are and the more consistent with the literature as the intra-subject variability is reduced. The lines at the bottom of the graph, on the other hand, indicate whether the t-test value is statistically significant.

6.1 Muscle Forces

EKSO subjects

Analyzing the results, from time T0 to time T1 there is a distinct improvement in the muscle forces of the pathological subjects, but these forces always have lower values than in the healthy subjects. It is also observed that the average gait patterns of the pathological subjects are concordant with the patterns of the healthy ones. From the point of view of standard deviations, the red bands identifying the T1 population show a wider range than the T0 population in all 6 muscle groups, thus implying greater variability between the subjects analyzed.

Considering in this specific case the outputs of the t-test as:

- EKSO T0 vs EKSO T1 as black (k)
- EKSO T0 vs CS as blue (b)
- EKSO T1 vs CS as red (r)

it emerges that in the case of the *Ankle Plantar Flexors group*, *Ankle Dorsi Flexors group*, and *Posterior Kinetic chain* the t-test between EKSO at time T0 and EKSO at time T1 has shown statistically significant differences along the entire gait cycle, while in the case of EKSO vs CS at time T1 there are statistically significant differences along a large part of the gait but not completely.

108

On the contrary, in the remaining muscle groups, the t-test of the EKSO subjects did not show statistically significant differences too pronounced, except in the case of *the Knee Extensors group* where the result of the t-test between EKSO T1 vs CS was also relevant.

In the case of the *Anterior Kinetic chain*, on the other hand, there were statistically significant differences along the stride cycle only in the case of EKSO T1 vs CS, while in the *Knee Flexors group* we have them only in the case of EKSO T0 vs CS.

In general, it can be observed that the comparison of these two groups shows improvements at time T1 in that all mean values of muscle forces are increasing in all six muscle groups, and there are no abnormalities in the trials.

FKT subjects

Looking at the results it can be seen that, from time T0 to time T1, there is a reduction in muscle strength in all muscle groups. The average trajectories of the gait cycle at time T1 are not consistent with the values and with the muscular strength peaks of the healthy subjects, especially in the case of the *Ankle Plantar Flexors Group, Posterior Kinetic chain*, and *Knee extensor group* where the strength values of the FKT T1 group are 50% lower than those of the CS group.

At time T0, on the other hand, except for the Knee Extensor group, all the trials were relatively consistent with the trends in healthy subjects.

Considering the standard deviations between the subjects, in all cases at time T1 the green bands are quite evident, demonstrating that there is considerable variability in this group. Even at time T0, it is important to emphasize that there is variability, especially in the case of the *Anterior Kinetic chain* and the *Knee Extensor group.*

Considering in this specific case the outputs of the t-test as:

- FKT T0 vs FKT T1 as black (k)
- FKT T0 vs CS as yellow (y)
- FKT T1 vs CS as green (g)

in the case of the *Ankle plantar flexor group*, *Anterior Kinetic chain*, and *Knee flexors group, statistically* significant differences are observed between the FKT subjects throughout the gait cycle. The differences between FKT T0 and CS are also greater in these graphs and except for the *Ankle plantar flexor group* there are also statistically significant differences during the entire gait cycle. Analyzing instead the FKT T1 versus CS case, the differences are predominantly seen in the *Ankle DorsiFlexors Group* where they are present during the whole gait cycle.

The *Knee Extensor Group* shows no statistically significant differences in any of the three groups to which the t-test was applied.

Analyzing the graphs, therefore, it is possible to state that the most significant muscle groups in the case of the FKT subjects are:

- Ankle Plantar Flexors group,
- Anterior Kinetic chain
- Knee Flexors group

where at time T1 there are no significant values.

EKSO subjects Vs FKT subjects at T0 time

These graphs show the starting conditions of the pathological subjects, who then were subjected to two different treatments.

In all muscle groups except for the *Knee Flexor group*, the average trends of the pathological subjects are similar to those of the healthy subjects, and the muscle values of the average EKSO and FKT forces are very similar to each other, although still lower than in the CS group.

The standard deviations are clearly greater in the case of the FKT group in all muscle groups, again implying greater variability in the data.

Considering in this specific case the outputs of the t-test as:

- EKSO vs FKT as black (k)
- EKSO vs CS as blue (b)
- FKT vs CS as yellow (y)

The t-test statistic shows that the results of EKSO vs. FKT are statistically significant in all muscle groups over the entire stride, which implies that the starting differences between the two groups of subjects are already considerable. This could be due to the inclusion and exclusion criteria of patients in EKSO therapy. In addition, the results show that in the case of the Ankle Dorsi flexor group, Anterior Kinetic chain, Knee Flexors group and Knee Extensor group, there are also statistically significant differences for EKSO vs. CS over the entire stride cycle, in the remaining muscle groups, however, the t-test was positive only in a portion of the stance phase. In the case of the comparison between FKT and CS, on the other hand, the differences were mainly shown in two muscle groups, namely Anterior Kinetic chain and Knee Flexors Group.

110

EKSO subjects Vs FKT subjects at T1 time

In this section, we will discuss the comparison of the results of subjects who have received different types of treatment. In general, it is observed that EKSO subjects almost always maintain an average muscle strength trend similar to the healthy controls, exception made forsome specific groups such as the *Ankle Dorsi Flexor Group* and *Knee Extensor Group*. In the case of the FKT group, on the other hand, there is a significant difference compared to the control group both in terms of the average muscle force values and in terms of the gait of the trials, in fact, in the case of the *Ankle Plantar Flexors Group*, *Posterior Kinetic chain* and *Knee Extensor group* the muscle forces are halved. It is also observed that in the FKT subjects, a great variability is shown, confirming what has been observed in the previous cases, although the same situation forEKSO population must be taken into account.

Considering in this specific case the outputs of the t-test as:

- EKSO vs FKT as black (k)
- EKSO vs CS as red (r)
- FKT vs CS as green (g)

It can be observed that the statistically significant differences obtained with the t-test are less evident than in the previously treated cases. Indeed, analyzing the comparison between the pathological subjects, in *Ankle Dorsal Flexors Group*, *Knee Flexors Group*, *Knee Extensor Group* and *Anterior Kinetic chain* there were no statistically significant differences, while in the remaining muscle groups the differences were only in the stance phase. The EKSO subjects show statistically significant differences during the whole stride only in the case of the *Ankle Dorsi Flexor Group*, whereas, in the knee musculature there are statistically significant differences between the stance phase and the swing phase. The FKT subjects, on the other hand, show statistically significant differences above all:

- During the Stance phase of the following muscular groups: *Ankle Plantar Flexors Group, Posterior Kinetic chain, Knee Flexors group.*
- During swing phase of *Ankle Dorsi Flexor group.*

General Comparison of Muscle Forces

In general, it can be observed that EKSO therapy appears to be effective in allowing patients to increase their muscle forces during the gait cycle, and even as the disease progresses, this innovative therapy allows them to maintain a constant gait cycle throughout muscle activity compared to patients undergoing conventional therapy, who do not maintain a regular gait cycle and forces. As mentioned above, this significant difference may result from the fact that the

inclusion criteria for EKSO therapy are very selective and subjects who were not able to participate may be in a more advanced state of the disease.

When analyzing and looking at all the graphs at the same time, the muscle groups most affected in Parkinson's disease are *Ankle Plantar Flexors Group, Posterior Kinetic Chain and Knee Extensor Group.*

6.2 Activations

Before proceeding with the discussion of the muscle activations divided into the four combinations described above, it is important to emphasize that, from a theoretical point of view, they represent the transition from neural activations u(t) to muscle activations a(t) and are expressed as a dimensionless numerical value, which varies between 0 and 1. In the present case, considering that on the x-axis there is a value varying from 0% to 100% representing the gait cycle and on the ordinates the muscle activations are represented, the dimensionless values will vary from 0 to 2.5.

EKSO subject

From the muscle activations it can be noticed that in the six muscle groups the population patterns at time T0 are similar to the ones at time T1 and all the trials are coherent with the healthy controls. In th*e Ankle Plantar Flexors group, Ankle Dorsi Flexors group* and *Posterior Kinetic chain* the trials are identical, which suggests that the EKSO therapy did not involve these muscle groups. In the case of Anterior Kinetic chain, Knee Flexors group and Knee Extensor group the results at time T1 are better than at time T0.

Analyzing the standard deviations, in most cases, from time T0 to time T1, there are no major differences, which means that there is identical variability between the two groups of subjects, but these differences are more pronounced in the *Knee Extensor Group.*

Considering in this specific case the outputs of the t-test as:

- EKSO T0 vs EKSO T1 as black (k)
- EKSO T0 vs CS as blue (b)
- EKSO T1 vs CS as red (r)

it emerges that in the case of the *Ankle Plantar Flexors group*, *Ankle Dorsi Flexors group*, and *Posterior Kinetic chain* the t-test between EKSO at time T0 and EKSO at time T1 has shown statistically significant differences along the entire gait cycle as it has been demonstrated with

the muscle force of the same subjects. In the case of confront between EKSO T0 and CS, it is possible to observe statistically significant differences during:

- The stance phase of *Ankle Plantar Flexors group, Posterior Kinetic chain and Knee Extensor group,*
- The swing phase of *Posterior Kinetic chain* and *Knee Extensor group.*

In the case of confront between EKSO T1 and CS, it is possible to observe statistically significant differences during:

- The stance phase of *Ankle Plantar Flexors group, Posterior Kinetic chain,* and *Knee Extensor group,*
- The swing phase of *Ankle Plantar Flexors group, Anterior Kinetic chain, Posterior Kinetic chain,* and *Knee Extensor group.*

In general, it is observed that statistically significant differences in muscle activations occur at time T1.

FKT subjects

The muscle activations of the FKT subjects show clear differences between time T0 and time T1 both in terms of values and trends along the step. The trends are not consistent with those of the healthy subjects. It is also observed that in the case of the *Knee Extensor Group* at time T0 there is a particular trend that oscillates between values 1 and 2, whereas, at time T1 the graph shows a linear trend with a decreasing muscle activation value during the stride cycle.

In the case of the *Ankle Plantar Flexors group*, *Posterior Kinetic chain* and *Knee extensor group* we have that muscle activations decrease as the disease progresses, while, in the remaining muscle groups we have the reverse mechanism. From the standard deviations it emerges that the green band is thicker than the yellow band as there are greater variabilities, but these variabilities between subjects in the same group also occur at time T1 especially in the case of the *Ankle Plantar Flexors group* and the *Knee flexors group*.

Considering in this specific case the outputs of the t-test as:

- FKT T0 vs FKT T1 as black (k)
- FKT T0 vs CS as yellow (y)
- FKT T1 vs CS as green (g)

it is possible to observe that in the case of the *Posterior Kinetic chain, Knee Flexors and Knee extensor groups* the t-test between FKT at time T0 and FKT at time T1 has shown statistically

significant differences along the entire gait cycle. In the case of the statistics between FKT at time T0 and CS there are statistically significant differences mainly in the swing phase, while at time T0 there are no statistically significant differences except for the swing phase of the Posterior Kinetic chain and the central interval of the *Knee Extensor group*.

EKSO vs FKT T0 subjects

From the graphs, it is possible to observe that the trends of the EKSO subjects are in line with those of the healthy subjects, whereas the FKT subjects show different trends, especially in the case of the *Knee Extensor group*, where the average trend is composed of a series of maximum and minimum peaks. In general, the mean values of the EKSO activations are greater than those of the healthy controls, while there are no different values in the FKT subjects. From the point of view of standard deviations, however, it is observed that the variability between the subjects is greater in the case of the FKT group except for the *Knee Extensor group*.

Considering in this specific case the outputs of the t-test as:

- EKSO vs FKT as black (k)
- EKSO vs CS as blue (b)
- FKT vs CS as yellow (y)

in contrast to the muscular forces, there are no statistically significant differences from the results of the t-test; in fact, only in the Knee Flexors group and in the stance phase of the Ankle Dorsi Flexors group was the comparison between the pathological subjects positive. The t-test between the EKSO subjects and the CS showed statistically significant differences in the stance phase of the Ankle Plantar Flexors group and in the mid-stance phase of the Knee Extensor groups, as was the case with the comparison between the FKT and CS.

EKSO vs FKT T1 subjects

Also in this case, as in the previous ones, concordant trends are observed between the control population and the EKSO population, while, in the case of the FKT subjects, the average trends in muscle activations deviate from the healthy subjects, especially in the case of the *Ankle Plantar Flexors group, Posterior Kinetic chain and Knee Extensor group*. In terms of standard deviations, greater variations were also found in the case of FKT subjects in all muscle groups. Considering in this specific case the outputs of the t-test as:

- EKSO vs FKT as black (k)

- EKSO vs CS as red (r)
- FKT vs CS as green (g)

it is observed that the t-test is statistically significant in only a few graphs. In detail, only these positive results occur:

- In the EKSO vs FKT case only in the stance phase and in the end of swing phase of the *Ankle Plantar Flexors Group* and in the middle of the Posterior Kinetic chain;
- In the EKSO vs CS case in the *Posterior Kinetic chain*, in the *Knee Extensor group,* the stance phase of *Ankle Plantar Flexors Group* and the swing phase of the *Anterior Kinetic chain;*
- In the FKT vs CS in the case of *Ankle DorsiFlexors group, Posterior Kinetic chain* and *Ankle Plantar Flexors group* during the swing phase and in the central interval of *Knee Extensor group*

General Comparison of Activation Force

Among the different muscle groups, it can be observed that there are no muscle groups that have a greater influence on muscle activations than others; in the case of the EKSO therapy, statistically significant differences are shown in the Ankle Plantar Flexors group, Ankle Dorsi Flexors group and in the posterior kinetic chain; in the comparisons with the FKT subjects at time T0 and T1, on the other hand, these muscle groups showed no statistically significant differences. As in the case of the muscle forces, however, it can be observed that in the case of the EKSO subjects, the values of the muscle activations increase with increasing time, whereas the opposite occurs in the case of the FKT subjects.

6.3 Final Considerations

Analyzing and comparing the muscle activations with the muscle forces of each group of previously treated subjects, it can be observed that with regard to the comparison of the EKSO population, the statistical results are consistent, thus demonstrating the effectiveness of robotic therapy on PD patients.

In the case of the FKT subjects who did not undergo robotic therapy, on the other hand, consistency of results can be observed in only two muscle groups, i.e. Ankle Dorsi Flexors

group and Knee flexors group, and it can therefore be stated that the therapy contributed to the improvement of the vastus internal muscle.

On the other hand, comparing the EKSO subjects with the FKTs at time T0 there is a coherence only with the biceps femoris, and the semimembranosus and semitendinosus muscles, while at time T1 there is a coherence only with the Ankle Plantar Flexors group.

In general, it can be affirmed that from a therapeutic point of view, the EKSO treatment can be considered effective with regard to muscular forces, while the muscular activations only partially influence the outcome of the therapy by allowing the values to increase after one month of treatment.

Chapter 7: Conclusions

In this work, it was evaluated whether the use of robotic EKSO therapy applied to individuals with Parkinson's disease was effective compared to conventional therapies. The major novelty of this contribution lays in the adoption of internal variables acquired dynamically in order to portray the impact of different therapies on the musculoskeletal system of subjects with Parkinson's disease. Using software such as MOtoNMS, OpenSim and CEINMS, it was possible to extract muscle forces, muscle activations and torques of 11 subjects, some of whom underwent EKSO therapy. From the analysis of the graphs, it is therefore possible to make some final considerations.

To achieve the results, it was essential to follow the pipeline [1] where, thanks to MOtoNMS, it was possible to obtain the *subject.trc* and *subject.mot* files, which were indispensable for the realization of the customized model on each subject in OpenSim. Afterwards the scaling procedure was implemented through an optimized workflow which is f based on body mass and the muscle optimizer tool. Subsequently, the data were calibrated on CEINMS after undergoing batch processing. It should be emphasized that the input evaluated the signals of eight superficial muscles extracted by means of the s-EMGs, but through CEINMS it was also possible to estimate the contribution of deeper muscles; in fact, a total of 15 muscles related to the lower limb were analyzed. The final output of CEINMS resulted in the graphical display of the muscle forces and muscle activations of each of the 15 muscles normalized from 0 to 1 over a range from 0% to 100% of the gait cycle where both the mean and standard deviation of the values could be observed. It is also necessary to consider the Torques of each subject's trials divided into Knee Angle and Ankle Angle, where again the mean and standard deviation values were normalized between 0 and 1.

By comparing the results of the subjects, we can make final considerations about the six different muscle group contributions. From the point of view of the EKSO group, it emerged that the robotic therapy showed promising results in terms of both muscle forces and activations, with increases in strength from time T0 to time T1 with statistically significant differences in all muscle groups. On the contrary, those who did not receive the innovative therapy did not show the same improvements from time T0 to T1. By observing both muscle forces and muscle activations in the FKT group, it can be seen that often after only three weeks, the values are halved or even the entire gait cycle is changed.

A further comparison was carried out between the EKSO and FKT subjects at both time T0 and T1, from which it emerged that in general, from the point of view of muscle strengths, EKSO therapy seems to be effective especially for the Ankle Plantar Flexors group, while, from the point of view of muscle activations, it does not seem to be particularly significant on the treatment.

In conclusion, it can be stated that EKSO robotic therapy seems to be effective on the muscle forces of Parkinson's disease patients but does not affect the muscle activations of the subjects too much.

In the future, it is desired to validate this therapy on a larger number of subjects in order to improve Parkinson's symptoms, especially in the gait cycle, keeping it as similar as possible to that of healthy subjects; in addition, the aim is to keep lower limb muscle activity active for longer.

Chapter 8: Appendix

Matlab Codes:

Hybrid Parameteic Optimizer

This code allows to estimate the best coefficients to run the hybrid model in CEINMS and it is customized only for Ekso Villa Margherita dataset.

```matlab
pathStart = uigetdir();
% Definition of the range of the coefficients
a = 0:10:40; a(1) = 1;
b = 0:25:100; b(1) = 1;
c = 0:50:200; c(1) = 1;
xDoc=xmlread(fullfile(([pathStart '\execution\Cfg\executionHybrid_elastic.xml'])));


% Extraction of the trials name
trials_dir = dir(fullfile(pathStart,'trials\simulation'));
for h = 3:length(trials_dir)
    trials_name{h-2} = trials_dir(h).name;
end


% Extraction of the execution trials name
exetrials_dir = dir(fullfile(pathStart,'execution\Setup\standardCalibration'));
for h = 3:length(exetrials_dir)
    exetrials_name{h-2} = exetrials_dir(h).name;
end
counter = 1;
% Iterative selection of the best coefficients


for n = 1:length(exetrials_name) % with this cycle the alculation will be performed over the whole trials
    system(['CEINMS -S "',
pathStart,'\execution\Setup\standardCalibration\',char(exetrials_name{n}),'"']);
    for i = 1:length(a) % this makes the alpha coefficient vary
        allListItemsA=xDoc.getElementsByTagName('alpha');
```

```matlab
            thisListItemA=allListItemsA.item(0);
            thisListItemA.setTextContent(num2str(a(i)))
        for k = 1%:length(b) % this makes the beta coefficient vary
            allListItemsB=xDoc.getElementsByTagName('beta');
            thisListItemB=allListItemsB.item(0);
            thisListItemB.setTextContent(num2str(b(k)))
        for j = 1%:length(c) % this makes the gamma coefficient vary
            allListItemsC=xDoc.getElementsByTagName('gamma');
            thisListItemC=allListItemsC.item(0);
            thisListItemC.setTextContent(num2str(c(j)))
            % save the new Cfg file containing the updated version of the coefficients and run
the simulation
            xmlwrite(fullfile(([pathStart '\execution\Cfg\executionHybrid_elastic.xml'])),xDoc);
            system(['CEINMS -S "',
pathStart,'\execution\Setup\standardCalibration\',char(exetrials_name{n}),'"']);
             % CEINMS output directory
            output_dir = fullfile(pathStart,
'\execution\simulations\standardCalibration\',char(trials_name{n}(1:end-4)));


            ObjFunComponentsAndWeightings = importdata(fullfile(output_dir,
'ObjectiveFunctionComponentsAndWeightings.sto'));
            F = sum(ObjFunComponentsAndWeightings.data(:,2)) +
sum(ObjFunComponentsAndWeightings.data(:,4)) +
sum(ObjFunComponentsAndWeightings.data(:,3));


            HybrParam(counter,1) = F;
            HybrParam(counter,2) = 1;
            HybrParam(counter,3) = a(i);
            HybrParam(counter,4) = b(k);
            HybrParam(counter,5) = c(j);
            counter = counter+1;
            disp(['Thats the iteration number ', num2str(counter), '! Hold on.'])
        end
    end
end
```

```matlab
[h, minFj] = min(HybrParam(:,1));
allListItemsA=xDoc.getElementsByTagName('alpha');
thisListItemA=allListItemsA.item(0);
thisListItemA.setTextContent(num2str(HybrParam(minFj,3)))
allListItemsB=xDoc.getElementsByTagName('beta');
thisListItemB=allListItemsB.item(0);
thisListItemB.setTextContent(num2str(HybrParam(minFj,4)))
allListItemsC=xDoc.getElementsByTagName('gamma');
thisListItemC=allListItemsC.item(0);
thisListItemC.setTextContent(num2str(HybrParam(minFj,5)))
% save the new Cfg file containing the updated version of the
% coefficients
xmlwrite(fullfile(([pathStart'\execution\Cfg\executionHybrid_elastic.xml'])),xDoc);


    % Run the simulation
    system(['CEINMS -S "',
pathStart,'\execution\Setup\standardCalibration\',char(exetrials_name{n}),'"']);


    clc
    disp(HybrParam(minFj,:))
    disp(['Trial ', char(trials_name{n}), ' just done! Press any key to go on'])
    %pause

end
```

Data Extraction and Visualization

```matlab
pathData = uigetdir();
pathFiles = fullfile(pathData,'\ceinms\trials\simulation');
files = files_name(dir(pathFiles));

mkdir([pathData,'\ceinms\graphs'])
 pathSave = [pathData,'\ceinms\graphs'];

%%%% Load standardCalibration data
    pathsC = fullfile(pathData,'ceinms/execution/simulations/standardCalibration');
    for i = 1:length(files)
        % Activations
        SC.activations.raw{i} = importdata(fullfile(pathsC,files{i}(1:end-
4),'Activations.sto'));
        SC.activations.data(:,:,i) = interp1D(SC.activations.raw{1,i}.data(:,2:end),101);
        SC.activations.labels = SC.activations.raw{1,1}.colheaders(:,2:end);
        % Muscle Forces
        SC.muscleforces.raw{i} = importdata(fullfile(pathsC,files{i}(1:end-
4),'MuscleForces.sto'));
        SC.muscleforces.data(:,:,i) = interp1D(SC.muscleforces.raw{1,i}.data(:,2:end),101);
        SC.muscleforces.labels = SC.muscleforces.raw{1,1}.colheaders(:,2:end);
        % Torques
        SC.torques.raw{i} = importdata(fullfile(pathsC,files{i}(1:end-4),'Torques.sto'));
        SC.torques.data(:,:,i) = interp1D(SC.torques.raw{1,i}.data(:,2:end),101);
        SC.torques.labels = SC.torques.raw{1,1}.colheaders(:,2:end);
    end
    disp('-- StandardCalibration model data have been stored..')
    clearvars -except SC files pathData pathSave


    figure
    for a = 1:size(SC.activations.data,2)
        subplot(5,3,a)
```

```matlab
    plot(mean(SC.activations.data(:,a,:),3),'LineWidth',2.5,'Color','k')
    hold on
    plot(mean(SC.activations.data(:,a,:),3)+std(SC.activations.data(:,a,:),0,3),'k--','LineWidth',0.5)
    plot(mean(SC.activations.data(:,a,:),3)-std(SC.activations.data(:,a,:),0,3),'k--','LineWidth',0.5)
    xlim([1 100])
    xlabel(['Gait cycle %'])
    ylim([0 1])
    ylabel(['Normalized excitation'])
    title(SC.activations.labels{a},Interpreter="none")
end
saveas(gca,[pathSave,'\activtions.png'])
% Muscle forces
figure
for mf = 1:size(SC.muscleforces.data,2)
    subplot(5,3,mf)
    plot(mean(SC.muscleforces.data(:,mf,:),3),'LineWidth',2.5,'Color','k')
    hold on
    plot(mean(SC.muscleforces.data(:,mf,:),3)+std(SC.muscleforces.data(:,mf,:),0,3),'k--','LineWidth',0.5)
    plot(mean(SC.muscleforces.data(:,mf,:),3)-std(SC.muscleforces.data(:,mf,:),0,3),'k--','LineWidth',0.5)
    xlim([1 100])
    xlabel(['Gait cycle %'])
    ylim([0 inf])
    ylabel(['Muscle force'])
    title(SC.muscleforces.labels{mf},Interpreter="none")
end
saveas(gca,[pathSave,'\muscleforces.png'])
% Torques
figure
for a = 1:size(SC.torques.data,2)
    subplot(1,2,a)
    plot(mean(SC.torques.data(:,a,:),3),'LineWidth',2.5,'Color','k')
```

```matlab
        hold on
        plot(mean(SC.torques.data(:,a,:),3)+std(SC.torques.data(:,a,:),0,3),'k--','LineWidth',0.5)
        plot(mean(SC.torques.data(:,a,:),3)-std(SC.torques.data(:,a,:),0,3),'k--','LineWidth',0.5)
        title(SC.torques.labels{a},Interpreter="none")
        xlim([1 100])
        xlabel(['Gait cycle %'])
        ylabel(['Joint moment'])
    end
    saveas(gca,[pathSave,'\torques.png'])


    save([pathSave,'\nmsData.mat'],"SC")
```

Matrix Group Muscle Functional Group

This matlab code is modified and use also for torque and activations.

```matlab
pathStoredT0 =
{'C:\Users\Marco\Documents\Progetti\Ekso_rehab\elaborations\subject_name\acquisition_date\ElaboratedData\ceinms\graphs\nmsData.mat', ... };
pathStoredT1 =
{'C:\Users\Marco\Documents\Progetti\Ekso_rehab\elaborations\subject_name\acquisition_date\ElaboratedData\ceinms\graphs\nmsData.mat',... };
weightsPd = [subject1_mass1, subject2_mass, …];
pathStoredCs =
{'C:\Users\Marco\Documents\Progetti\ModelloNMS_muscleoptimized\Controlli\subject_name\motonms\ElaboratedData\ceinms\graphs\nmsData.mat',... };
weightsCs = [subject1_mass1, subject2_mass, …];


% Loading of muscle forces from each simulation of each participant.
% Normalization in percentage of the body weight.
% the number in [] identify the columns of muscular groups
load(pathStoredT0{1})
tmp = SC.muscleforces.data/weightsPd(1)*100;
anklePlantFlex = sum(tmp(:,[3,4,9],:),2);
```

```matlab
ankleDorsiFlex = tmp(:,10,:);
kneeFlex = sum(tmp(:,[1,2,7,8],:),2);
kneeExt = sum(tmp(:,[6,11,12,13],:),2);
posteriorKin = sum(tmp(:,[3,4,9,1,2,7,8],:),2);
anteriorKin = sum(tmp(:,[1,2,7,8,10],:),2);
mfT0 = [anklePlantFlex,ankleDorsiFlex,kneeFlex,kneeExt,anteriorKin,posteriorKin];
clearvars SC anklePlantFlex ankleDorsiFlex kneeFlex kneeExt tmp


load(pathStoredT1{1})
tmp = SC.muscleforces.data/weightsPd(1)*100;
anklePlantFlex = sum(tmp(:,[3,4,9],:),2);
ankleDorsiFlex = tmp(:,10,:);
kneeFlex = sum(tmp(:,[1,2,7,8],:),2);
kneeExt = sum(tmp(:,[6,11,12,13],:),2);
posteriorKin = sum(tmp(:,[3,4,9,1,2,7,8],:),2);
anteriorKin = sum(tmp(:,[1,2,7,8,10],:),2);
mfT1 = [anklePlantFlex,ankleDorsiFlex,kneeFlex,kneeExt,anteriorKin,posteriorKin];
clearvars SC anklePlantFlex ankleDorsiFlex kneeFlex kneeExt tmp


for i = 2:length(pathStoredT0)
    load(pathStoredT1{i})
    tmp = SC.muscleforces.data/weightsPd(i)*100;
    anklePlantFlex = sum(tmp(:,[3,4,9],:),2);
    ankleDorsiFlex = tmp(:,10,:);
    kneeFlex = sum(tmp(:,[1,2,7,8],:),2);
    kneeExt = sum(tmp(:,[6,11,12,13],:),2);
    posteriorKin = sum(tmp(:,[3,4,9,1,2,7,8],:),2);
    anteriorKin = sum(tmp(:,[1,2,7,8,10],:),2);
    mfT0tmp = [anklePlantFlex,ankleDorsiFlex,kneeFlex,kneeExt,anteriorKin,posteriorKin];
    mfT0 = cat(3,mfT0,mfT0tmp);
    clearvars SC anklePlantFlex ankleDorsiFlex kneeFlex kneeExt tmp
    load(pathStoredT1{i})
    tmp = SC.muscleforces.data/weightsPd(i)*100;
    anklePlantFlex = sum(tmp(:,[3,4,9],:),2);
    ankleDorsiFlex = tmp(:,10,:);
```

```matlab
    kneeFlex = sum(tmp(:,[1,2,7,8],:),2);
    kneeExt = sum(tmp(:,[6,11,12,13],:),2);
    posteriorKin = sum(tmp(:,[3,4,9,1,2,7,8],:),2);
    anteriorKin = sum(tmp(:,[1,2,7,8,10],:),2);
    mfT1tmp = [anklePlantFlex,ankleDorsiFlex,kneeFlex,kneeExt,anteriorKin,posteriorKin];
    mfT1 = cat(3,mfT1,mfT1tmp);
    clearvars SC anklePlantFlex ankleDorsiFlex kneeFlex kneeExt tmp
end

mfBandsT0 = getBands(mfT0);
mfT1 = mfT1(:,:,[1:22,25:end]);
mfBandsT1 = getBands(mfT1);

load(pathStoredCs{1})
tmp = SC.muscleforces.data/weightsCs(1)*100;
anklePlantFlex = sum(tmp(:,[3,4,9],:),2);
ankleDorsiFlex = tmp(:,10,:);
kneeFlex = sum(tmp(:,[1,2,7,8],:),2);
kneeExt = sum(tmp(:,[6,11,12,13],:),2);
posteriorKin = sum(tmp(:,[3,4,9,1,2,7,8],:),2);
anteriorKin = sum(tmp(:,[1,2,7,8,10],:),2);
mfCs = [anklePlantFlex,ankleDorsiFlex,kneeFlex,kneeExt,anteriorKin,posteriorKin];
clearvars SC anklePlantFlex ankleDorsiFlex kneeFlex kneeExt tmp

for i = 2:length(pathStoredCs)
    load(pathStoredCs{i})
    tmp = SC.muscleforces.data/weightsCs(i)*100;
    anklePlantFlex = sum(tmp(:,[3,4,9],:),2);
    ankleDorsiFlex = tmp(:,10,:);
    kneeFlex = sum(tmp(:,[1,2,7,8],:),2);
    kneeExt = sum(tmp(:,[6,11,12,13],:),2);
    posteriorKin = sum(tmp(:,[3,4,9,1,2,7,8],:),2);
    anteriorKin = sum(tmp(:,[1,2,7,8,10],:),2);
    mfCstmp  = [anklePlantFlex,ankleDorsiFlex,kneeFlex,kneeExt,anteriorKin,posteriorKin];
    mfCs = cat(3,mfCs,mfCstmp);
```
126

```matlab
        clearvars SC anklePlantFlex ankleDorsiFlex kneeFlex kneeExt tmp
end


mfBandsCs = getBands(mfCs);


% Statistica and plots


addpath('..\..\..\Programmi\spm1dmatlab-master')
labels = {'Ankle Plantar Flexors group', 'Ankle Dorsi Flexors group', 'Knee Flexors group',
'Knee Extensors group', 'Anterior kinetic chain', 'Posterior kinetic chain'};
for k = 5:length(labels)
    statisticsSPM_1indipendent2paired(mfBandsCs, mfBandsT0, mfBandsT1, k, labels)
    %legend('Normative bands', 'Before therapy','After therapy')
    print(gcf,                                      ['C:\Users\Marco\Documents\PhD\PhD-
Thesis\tesi\figures\figures6\',labels{k},'.tiff'],'-r600','-dtiff')
end
```

Statistics SPM

```matlab
function statisticsSPM_1indipendent2paired(indipendentGroup, pairedGroup1, pairedGroup2,
k, label)
% j = [1:3,7:11];
%%%%%%%%% Statistics %%%%%%%%%%
yA = pairedGroup1.MATP{1,j(k)}(1:100,:)';
yB = pairedGroup2.MATP{1,j(k)}(1:100,:)';
yC = indipendentGroup.MATP{1,k}(1:100,:)';


if size(yA,1) ~= size(yB,1)
    minCol = min(size(yA,1),size(yB,1));
    yA = yA(1:minCol,:);
    yB = yB(1:minCol,:);
end
% Inizialization of the statistic test
rng(0)
```

```matlab
alpha      = 0.05;
two_tailed = true;
iterations = 1000;


% Non parametric paired test to compare the same sample in two different time frames, yA
and yB
snpm1      = spm1d.stats.nonparam.ttest(yA, yB);
snpmi1     = snpm1.inference(alpha, 'two_tailed', two_tailed, 'iterations', iterations);


% Non parametric test to compare two different samples, yA and yC
iterations = 2000;
snpm2      = spm1d.stats.nonparam.ttest2(yA, yC);
snpmi2     = snpm2.inference(alpha, 'two_tailed', two_tailed, 'iterations', iterations);


% Non parametric test to compare two different samples, yB and yC
iterations = 2000;
snpm3      = spm1d.stats.nonparam.ttest2(yB, yC);
snpmi3     = snpm3.inference(alpha, 'two_tailed', two_tailed, 'iterations', iterations);
%%%%%%%%% Plot of the results %%%%%%%%%

h = figure('units','centimeters','Position',[4 4 7 4]);
f1 = fill([1:100 100:-
1:1],[indipendentGroup.SUPP(1:100,k)',fliplr(indipendentGroup.INFP(1:100,k)')],[0.88 0.08
0.24],'FaceAlpha',0.4,'LineStyle','none');
hold on
f2 = fill([1:100 100:-1:1],[pairedGroup1.SUPP(1:100,j(k))',fliplr(pairedGroup1
.INFP(1:100,j(k))')], [0.3922, 0.5843, 0.9294], 'FaceAlpha',0.3,'LineStyle','none');
f3 = fill([1:100 100:-1:1], [pairedGroup2.SUPP(1:100,j(k))',fliplr(pairedGroup2.
INFP(1:100,j(k))')] ,[0.0391, 0.2148, 0.8164],'FaceAlpha',0.3,'LineStyle','none');

plot(pairedGroup1.MP(:,j(k)),'color',[0.3922, 0.5843, 0.9294],'LineStyle','-.','LineWidth',1.5)
plot(pairedGroup2.MP(:,j(k)),'color',[0.0391, 0.2148, 0.8164],'LineStyle','-.','LineWidth',1.5)
title([label{k}])
%ylim([0,inf])
xlabel('gait cycle[%]')
```

```matlab
xlim([1 100])
ylabel('Joint torque [N * heigh % body weight]')
grid on
set(gca,'fontsize',5)
hold off
%%%%%%%%% Plot the statistics %%%%%%%%%
rectPos = ylim;
rectWidth = (rectPos(2)-rectPos(1))/25;
% Plot of the first p-values' comparison yA vs yB
p_values1 = snpmi1.p;
if isempty(p_values1)
    rectangle('Position', [1,rectPos(1),100,rectWidth],...
        'Facecolor',[1,1,1],'EdgeColor','w')
else
    num_intervals1 = length(snpmi1.clusters);
    for intervals1 = 1:num_intervals1
        endpoints1(:,intervals1) = round(snpmi1.clusters{1, intervals1}.endpoints);
        rectangle('Position', [endpoints1(1,intervals1),rectPos(1),endpoints1(2,intervals1)-
endpoints1(1,intervals1),rectWidth],...
            'Facecolor',[0.88 0.08 0.24],'EdgeColor','w')
    end
end
% Plot of the first p-values' comparison yA vs yC
p_values2 = snpmi2.p;
if isempty(p_values2)
    rectangle('Position', [1,rectPos(1)-
rectWidth,100,rectWidth],'Facecolor',[1,1,1],'EdgeColor','w')
else
    num_intervals2 = length(snpmi2.clusters);
    for intervals2 = 1:num_intervals2
        endpoints2(:,intervals2) = round(snpmi2.clusters{1, intervals2}.endpoints);
        rectangle('Position', [endpoints2(1,intervals2),rectPos(1)-
rectWidth,endpoints2(2,intervals2)-endpoints2(1,intervals2),rectWidth],...
            'Facecolor',[0.3922, 0.5843, 0.9294],'EdgeColor','w')
    end
```

```matlab
end
% Plot of the first p-values' comparison yC vs yB
p_values3 = snpmi3.p;
if isempty(p_values3)
    rectangle('Position', [1,rectPos(1)-2*rectWidth,100,rectWidth], 'Facecolor', [1,1,1], ...
    'EdgeColor','w')
else
    num_intervals3 = length(snpmi3.clusters);
    for intervals3 = 1:num_intervals3
        endpoints3(:,intervals3) = round(snpmi3.clusters{1, intervals3}.endpoints);
        rectangle('Position', [endpoints3(1,intervals3),rectPos(1)-
2*rectWidth,endpoints3(2,intervals3)-endpoints3(1,intervals3),rectWidth], ...
'Facecolor',[0.0391, 0.2148, 0.8164],'EdgeColor','w')
    end
end
ylim([rectPos(1)-2*rectWidth inf])
end
```

Figure Appendix

In this thesis work, only some of the graphs obtained have been reported in the results chapter, in particular, the torques that are processed directly by CEINMS and the graphs of individual subjects have not been discussed. A brief list of these figures will therefore follow.

Torques of all subjects
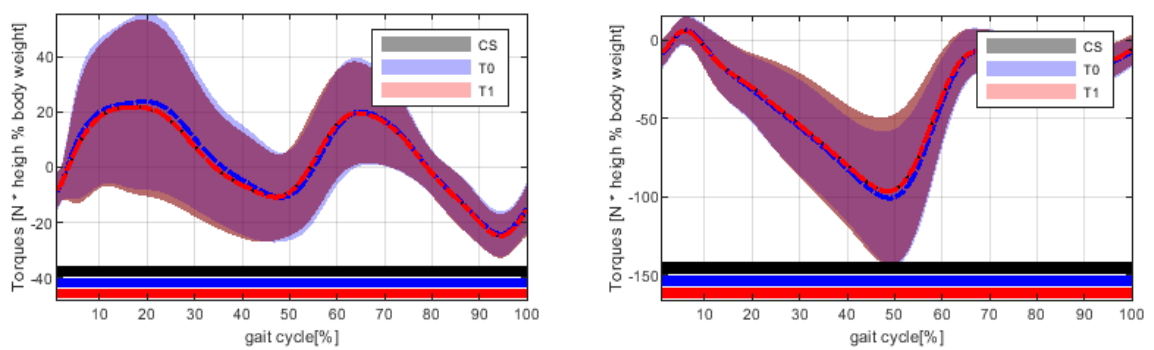
Figure 8.1: Representation of Torques of EKSO subjects, Knee angle and Ankle angle are represented respectively.
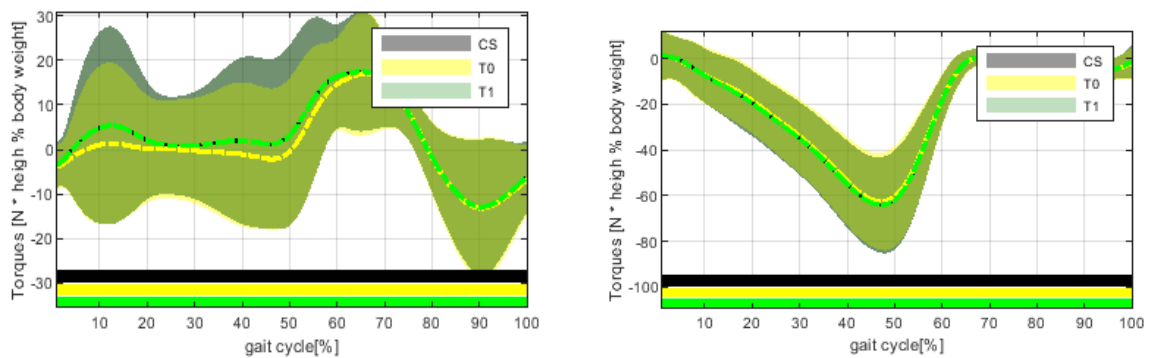
Figure 8.2: Representation of Torques of FKT subjects, Knee angle and Ankle angle are represented respectively.
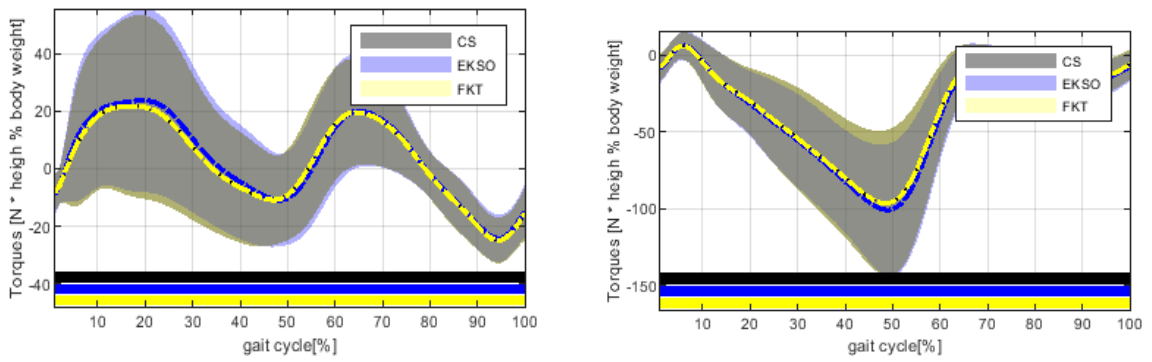
Figure 8.3: Representation of Torques of T0 subjects, Knee angle and Ankle angle are represented respectively.
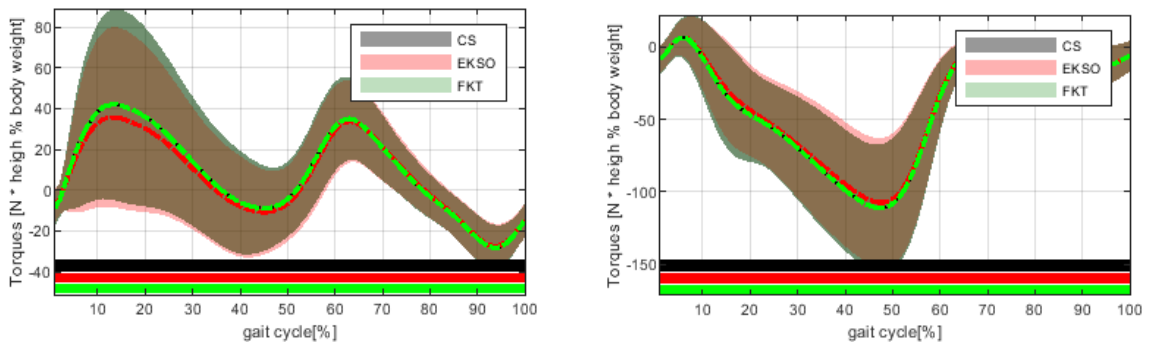
Figure 8.4: Representation of Torques of T1 subjects, Knee angle and Ankle angle are represented respectively.

Muscles Groups Representation of Single Subjects
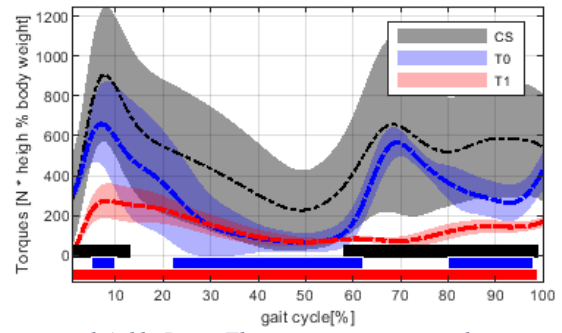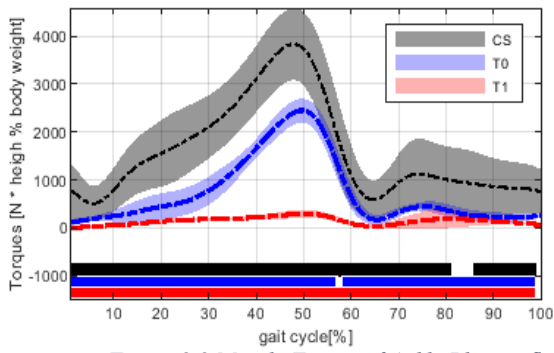
S1 Muscle Forces
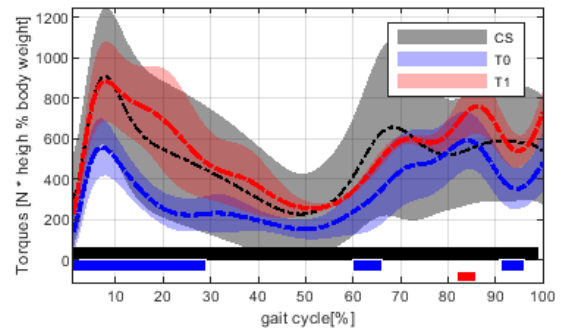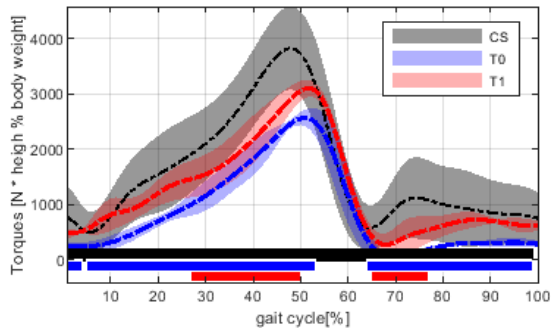
Figure 8.5 Muscle Forces of Ankle Plantar flexors group and Ankle Dorsi Flexors group respectively.
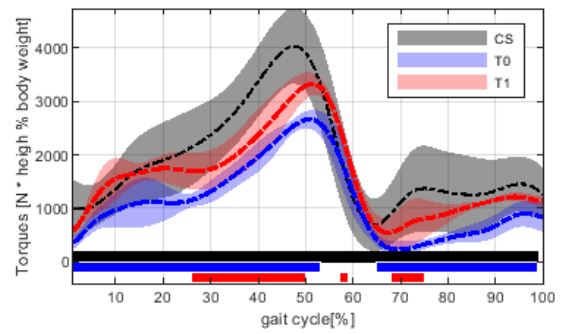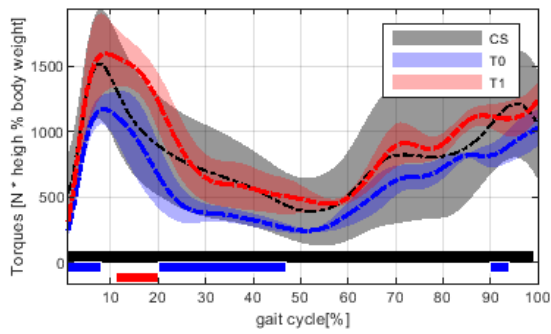
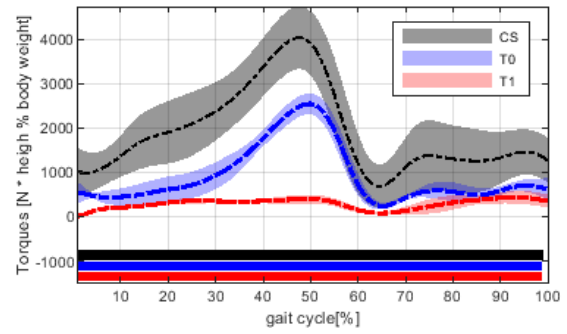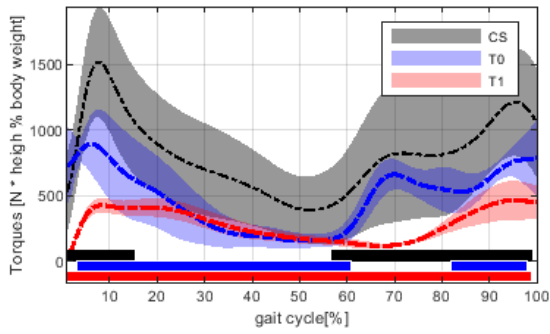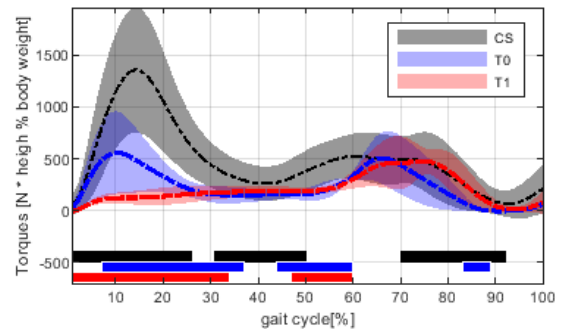*Figure 8.6 Muscle Forces of Anterior and Posterior Kinetic chain respectively.*
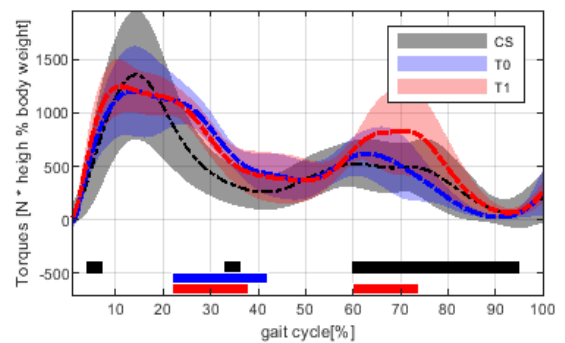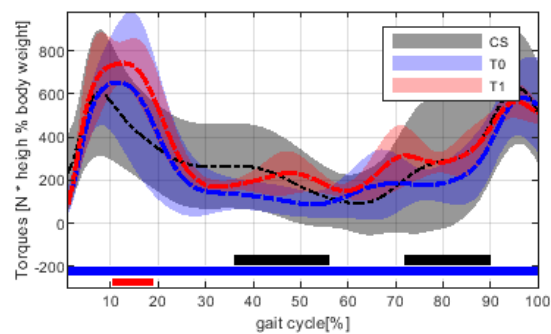
Figure 8.7 Muscle Forces of Knee flexors group and Knee extensors group respectively.

Figure 8.8 Muscle Forces of Ankle Plantar flexors group and Ankle Dorsi Flexors group respectively.

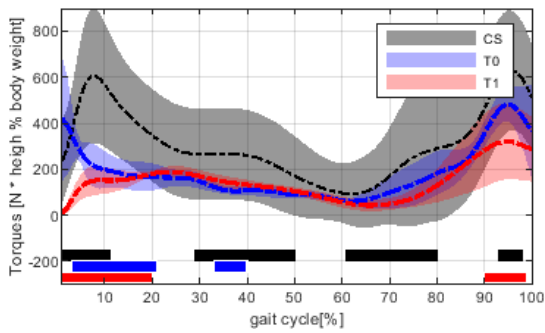*Figure 8.9 Muscle Forces of Anterior and Posterior Kinetic chain respectively.*

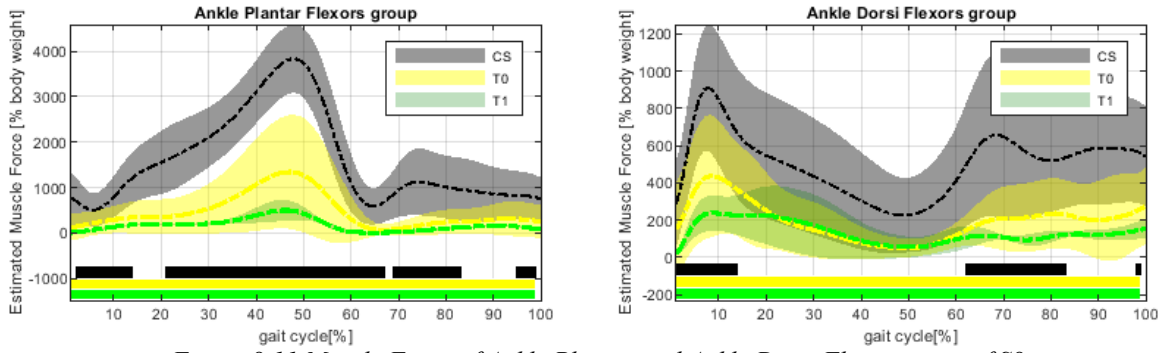*Figure 8.10 Muscle Forces of Knee flexors group and Knee extensors group respectively.*

134

Figure 8.11 Muscle Force of Ankle Plantar and Ankle Dorsi Flexor group of S8
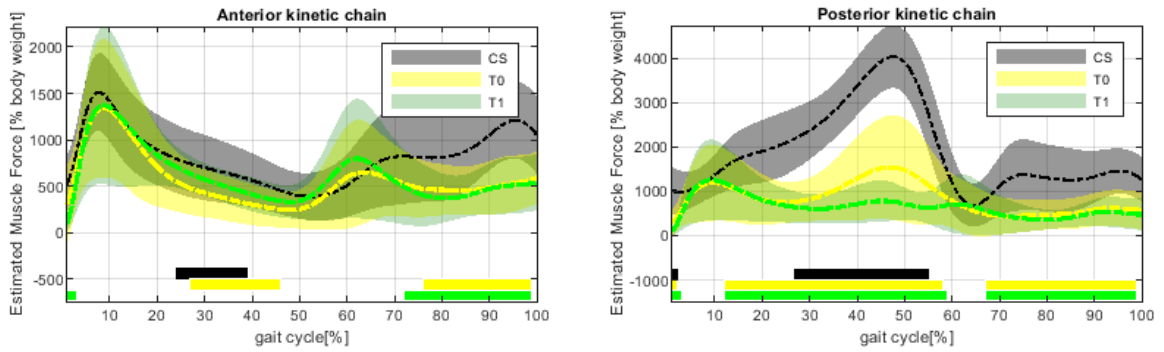

Figure 8.12 Muscle Force of Anterior and Posterior Kinetic chain of S8 133
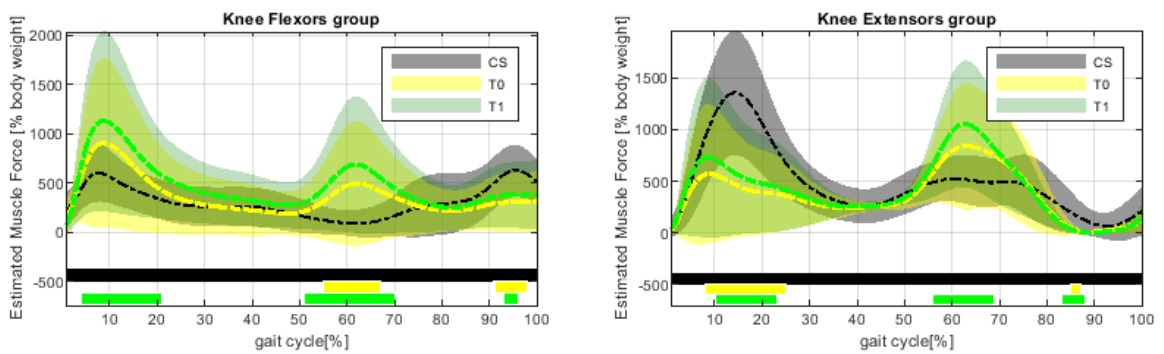

Figure 8.13 Muscle Force of Knee Flexor and Extensor group of S8
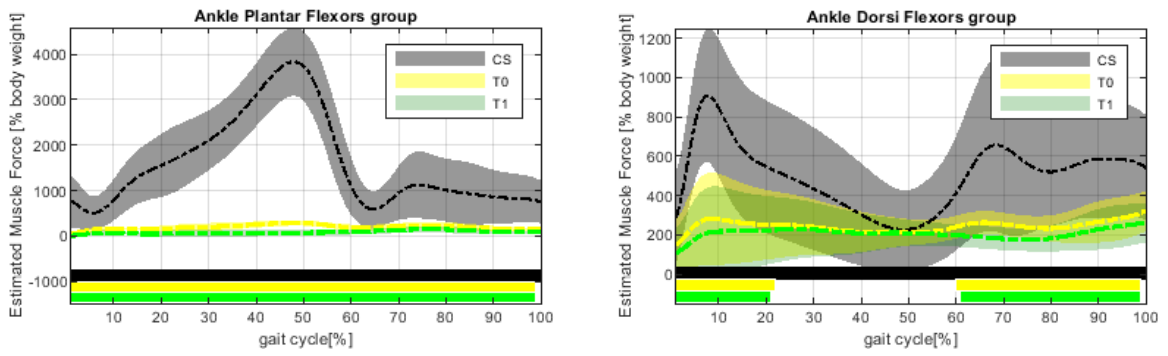
S11 Muscle Force

Figure 8.14 Muscle Force of Ankle Plantar and Ankle Dorsi Flexor group of S11
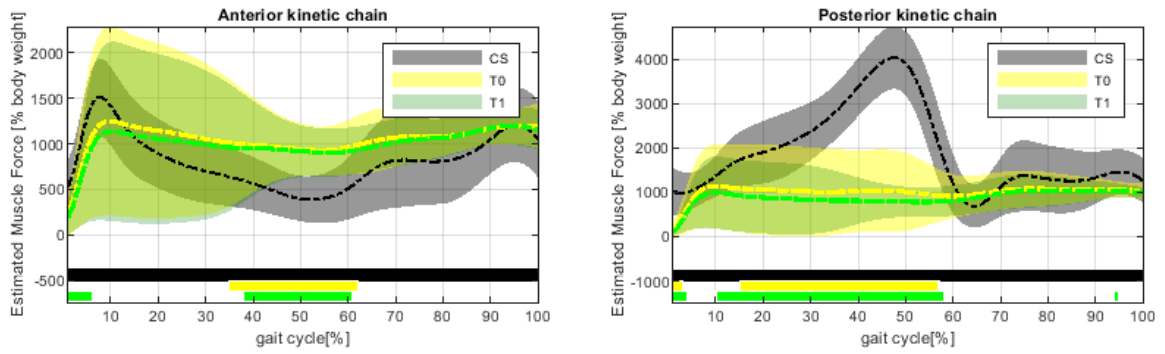

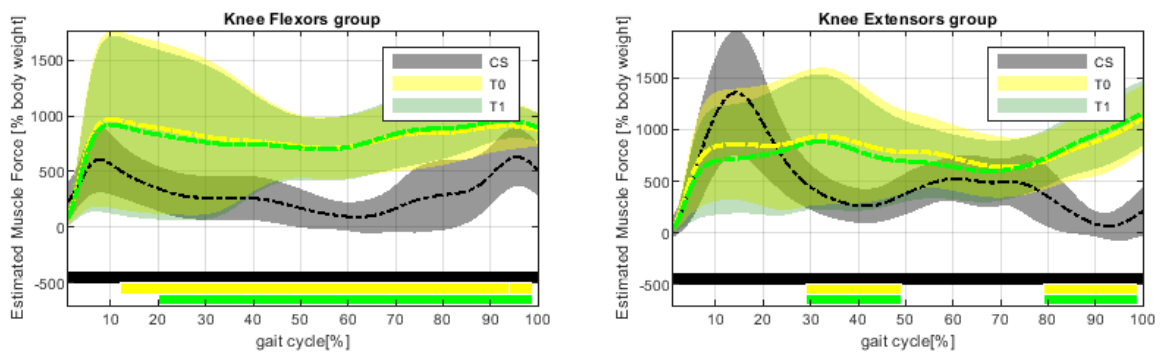*Figure 8.15 Muscle Force of Anterior and Posterior Kinetic chain of S11*

Figure 8.16 Muscle Force of Knee Flexor and Extensor group of S11

Bibliography

[1] M. Romanato, F. S. (2022). Quantitative assessment of training effects using EksoGT® exoskeleton in Parkinson's disease patients: A randomized single blind clinical trial. *Elsevier*.

[2] A. Leardini, Z. Sawacha, G. Paolini, S. Ingrosso, R. Nativo, M.G. Benedetti. *A new anatomically based protocol for gait analysis in children.*, 2007.

[3] Marco Romanato, Daniele Volpe, Annamaria Guiotto, Fabiola Spolaor, Massimo Sartori, Zimi Sawacha. «Electromyography-informed modeling for estimating muscle activation and force alterations in Parkinson's disease.» *Computer Methods in Biomechanics and Biomedical Engineering*, 2021.

[4] Zhe Zhang, S.-D. C. (2020). Autonomic Dysfunctions in Parkinson's Disease: Prevalence, Clinical Characteristics, Potential Diagnostic Markers, and Treatment. *Hindawi*.

[5] Alice De Luca1, A. B. (2019). Exoskeleton for Gait Rehabilitation: Effects of Assistance, Mechanical Structure, and Walking Aids on Muscle Activations. *Applied Science MDPI*, 21.

[6] Maria Grazia Benedetti, E. B. (2017). SIAMOC position paper on gait analysis in clinical practice: General requirements, methods and appropriateness. Results of an Italian consensus conference. *SIAMOC*, (p. 9).

[7] Aurelio Cappozzo, Ugo Della Croce, Alberto Leardini, Lorenzo Chiari. «Human movement analysis using stereophotogrammetry.» *ELSEVIER*, 2004.

[8] R.B. Davis, D. Tyburski, J.R. Gage «A gait analysis data collection and reduction tecnique.» *Human Moviment Science*, 1991

[9] A. Cappozzo, F. Catani, U. della Croce, A. Leardini. «Position and orientation in space of bones during movement: anatomical frame definition and determination.» 1995.

[10] Saladin, Kenneth S., *Anatomia umana*, ed. by Raffaele De Caro and Sergio Galli, 3. ed. italiana.

[11] Aiello, A. «Muscoli: Origini e Inserzioni.» s.d.

[12] Perry, J. «The Gait Analysis .» 1992.

[13] Tim Morgan, DC. «Biomechanics & Theories of Human Gait.» In *Boston Sports Medicine Performance Group* . 2012.

[14] J.L. Hicks, T.K. Uchida, A. Seth, A. Rajagopal, S.L. Delp. «Best Practices for Verification and Validation of Musculoskeletal Models and Simulations of Movement.» 2015.

[15] Sherwood, L. «Fondamenti di Fisiologia Umana, Quarta Edizione.» Di Piccinin Editore. 2012.

[16] Winter, D. A. «Biomechanics and Motor control of Human Movement, Fourth Edition.» 2009.

[17]Julien Stelletta, Yoann Lafon. «Hill-Type Muscle Model.» In *Biomechatronics* . 2019.

[18] D.G. Thelen, F.C. Anderson, S.L. Delp. «Generating dynamic simulations of movement using computed muscle controls.» 2003

[19] Massimo Sartori, Dario Farina, David G. Lloyd. «Hybrid neuromusculoskeletal modeling to best track joint moments using a balance between muscle excitations derived from electromyograms and optimization.» *Biomechanics Journal*, 2014.

[20] D. G. Llyod, T.F. Besier. «An EMG-driven musculoskeletal model to estimate muscle forces.» 2002.

[21]M.F. Rabbi, C. Pizzolato, D.G. Lloyd, C.P. Carty, D. Devaprakash, L.E. Diamond. «Non negative matrix factorization is the most appropriate method for extraction of muscle synergies in walking and running.» 2020.

[22]Riccardo Ballarini, Marco Ghislieri , Marco Knaflitz and Valentina Agostini. «An Algorithm for Choosing the Optimal Number of Muscle Synergies during Walking.» 2021.

[23]Scott L. Delp, Frank C. Anderson, Allison S. Arnold, Peter Loan, Ayman Habib, Chand T. John, Eran Guendelman, and Darryl G. Thelen. «OpenSim: Open-Source Software to Create and Analyze Dynamic Symulation of movement.» *IEEE TRANSACTIONS ON BIOMEDICAL ENGINEERING*, 2007.

[24] A. Seth, M. Sherman, J.A. Reinbolt, S.L. Delp. *OpenSim: a musculoskeletal modeling and simulation framework for in silico investigation and exchange.*, 2015.

[25] Human Movement Bioengineering Course Notes

[26]Hairong Chen, Enze Shao, Dong Sun, Rongrong Xuan, Julien S. Backer, Jaodong Gu. «Effects of footwear with different longitudinal bending stiffness on biomechanical characteristics and muscular mechanics of lower limbs in adolescent runners.» 2022.

[27] A. Seth, M. Sherman, J.A. Reinbolt, S.L. Delp. *OpenSim: a musculoskeletal modeling and simulation framework for in silico investigation and exchange.*, 2015.

[28]Modenese, E. Ceseracciu, M. Reggiani, D.G. Lloyd. «Estimation of musculotendon parameters for scaled and subject specific musculoskeletal models using an optimization tecnique.» *Journal of Biomechanics.*, 2016.

[29] E. Ceseracciu, M. Reggiani, *CEINMS User Guide Documentation, Release 0.9.0.* 2015

[30] C. Pizzolato, D.G. Lloyd, M. Sartori, E. Ceseracciu, T.F. Besier, B.J. Fregly, M. Reggiani,. «CEINMS: A toolbox to investigate the influence of different neural control solutions on the prediction of muscle excitation and joint moments during dynamic motor tasks.» 2015.

[31]«Vicon Nexus Product Guide 8.1.» 2015.

[32]A. Mantoan, M. Reggiani, M. Sartori, Z. Sawacha, C. Pizzolato, C. Cobelli. «A MATLAB generic tool to efficiently process C3D data files for applications in OpenSim, XXIV.» *Congress of International Society of BIomechanics (ISB 2013), Nadal, Brazil.* 2013.

[33]Alice Mantoan, Claudio Pizzolato, Massimo Sartori, Zimi Sawacha, Claudio Cobelli, Monica reggiani. «MOtoNMS: A MATLAB toolbox to process motion data for neuromusculoskeletal modeling and Simulation.» 2015.

[34]Ben Serrien, Maggy Goossensb, Jean-Pierre Baeyensa. «Statistical parametric mapping of biomechanical one-dimensional data with Bayesian inference.» 2019.

Ringraziamenti

Vorrei Ringraziare la Prof Zimi Sawacha per avermi dato l'opportunità di svolgere questo percorso di tesi.

Un doveroso ringraziamento agli Ingegneri Marco Romanato e Giulio Rigoni che mi hanno aiutata e supportata durante l'intero svolgimento del progetto.

Un enorme grazie va anche alla mia famiglia che mi ha permesso di studiare a Padova e di frequentare il corso che ho sempre voluto fare, la quale mi ha sempre supportata anche nei giorni NO e nei momenti più bui.

Ringrazio Davide che mi ha sempre spronata a dare il meglio di me e che mi è stato accanto nonostante la distanza di questi due anni.

Ringrazio anche il gruppo 104 che ha reso epico questo ultimo anno.

Un grazie speciale va anche a tutti i miei compagni di avventura (Giulia, Giuliana, Gianluca, Domenica, Valentina, Francesca, Chiara e Virna) che hanno reso magnifico questo percorso.

Grazie a tutti coloro che hanno creduto in me
Un immenso abbraccio a tutti,
Vi voglio bene !

Gloria